INVESTIGATION OF LINKS AND CROSSTALK BETWEEN AUTOPHAGY AND DNA DAMAGE RESPONSES

by

SİNEM DEMİRBAĞ SARIKAYA

Submitted to the Faculty of Engineering and Natural Sciences

in partial fulfilment of

the requirements for the degree of

Doctor of Philosophy

Sabanci University

June 2021

ABSTRACT

INVESTIGATION OF LINKS AND CROSSTALK BETWEEN AUTOPHAGY AND DNA DAMAGE RESPONSES

SİNEM DEMİRBAĞ SARIKAYA

Ph.D. Dissertation, June 2021

Thesis Supervisor: Assoc. Özlem Kutlu

Thesis Co-advisor: Prof. Devrim Gözüaçık

Keywords: DNA damage, DNA Repair, Autophagy, Chemotherapeutics, NHEJ, ATG5, KU70

Autophagy is a well conserved intracellular degradation system that is essential for the maintenance of cellular homeostasis and protects cells from energy crisis, oxidative stress, hence DNA damage under stress conditions. Autophagy also, contributes to genomic stability by modulating various repair proteins and eliminating micronuclei carrying damaged DNA. DNA double strand breaks (DSB) are considered among the most lethal DNA damage types and repaired by two main repair systems: NHEJ and HRR. Upon DNA damage induction, autophagy activation supports HR mediated DSB repair but, impairment of autophagy causes hyperdependency on an error prone DSB repair, NHEJ. During the thesis study, we identified a novel and direct interaction between autophagy and DSB DNA repair through autophagy marker protein, ATG5 and NHEJ repair proteins. ATG5-KU70 protein interaction increased under DNA damage induction by chemotherapeutic drugs. Depletion of ATG5 protein caused delayed DSB repair through declined p-H2AX resolution. KU70 was not the target of autophagy under autophagic stimulation, which implies an autophagy independent role for ATG5-KU70 interaction. All the results indicated that KU70 is a novel interaction partner of ATG5 and

this interaction is important for the repair of DSB damage under chemotherapeutic drug induced genotoxic stress.

ÖZET

OTOFAJI ILE DNA HASAR YANITLARI ARASINDAKI BAĞLANTI VE KARŞILIKLI ETKILEŞIMIN ARAŞTIRILMASI

SİNEM DEMİRBAĞ SARIKAYA

Ph.D. Dissertation, June 2021

Thesis Supervisor: Assoc. Özlem Kutlu

Thesis Co-advisor: Prof. Devrim Gözüaçık

Keywords: DNA damage, DNA Repair, Autophagy, Chemotherapeutics, NHEJ, ATG5, KU70

Otofaji, hücresel homeostazın korunması için gerekli olan ve hücreleri enerji krizinden, oksidatif stresten, dolayısıyla stres koşulları altında DNA hasarından koruyan iyi korunmuş bir hücre içi geri dönüşüm sistemidir. Otofaji ayrıca çeşitli onarım proteinlerini modüle ederek ve hasarlı DNA taşıyan mikronükleusları ortadan kaldırarak genomik stabiliteye katkıda bulunur. DNA çift zincir kopmaları (DSB), en ölümcül DNA hasar türleri arasında kabul edilir ve iki temel onarım sistemi tarafından onarılır: NHEJ ve HRR. DNA hasarı uyarımı sonrası otofaji aktivasyonu, HR aracılı DSB onarımını destekler, ancak otofajinin bozulması, hataya açık bir DSB onarımına, NHEJ'ye aşırı bağımlılığa neden olur. Bu tez çalışması sırasında, otofaji marker proteini, ATG5 ve NHEJ onarım proteinleri aracılığıyla otofaji ve DSB DNA onarımı arasında yeni ve doğrudan bir etkileşim belirledik. ATG5-KU70 protein etkileşimi, kemoterapötik ilaçlar tarafından DNA hasarı indüksiyonu altında arttı. ATG5 proteininin eksikliği, azalan p-H2AX çözünürlüğü yoluyla gecikmiş DSB onarımına neden oldu. KU70, otofajik stimülasyon altında otofajinin hedefi değildi ve bu nedenle ATG5-KU70 etkileşiminin otofajiden bağımsız bir rolü olabileceği düşünülebilir. Tüm sonuçlar, KU70'in ATG5'in yeni bir

etkileşim ortağı olduğunu ve bu etkileşimin kemoterapötik ilaca bağlı genotoksik stres altında DSB hasarının onarımı için önemli olduğunu gösterdi.

‘Dedicated to myself, my husband, my son and my family’

ACKNOWLEDGEMENTS

First of all, I would like to express my gratitude to my dear supervisor Prof. Devrim Gözüaçık. The moment he accepted me into his lab was a great turning point for me. And I felt this transformation deeply throughout my entire doctoral journey. He was always very motivated, his scientific curiosity was very fresh and strong, and this allowed me to have a very productive and fulfilling PhD. Without his great supervision, scientific motivation and encouragement, this work would not have been this way. It was a great chance for me to do my thesis in his lab.

In addition, I would like to thank you my co-advisor Özlem KUTLU and my thesis committee: Prof. Meltem Müftüoğlu and Asst. Prof. Ogün Adebali for their key touches on the points I got stuck in during my thesis process.

And of course, I would like to thank my laboratory members Nur, Gülfem and Yunus for their support during my doctoral process.

I would like to specially thank you my dear friends, Hümeyra Nur Kaleli and Şükriye Bilir. These girls have always guided me in the right way and they were always there for me whenever I called.

Finally, to myself, this was the period when I believed in myself the most and got the most help from myself. Then, my husband was the second architect of this process. When he carried me from home to school, he carried all my stress and problems while carrying me from home to school.

And, to my family, because I owe it all to you.

Thank you.

This project is supported by TUBITAK-1001-Scientific and Technological Research Projects Funding Program, Project No: 117Z244. I would like to thank you Sabanci University for providing me financial support as PhD scholarship student.

TABLE OF CONTENTS

1. INTRODUCTION 14
1.1 DNA DAMAGE 14
1.2 DNA DAMAGE RESPONSES 16
1.3 DNA REPAIR 21
1.3.1 Base Excision Repair 22
1.3.2 Nucleotide Excision Repair (NER) 25
1.3.3 Mismatch Repair (MMR) 29
1.3.4 Homologous Recombination Repair (HR) 31
1.3.5 Non-homologous end joining 34
1.4 AUTOPHAGY 35
1.4.1 Mechanism of autophagy 39
1.5 CROSSTALK BETWEEN AUTOPHAGY AND DSB REPAIR 40
2. MATERIALS AND METHODS 49
2.1 PLASMIDS, CONSTRUCTS and SIRNAs 49
2.2 CELL CULTURE 50
2.2.1 Cell Line Maintenance 50
2.2.2 Cell Transfections 50
2.2.3 DNA Damage Induction in Cell Culture 50
2.2.4 DNA Damage Repair Induction (Recovery Experiment) 51
2.2.5 Autophagy Induction in Cell Culture 51
2.3 CELL FRACTINATION 52
2.4 PROTEIN ISOLATION 52
2.5 IMMUNOBLOTTING TESTS 53
2.6 IMMUNOPRECIPITATION ANALYSES 55
2.7 IMMUNOFLUORESCENCE ANALYSES 56
2.8 GEL FILTRATION (FPLC) ANALYSES 57
2.9 RNA ISOLATION and RT-PCR ANALYSIS 58
2.10 STATISTICAL ANALYSES 60
3. RESULTS 61
3.1 CLONING STUDIES OF ATG5 61
3.2 PRELIMINARY DATA PRIOR TO THE PROJECT DESIGN 64

3.3 CONFIRMATION AND CHARACTERIZATION OF ATG5-KU70 AND ATG5-KU80 INTERACTION IN CONTROL AND DNA DAMAGE INDUCED CONDITIONS 67
3.4 ANALYSIS THE DYNAMICS OF ATG5-KU70 INTERACTION. 68
3.5 KU70 INTERACT WITH N-TERMINAL PART OF ATG5 78
3.6 ANALYIS THE EFFECT OF AUTOPHAGIC STIMULI ON DNA DSB INDUCTION 80
3.7 ANALYIS THE EFFECT OF AUTOPHAGY ACTIVATION AND INHIBITION ON KU70 TURNOVER 85
3.8 ANALYIS THE EFFECT OF DNA DSB DAMAGE RESPONSE ON AUTOPHAGY ACTIVATION 87
3.9 THE FUNCTIONAL ROLE OF ATG5-KU70 INTERACTION IN DNA DAMAGE REPAIR 88
3.9.1 Analysis the effect of ATG5 over etoposide induced DNA DSB damage and following repair process 90
3.9.2 ATG5 rescue recovers the delay in DNA DSB repair induced by etoposide. 92
3.9.3 ATG5 is not included in p-H2AX foci formation upon DNA DSB induction by Etoposide. 93
3.9.4 Loss of ATG5-Ku70 interaction enables recovery of genotoxic stress induced by etoposide. 95
3.10 ANALYSIS THE EFFECT OF DNA DAMAGE ON ATG5 AND DNA REPAIR GENE EXPRESSION LEVEL 96
4. DISCUSSION 101
5. CONCLUSION AND FUTURE ASPECTS 1
6. APPENDIX A 1
7. PUBLICATIONS 1
Publication List 63
Poster presentation 66

LIST OF TABLES

Table 2.3.1: List of six major DNA repair pathway and abnormalities associated with these repair systems…….21

Table 2.5.1: The ingredients of home-made separating gel for SDS-PAGE ……51

Table 2.5.2: The ingredients of home-made stacking gel for SDS-PAGE…….51

Table 3.2.1: The list of studies in the literature conducted on the association between autophagy and DNA repair systems…….1-7

LIST OF FIGURES

FIGURE 1.1.1 SCHEMATIC REPRESENTATION OF THE COMMON DNA LESIONS OCCURS IN GENOMIC DNA. 15

FIGURE 1.2.1 SCHEMATIC REPRESENTATION OF DNA DAMAGE RESPONSE (DDR) SIGNALING PATHWAY..... 19

FIGURE 1.2.2 THE EFFECTS OF THE DNA DAMAGE RESPONSE ON CELLULAR FATE 20

FIGURE 1.3.1.1 SCHEMATIC REPRESENTATION OF THE BER PATHWAY…..23

FIGURE 1.3.2.1 SCHEMATIC REPRESENTATION OF THE NER PATHWAY. ... 26

FIGURE 1.3.3.1 SCHEMATIC REPRESANTATION OF MMR PATHWAY..... 29

FIGURE 1.4.1 SCHEMTAIC REPRESENTATION OF AUTOPHAGY PATHWAY. 36

FIGURE 1.4.2 SCHEMATIC REPRESENTATION OF ATG5-ATG12-ATG16 CONJUGATION SYSTEM. 40

FIGURE 1.5.1 SCHEMATIC REPRESENTATION OF THE HR PATHWAY AND ITS CROSSTALK WITH THE AUTOPHAGY PROCESS..... 45

FIGURE 1.5.2 SCHEMATIC REPRESENTATION OF THE NHEJ PATHWAY AND ITS CROSSTALK WITH THE AUTOPHAGIC PROCESS.. 48

FİGURE 3.1.1 SCHEMATIC REPRESENTATİON OF ATG5 FRAGMENTS SIZES 61
FİGURE 3.1.2 IMMUNOBLOTTING RESULTS OF DIFFERENT 193-275 AND 1-79, 80-192 CLONES..... 62
FIGURE 3.1.3 SCHEMATIC REPRESENTATION OF CLONING STEPS OF ATG5 FRAGMENTS. 63
FIGURE 3.1.4 IMMUNOBLOTTING EXPERIMENT RESULT OF ATG5 FRAGMENTS OVEREXPRESSED CELLS UNDER ETOPOSIDE TREATMENT.. 64
FIGURE 3.2.1 SILAC-BASED LC-MS/MS ANALYSIS RESULTS OF HEK/293T AND HELA CELLS. 65
FIGURE 3.2.2 ATG5 IMMUNOPRECIPITATION EXPERIMENTS TO TEST ATG5-KU70 AND ATG5-KU80 BINDING IN A) HELA AND B) HEK/293T CELLS.66
FIGURE 3.3.1 ATG5 IMMUNOPRECIPITATION EXPERIMENT RESULTS TO CONFIRM KU70 AND KU80 BINDINGS 67-68
FIGURE 3.4.1 GEL FILTRATION TESTS OF HELA CELL-DERIVED TOTAL LYSATES. 69
FIGURE 3.4.2 REPRESENTATIVE CHROMATOGRAM SHOWING PEAKS OF THE MOLECULAR WEIGHT MARKER MIX. 70
FIGURE 3.4.3 REPRESENTATIVE CHROMATOGRAMS OF DMSO TREATED CONTROL CELL LYSATES. 70
FIGURE 3.4.4 OD595 ABSORBANCE CONFIRMATION OF THE MARKER PEAKS OF THE GEL FILTRATION OVER SUPERDEX 200 COLUMN..... 71
FIGURE 3.4.5 ENDOGENOUS ATG5-IMMUNOPRECIPITATION EXPERIMENTS PERFORMED IN HEK/293T CELLS. 71
FIGURE 3.4.6 ENDOGENOUS ATG5-IMMUNOPRECIPITATION EXPERIMENTS PERFORMED IN HEK/293T CELLS. 73
FIGURE 3.4.7 ENDOGENOUS ATG5-IMMUNOPRECIPITATION EXPERIMENTS PERFORMED IN HELA CELLS.. 73
FIGURE 3.4.8 ENDOGENOUS ATG5-IMMUNOPRECIPITATION EXPERIMENTS PERFORMED IN HELA CELLS. 74
FIGURE 3.4.9 ENDOGENOUS ATG5-IMMUNOPRECIPITATION EXPERIMENTS PERFORMED IN HEK293T CELLS. 75

FIGURE 3.4.10 COLOCALIZATION EXPERIMENTS OF KU70 AND ATG5 UNDER DNA DSB DAMAGE INDUCTION BY ETOPOSIDE IN HEK293T CELLS. 76
FIGURE 3.4.11 QUANTIFICATION OF CONFOCAL MICROSCOPY ANALYSIS IN HEK293T CELLS..... 77
FİGURE 3.4.12 CELLULAR FRACTIONATION WERE PERFORMED AFTER DOXORUBICIN TREATMENT. (+), DOXORUBICIN; (-), DMSO IN HEK293T CELLS.. 78
FIGURE 3.5.1 ATG5 IMMUNOPRECIPITATION ANALYSIS IN HEK293T CELLS. 79
FIGURE 3.6.1 THE EFFECT OF AUTOPHAGIC ACTIVITY ON P-H2AX FOCI FORMATION IN MEF CELLS. 81
FIGURE 3.6.2 QUANTIFICATION OF CONFOCAL MICROSCOPY ANALYSIS IN MEF CELLS.. 82
FIGURE 3.6.3 IMMUNOBLOTTING RESULTS OF EBSS TREATED MEF CELLS. 82
FIGURE 3.6.4 ANALYSIS THE EFFECT OF AUTOPHAGIC ACTIVATION ON DNA DSB DAMAGE IN MEF CELLS. 83
FIGURE 3.6.5 QUANTIFICATION OF CONFOCAL MICROSCOPY ANALYSIS IN MEF CELLS 84
FIGURE 3.6.6 THE EFFECT OF AUTOPHAGY ACTIVATION ON DNA DSB DAMAGE IN MEF CELLS... 85
FIGURE 3.7.1 THE EFFECT OF AUTOPHAGY ACTIVATION AND INHIBITION ON KU70 DEGRADATION IN MEF CELLS. 86
FIGURE 3.8.1 THE EFFECT OF ETOPOSIDE INDUCED DNA DAMAGE AND REPAIR ON AUTOPHAGY ACTIVATION. 87
FIGURE 3.9.1 COLOCALIZATION ANALYSIS BETWEEN ATG5 AND KU70 UNDER DNA DAMAGE AND REPAIR INDUCING CONDITIONS IN HELA CELLS 88
FIGURE 3.9.2 QUANTIFICATION OF DNA DAMAGE AND REPAIR INDUCED ATG5-KU70 COLOCALIZATION IN HELA CELLS. 89
FIGURE 3.9.1.1 THE EFFECT OF ATG5 DEPRIVATION ON DNA DSB DAMAGE AND REPAIR PERIODS IN ATG5KO AND ATG5WT HELA CELLS..... 90

FIGURE 3.9.1.2 THE EFFECT OF ATG5 DEPRIVATION ON DNA DSB DAMAGE AND REPAIR PERIODS IN ATG5KO AND ATG5WT HELA CELLS..... 91
FIGURE 3.9.2.1 THE EFFECT OF ATG5 RESCUE ON DNA DSB DAMAGE AND DSB REPAIR PROCESS IN ATG5KO HELA CELLS. ……92
FIGURE 3.9.3.1 COLOCALIZATION ANALYSIS BETWEEN ATG5 AND P-H2AX UNDER DNA DAMAGE INDUCTION BY ETOPOSIDE IN HELA CELLS..... 94
FIGURE 3.9.3.2 COLOCALIZATION ANALYSIS OF ATG5 AND P-H2AX UNDER THE DNA DSB DAMAGE INDUCING CONDITION IN HELA CELLS..... 95
FIGURE 3.9.4.1 CELLULAR VIABILITY OF ATG5WT AND ATG5 KO CELLS UNDER THE DNA DSB DAMAGE AND REPAIR CONDITIONS..... 95
FIGURE 3.10.1 EFFECT OF DNA DAMAGE INDUCED BY ETOPOSIDE AND CISPLATIN ON ATG5 MRNA LEVELS. ……97
FIGURE 3.10.2 EFFECT OF DNA DAMAGE INDUCED BY ETOPOSIDE AND CISPLATIN ON KU70 MRNA LEVELS..... 97
FIGURE 3.10.3 EFFECT OF DNA DAMAGE INDUCED BY ETOPOSIDE AND CISPLATIN ON KU80 MRNA LEVELS..... 98
FIGURE 3.10.4 EFFECT OF DNA DAMAGE INDUCED BY ETOPOSIDE AND CISPLATIN ON DNA-PKCS MRNA LEVELS. 99
FIGURE 3.10.5 THE EFFECT OF DNA DAMAGE ON ATG5, KU70 AND KU80 PROTEİN LEVELS..... 99

LIST OF ABBREVIATIONS

ATG: Autophagy-related genes

AMPK: AMP activated protein kinases

mTOR: Mammalian target of rapamycin

PI3K: Class-III-Phosphotidylinostiol-3-Kinase

PIP3: Phosphotidylinositol-3-phosphate

LC3: Microtubule-associated protein 1 light chain 3

EXO1: Exonuclease 1

BLM: BLM RecQ like helicase

EBSS: Earl's balanced salt solution

XRCC4: X-ray repair cross complementing 4

PNKP: polynucleotide kinase 3'-phosphatase

APLF: Aprataxin and PNKP like factor

WRN: WRN RecQ like helicase

ATM: ATM serine/threonine kinase

ATR: ATR serine/threonine kinase

RAD50: RAD50 double strand break repair protein

DNA-PKcs: Protein kinase, DNA-activated, catalytic subunit

MRE11: MRE11 homolog, double strand break repair nuclease

NBS1: Nijmegen breakage syndrome 1 (nibrin)

RNF8: Ring finger protein 8

MDC1: Mediator of DNA damage checkpoint 1

Rap80: Receptor associated protein 80

ATRIP: ATR interacting protein

BAX: BCL2 associated X, apoptosis regulator

PUMA: BCL2 binding component 3

WIP1: WD repeat domain, phosphoinositide interacting 1

MDM2: MDM2 proto-oncogene

XPC: XPC complex subunit, DNA damage recognition and repair factor

BRCA1: BRCA1 DNA repair associated

CtIP: CTBP-interacting protein

FLNA: Alpha filamin

XRCC6/KU70: X-Ray Repair Cross Complementing 6

XRCC5/KU80: X-Ray Repair Cross Complementing 5

1. INTRODUCTION

1.1 DNA DAMAGE

Genetic information is stored in DNA and sustaining its integrity is crucial to maintain life of organisms. About 10,000 DNA lesions occur in each human cell on each day as a result of daily cellular functions (Lindahl & Barnes, 2000) There are various mechanisms which have been evolutionarily sustained to sense and neutralize potential DNA lesions that can be threatening for genomic integrity (Jackson & Bartek, 2009). For instance, during DNA replication some nucleotides can be incorporated into the newly replicated DNA strands incorrectly and result in mismatch base conjugation or different byproducts. As an example of these byproducts, Reactive Oxygen Species (ROS) or Reactive Nitrogen species (RNS) which produced in multiple subcellular sites during normal physiological cellular processes are cause of different DNA lesions involving single- or double-stranded breaks, base insertions, and apurinic/apyrimidinic sites (AP) (Cadet & Wagner, 2013; Van Houten et al., 2018). In addition to endogenous DNA damaging agents ROS and RNS, there are exogenous agents, such as ionizing radiations (i.e., X-rays), cosmic radiation, mutagenic chemicals, and ultraviolet (UV) light that cause formation of DNA lesions that require correction by cells daily (N. Chatterjee & Walker, 2017; Tubbs & Nussenzweig, 2017). Similar to all other natural molecules, DNA is also exposed to regular decay processes. For example, a DNA molecule under the attack of alkylation, oxidation and deamination, which are mutagenic if not corrected, is exposed to the decay because of wrong base pairing and so, base insertions during DNA replication (Lindahl, 1993). Single-stranded break (SSB) is another type of DNA lesion that arises spontaneously as a result of UV or gamma irradiation exposure (Abbotts & Wilson, 2017)

or occurs in case of DNA replication, stalling of replication fork and collision of the transcriptional machinery (Hossain et al., 2018). Double-stranded breaks (DSBs) are also the most severe DNA lesions that the cell is exposed to and occurs if each strand of the DNA is severed as a consequence of SSBs accumulation or presence of various adjacent SSBs (Abbotts & Wilson, 2017). Consequently, genomic integrity of the cells is continuously under a number of attacks of DNA damaging agents and to overcome these different attacks, cells have developed sophisticated mechanisms to detect, record and repair these widespread DNA lesions.

DNA lesion	Apurinic site	Strand cross-linking	Bulky Lesion	Mismatch	Double-Stranded Break
Main causes	Cellular metabolism	UV radiation	UV radiation	Replication errors	IR; Replication fork stallation
DDR	BER	FANCONI	NER	MMR	NHEJ; MMEJ; SSA; HDR

Figure 1.1.1 Schematic representation of the common DNA lesions that occur in genomic DNA. In the following part, the table demonstrates the type and main cause of DNA lesion and leading DNA repair pathway employed for its resolution (Jackson & Bartek, 2009).

1.2 DNA DAMAGE RESPONSES

The DNA damage response (DDR) system acts as an intracellular warning system constantly tracking the genomic integrity and controlling the accurate transfer of the genetic information to daughter cells (Jackson & Bartek, 2009). Proteins of the phosphatidylinositol 3-kinase-like protein kinases (PIKKs) family; ATM, ATR and DNA-PK and poly (ADP)ribose polymerase (PARP) family are the mediators of the DDR system in the cells. ATM and DNA-PK exerts their functions upon DNA damaging agent's exposure such as ionizing radiation that conclude in DSBs ((Harper & Elledge, 2007; Meek et al., 2008)). ATM has a number of substrates however, DNA-PK performs its function by controlling a small number of proteins employed in DSB end joining. At the early onset of DSB induction, the MRN complex binds to double-stranded DNA ends (Ciccia & Elledge, 2010). The MRN complex consists of MRE11, RAD50, and NBS1 proteins. MRE11 functions as an endo- and exonuclease to be able to resect DNA ends at the DSB. Moreover, recruitment of DDR factors containing ATM and different signaling molecules to the DSB requires the MRN complex (Ciccia & Elledge, 2010). It is accepted that induction of ATM kinase is stimulated by structural changes in chromatin structures upon DNA breakage however, it is seen that MRN-guided recruitment of ATM to the DSB after its activation leads to notable amplification in activation of ATM (Ciccia & Elledge, 2010; Kitagawa et al., 2004). When the activated ATM kinase arrives at the DSB, it phosphorylates a number of target proteins which promote cellular damage response. The histone protein, H2AX, is one of the leading targets of ATM inside of the chromatin and its phosphorylated form, γH2AX, functions as a platform to recruit other DDR proteins and elevate signaling pathways. Once MDC1 is recruited by γH2AX, it recruits MRN and ATM proteins to the site covering DSBs and so, ATM signaling is

enhanced (Ciccia & Elledge, 2010). MDC1 also recruits an E3 ubiquitin ligase, RNF8, to the DSB site and ubiquitin chains are conjugated to histone H2A. Brca1 complex involving Rap80 and Abraxas proteins bind to ubiquitin chains and recruits to the DSB region (Ciccia & Elledge, 2010). In contrast to ATM, which responds to DSBs, ATR exerts its function in concentrating with ATRIP at RPA-coated ssDNA regions that occur in stalled replication forks and at single-strand–double strand junctions that emerge as intermediates of DNA repair pathways, at resected DSBs (Cimprich & Cortez, 2008), (Byun et al., 2005). ATR is essentially required for cell survival under physical conditions because of its function in resolution of stalled replication forks (E. J. Brown & Baltimore, 2000; Eric J. Brown & Baltimore, 2003). Markedly, even though activation of ATM and ATR are triggered by different stimuli, they share considerably overlapped substrates (Goldstein & Kastan, 2015; Kastan & Bartek, 2004)

The only two members of the PARP family- PARP1 and PARP2- have been indicated in the DDR (Schreiber et al., 2006). PARP1 and PARP2 are induced in the presence of SSBs and DSBs and recruit DDR mediators by catalyzing the insertion of poly (ADP-ribose) chains on proteins to chromatin at the damaged region (Schreiber et al., 2006).

Most of the current knowledge about the DDR is built on the function of two kinases, ATM and ATR. After ATM and ATR detect the DNA lesions, they phosphorylate DDR amplifier proteins which can recruit ATM/ATR substrates (Zhou & Elledge, 2000). Additionally, ATM and ATR phosphorylate DDR effector proteins directly or indirectly by various kinases such as CHK1, CHK2, CK2, p38 and MK2 (Harper & Elledge, 2007).

The DDR was involved in various decision points of physiological processes including the choice of undergoing apoptosis, going into terminal differentiation during senescence, elevated immune surveillance (Gasser & Raulet, 2006; Zhou & Elledge, 2000). ATM and ATR are essentially involved in different DNA repair processes, NHEJ, HR, ICL repair NER and replication fork stability. During DDR, the decision steps are firstly in favor of fast post-translational modifications involving phosphorylation and inhibition of CDC25 which is the cell cycle phosphatase essential for activation of CDK. A remarkable part of the decision processes is in favor of slow transcriptional returns providing processing of information over a period of time. The ultimately examined player of the short response is p53. P53 has tremendous roles in different vital cellular processes such as activation of cell cycle arrest, senescence or apoptosis in the presence of DNA damage. P53 exerts its function via transcriptionally regulating p21 which is the CDK inhibitor and the pro-apoptotic proteins BAX and PUMA (Riley et al., 2008). In response to DNA damage, ATM and CHK2 regulates p53 and also, p53 directly induces DNA repair pathways. For instance, by regulating XPC and DDB2 and activating dNTP synthesis, p53 induces NER (Ford, 2005). After DSB formation, ATM induces p53 in a periodic cycle through a transcriptional circle which encompasses p53 targets WIP1 phosphatase and the MDM2 E3 ubiquitin ligase that switch off ATM and p53 separately (Batchelor et al., 2009). Through this mechanism, the cell has a clock mechanism that induces p53 transcriptional stimulations in an oscillating manner based on repair of the initial DNA damage. Depending on the clock-like mechanism, each transcriptional pulse takes place in a different proteomic circumstance and could confer different information for the cell by directing cells towards different fates such as apoptosis or senescence.

Now, it is clearly known that ATM and ATR organize a wider range of cellular processes than assumed before, harboring DNA replication and repair, transcription, RNA splicing and metabolic signaling (Bennetzen et al., 2010; Matsuoka et al., 2007; Paulsen et al., 2009). Attenuation of these activities gives rise to DNA damage caused genomic instability.

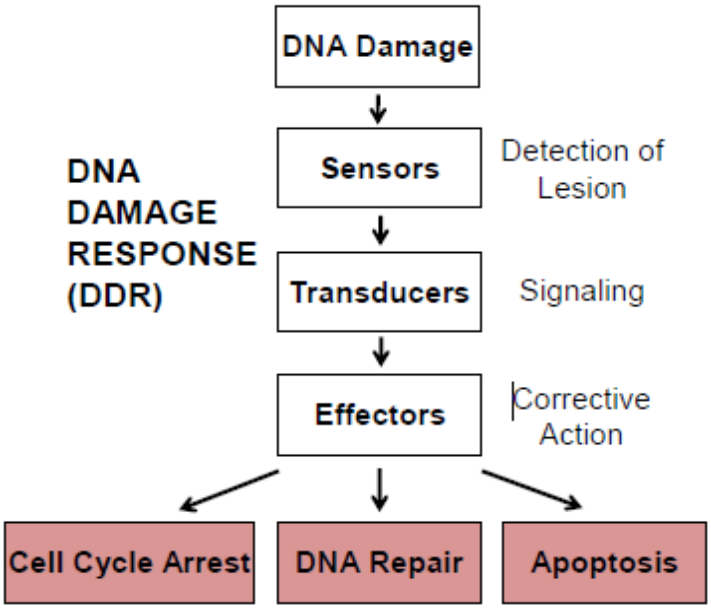

Figure 1.2.1 Schematic representation of DNA damage response (DDR) signaling pathway (Ray & Fry, 2015).

Positioning of DDR players to the damaged DNA sites is started by sensory proteins which has capability to directly recognize specific DNA lesions and induce the DDR (Zhou & Elledge, 2000). The studies conducted in mammalian and yeast cells have revealed that strained binding of sensory proteins to the chromatin is enough to uncover the DDR cascade in the presence or absence of DNA damage (Bonilla et al., 2008; E.

Soutoglou & Misteli, 2008). Further regulation of DNA repair settles in the site of DNA damage occupied by DDR-controlled factors and it can be seen as distinct nuclear foci under the microscopy. These foci structures are extremely dynamic and controlled by spatiotemporal regulation (Ziv et al., 2006) which is considered to offer a dynamic repair choice, most likely in an enhanced order. Clustering of the DDR cascade is governed by a range of post-translational modifications consisting of sumoylation, poly (ADPribosylation), acetylation, methylation, and phosphorylation activated through the DNA damage response (Bergink & Jentsch, 2009; Harper & Elledge, 2007; Kleine & Lüscher, 2009; Misteli & Soutoglou, 2009). There is a broad spectrum of proteins which specifically detects these post-translational modifications and mediates the recruitment to DNA damage sites.

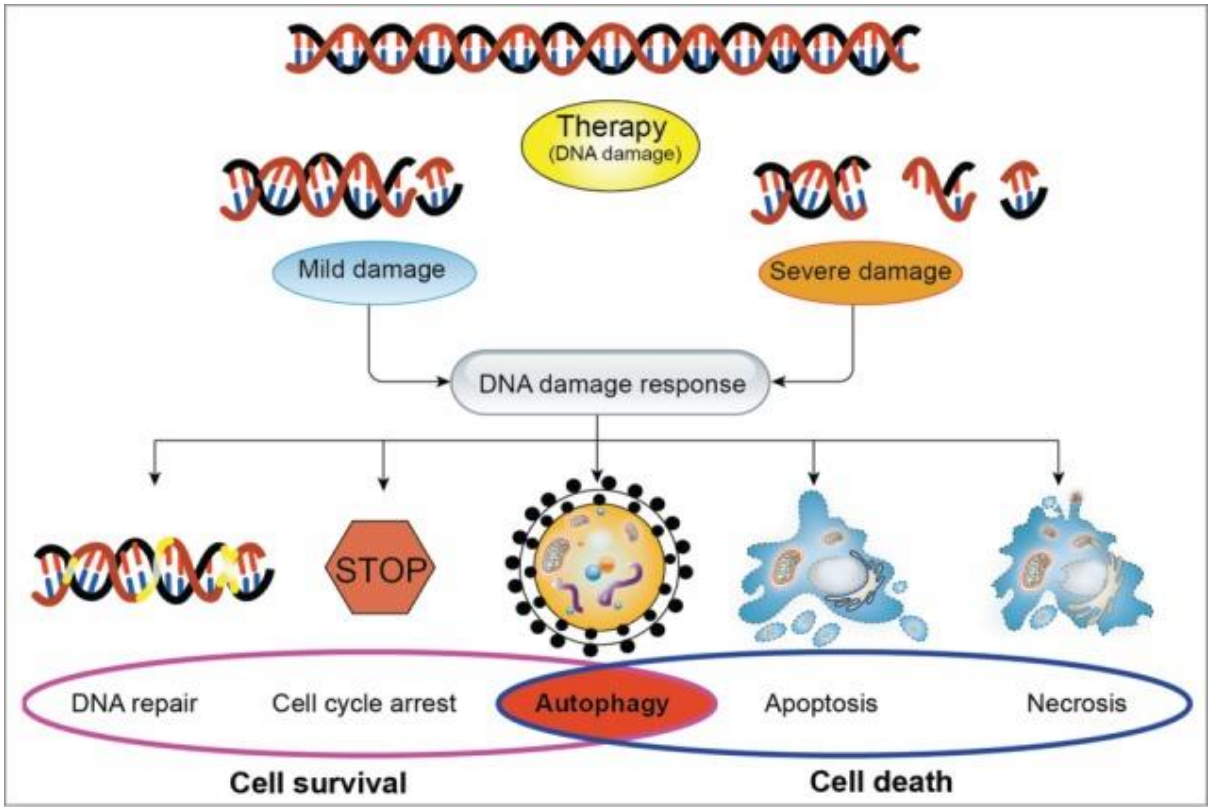

Figure 1.2.2: The effects of the DNA damage response on cellular fate

1.3 DNA REPAIR

DNA repair is precisely identified as the cellular responses related with the recovery of the natural base pair sequence and construction of damaged DNA. Once DNA damage is detected, signal is delivered to the mechanisms controlling the cell cycle progression to retard or pause cell division. The slowing down of cell division initiates a state that provides the cell to adapt the suitable mechanism for repairing the lesion (Carusillo & Mussolino, 2020). Major DNA repair systems are classified into six different pathways and each repair pathway consists of a range of biochemical events promoting sensing, excision, and recovery of the natural DNA sequence (D'Andrea, 2015).

1.3.1. Base Excision Repair

Table 1.3.1: List of six major DNA repair pathway and abnormalities associated with these repair systems. (D'Andrea 2015)

DNA Damage Repair Pathway	Function	Examples of Gene Mutation	Examples of Altered Expression of a Normal Gene	Effect of Loss of Pathway on Clinical Response
Base-excision repair (BER)	Repair of damaged bases or single-strand DNA breaks	None reported	None reported	None reported
Mismatch repair (MMR)	Repair of mispaired nucleotides	Mutation of *MSH2*, *MSH6*, and *MLH1* in Turcot syndrome (brain and colon tumors) and *HNPCC* (colon and gynecologic cancers)	Loss of expression of *MSH2* or *MLH1* in sporadic colon cancer	Resistance to DNA monoadducts Sensitivity to DNA crosslinks
Nucleotide-excision repair (NER)	Excision of a variety of helix-distorting DNA lesions	Mutation of *XPA*, *XPB*, *XPC*, *XPE*, *XPF*, or *XPG* in xeroderma pigmentosum (skin cancer) Variant expression of *ERCC1* or *XPD* in lung cancer	Loss of *XPA* expression in testicular germ-cell tumors	Sensitivity to DNA adducts
Homologous recombination (HR)	Repair of double-strand DNA breaks	*BRCA1/2* mutated in early-onset breast/ovarian, prostate, pancreas, and gastric cancers *FANC* genes mutated in Fanconi anemia	Loss of expression of *BRCA1/2* in ovarian and lung cancers Loss of *NBS1* expression in prostate cancer	Sensitivity to DNA double-strand breaks
Nonhomologous end joining (NHEJ)	Repair of double-strand DNA breaks	DNA ligase IV mutated in Lig4 syndrome (leukemia) Artemis mutated in Omenn syndrome (lymphoma)	Loss of *Ku70* expression in cervical, rectal, and colon cancers Loss of *Ku86* expression in rectal cancer	Sensitivity to DNA double-strand breaks
Translesional synthesis (TLS)	Bypass of DNA adducts during DNA replication	DNA pol E mutated in xeroderma pigmentosum variant (XPV; skin cancers)	Pol β overexpressed in uterus, ovary, prostate, and stomach cancers Pol iota overexpressed in breast cancer	Resistance to DNA adducts

Base excision repair (BER) is one of the major single strand break repair systems (Robertson et al., 2009) BER restorates non-bulky single-base DNA lesions caused by alkylation, oxidation or deamination of bases. BER activation occurs in the nucleus during primarily G1 phase of the cell cycle (Dianov & Hübscher, 2013). In this repair pathway, following chromatin remodeling at the damaged DNA site, the lesion is detected by a specific DNA glycosylase (Odell et al., 2013). There are 11 different DNA glycosylases that can recognize and cut out a damaged base from unaffected helices and flipping out bases from the major groove (Huffman et al., 2005; Krokan & Bjoras, 2013). Two different types of glycosylases are addressed in the BER pathway in terms of their function. One type of glycosylases is monofunctional that have only a glycosylase activity and uracil glycosylases. N-methylpurine DNA Glycosylase (MPG), and MutY Homolog (MUTYH) are examples of these glycosylases. Another type of glycosylases are bifunctional with a glycosylase and an additional 3'AP lyase activity. The Nth-like DNA glycosylase 1 (NTHL1), Nei-like DNA glycosylase 1 (NEIL1) and Nei-like DNA glycosylase 2 (NEIL2) are the examples of these glycosylases (Jacobs & Schär, 2012). In addition, there are NEIL3 and DNA glycosylase (OGG1) which bear mono- and bifunctional activity (Svilar et al., 2011). As a result of the monofunctional glycosylases activity, an abasic site is generated and it is directed to the short-patch-repair pathway.In

case of the bifunctional glycosylase's activity, the long-patch repair pathway of BER is activated (Dianov & Hübscher, 2013).

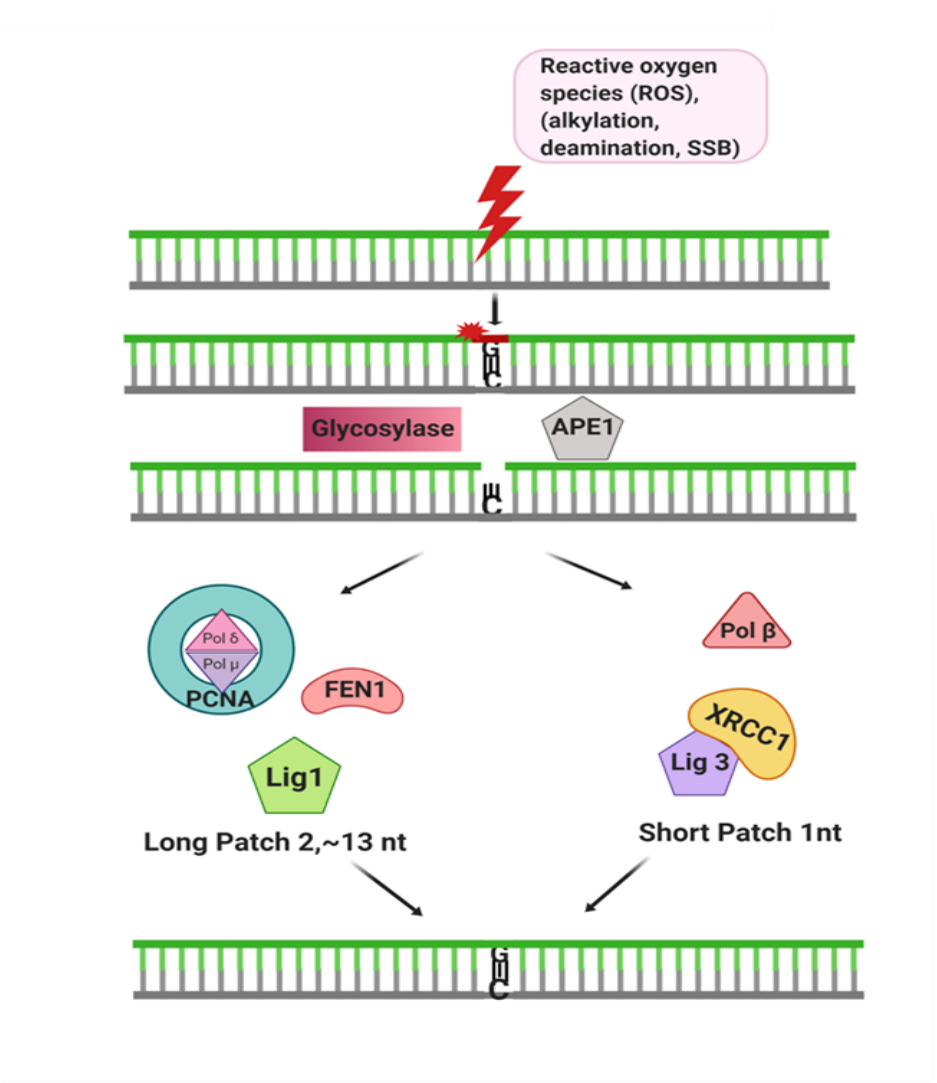

Figure 1.3.1.1: Schematic representation of the BER pathway.

During short patch repair pathway, the AP endonuclease (APE1 in human cells) cut out the phosphodiester bond 5′ to the abasic site and give rise to 3′-hydroxyl and a 5′-2-deoxyribose-5′-phosphate (5′-dRP). The exposed 3'-hydroxyl group is invaded by DNA polymerase β (POL β). The repair gap is then modified by the 5′-dRP lyase activity of POL β. Finally, the gap is fulfilled by the POL β and ligated by LIG1 (DNA ligase 1) or

a complex of LIG3 (DNA ligase 3) and XRCC1 (X-ray repair cross-complementing protein 1) (Almeida & Sobol, 2007).

During Long patch repair, the repair gap emerges as a result of bifunctional glycosylase function, and it is modified by the 3′ phosphodiesterase activity of APE1. Hereafter, a synthesis occurs in a strand-displacement manner to fill the emerging gap by the activity POL β (in non-proliferating cells) or POL δ/ε (in proliferating cells) enzymes. To accomplish the repair, flap endonuclease 1 (FEN1) excises the displaced 5′-flap structure and lastly, ligation is performed by LIG1 (Akbari et al., 2009; Svilar et al., 2011). Whilst the repair of 8-oxo-G lesions by BER at CAG repeats is associated with trinucleotide repeat instability, downregulation of OGG1 is found as related with cancer, neurodegenerative diseases and aging (N. Chatterjee & Siede, 2013; P. Chatterjee et al., 2015; Curtin, 2012; de Souza-Pinto et al., 2009; Kovtun & McMurray, 2007; Krokan & Bjoras, 2013; Møllersen et al., 2012). POL β mutations are discovered specifically in solid cancers. Also, it is found that POL β variants can have dominant negative and sequence specific mutative functions (Lang et al., 2007; Murphy et al., 2012; Starcevic et al., 2004; L. Wang et al., 1992) It has been also revealed that PARP1 is needed in the repair of purine base damage and single strand break repair mediated by a sub-pathway of BER (Krokan & Bjoras, 2013; Reynolds et al., 2015). Lastly, short, and long patch BER are also shown to be operated in mitochondria through the activity of another enzyme, POL γ. All this research points out the significance of the BER system in the maintaining of global genome stability (Akbari et al., 2008; P. Liu & Demple, 2010).

1.3.2 Nucleotide Excision Repair (NER)

Nucleotide excision repair is a second SSB repair system and is responsible for removal of bulky DNA adducts which modify the DNA helix structure and prevent the accurate functioning of polymerases (Gillet & Schärer, 2006). In this manner, UV-induced cyclobutane pyrimidine dimers (CPDs), 6-4 pyrimidine-pyrimidone photoproducts (6-4PPs), benzo[a]pyrene adducts, or damages emerged from chemotherapeutic agent exposure are the major targets of the NER system. At the onset of the NER, chromatin remodeling is performed by NER and chromatin components therefore, a way is opened on the particular DNA lesions for functioning of NER machinery (Scharer, 2013). NER pathway can be branched into two sub-pathways: global genome NER (GG−NER) and transcription−coupled NER (TC−NER) (Iyama & Wilson, 2013; Menck & Munford, 2014). The placement of lesions and protein complexes dictates which sub-pathway will be activated during NER.

In the GG-NER pathway, DNA damage is sensed by the XPC (Xeroderma Pigmentosum, complementation group C), RAD23B (UV excision repair protein Radiation sensitive 23B) and CETN2 (Centrin 2) protein complex. This protein complex scans and detects transient single−stranded DNA (ssDNA) resulting from interrupted base pairing throughout the genome (Fagbemi et al., 2011; Masutani et al., 1994; Nishi et al., 2005). Once this complex binds to the reverse strand of the lesion, transcription factor II H (TFIIH), a transcription initiation and repair factor involving ten protein subunits, recruits to the site and initiates GGR-coupled repair (Compe & Egly, 2012; Iyama & Wilson, 2013; Katoh et al., 2000; Volker et al., 2001). In case of repair of UV-induced CPDs, ultraviolet-damaged DNA damage−binding protein (UV–DDB) complex which bear

DDB1 (XPE−binding factor) and the GG−NER−specific protein DDB2 specifically binds to UV-radiation caused lesions and then activates the XPC binding to the lesions (Chu & Chang, 1988; Scrima et al., 2008; Wakasugi et al., 2002). The lesions that the XPC binds turn to a substrate for the transcription initiation factor II H (TFIIH) complex. In the last step, gap filling, and double excision is synchronized to avoid ssDNA gap formation and potential DDR signal activation (Marini et al., 2006; Marti et al., 2006; Mocquet et al., 2008).

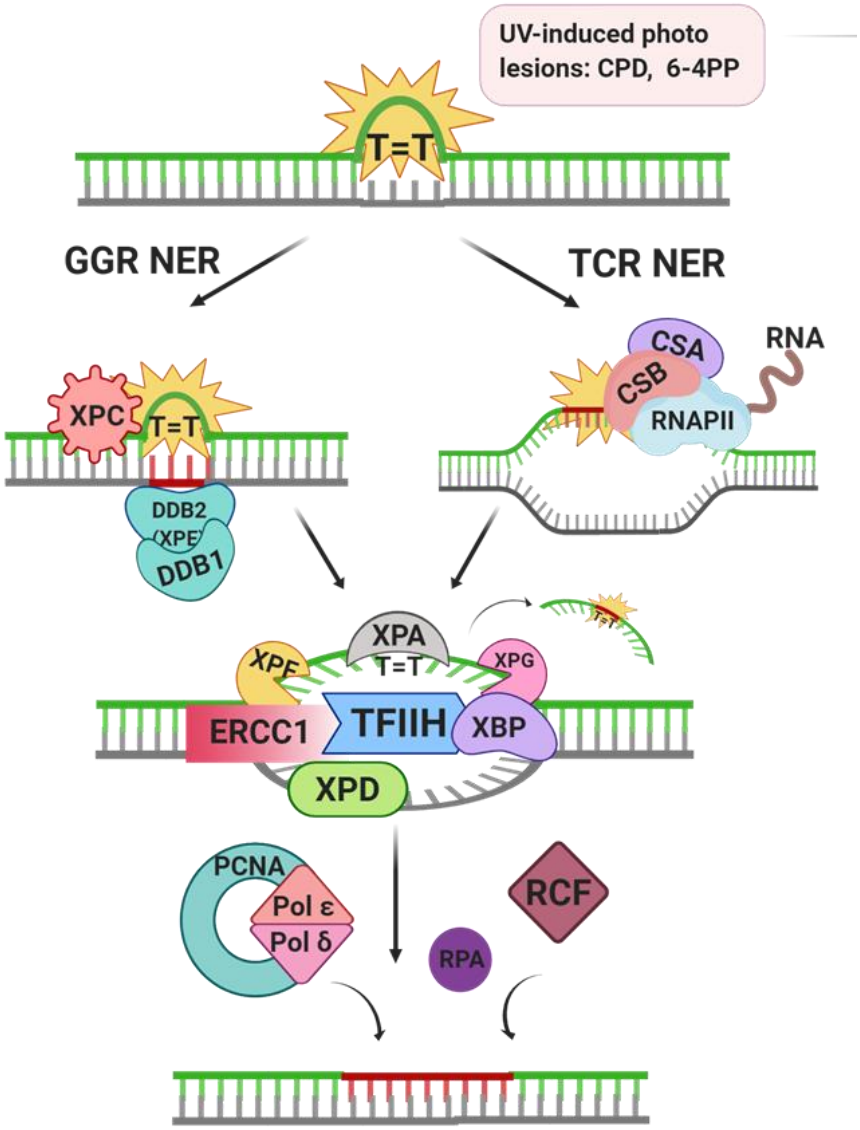

Figure 1.3.2.1: Schematic representation of the NER pathway.

In the cleavage step of GG-NER, all the proteins are assembled to NER. During the incision, structure specific endonucleases XPF–ERCC1 and XPG are employed to cleave the damaged region near the 5′ and 3′ end of the lesion respectively (Fagbemi et al., 2011). The last step of gap-filling and ligation accomplished with a number of proteins including the replication proteins PCNA (proliferating cell nuclear antigen), RFC (replication factor C), POL δ, POL ε or POL κ, and XRCC1–LIG3 or LIG1. The decision about which polymerase will be used depends on the proliferative condition of the cell. For instance, non-proliferative cells dominantly use POL ε but proliferating cells use mainly NER polymerase POL δ and POL κ. Similarly, LIG1 is preferred by replicating cells for ligation but, XRCC1–LIG3 complex mediates ligation in non-replicative cells since dNTPs and LIG1 are poorly expressed in these cells (Moser et al., 2007).

The second sub-pathway of NER, TC-NER, is activated by a stalled RNA polymerase II when lesions form on actively transcribed genes. TC−NER−specific proteins CSA (Cockayne syndrome WD repeat protein A) and CSB (Cockayne syndrome protein B) are then recruited to the lesion for damage detection. This protein complex also is required for assembly of different TC−NER components such as the key NER factors (different from the GG−NER− specific UV–DDB and XPC complexes) and TC−NER−specific proteins, such as UVSSA (UV−stimulated scaffold protein A), USP7 (ubiquitin specific processing protease 7), XAB2 (XPA−binding protein 2) and HMGN1 (high mobility group nucleosome−binding domain−containing protein 1) (Fousteri et al., 2006; Schwertman et al., 2012) After localization of the CSA-CSB complex to the lesion, it turns back RNA polymerase II by uncovering the lesion. Subsequently, TFIIH recruits to the lesion and causes unwinding of DNA forming a bubble in the length of 30bp

approximately. The order of next steps is presumably shared with GG-NER and the lesion is eliminated from the transcribed strand (Marteijn et al., 2014).

Aberrations in NER pathway leads to a range of human disorders e.g Xeroderma Pigmentosum (XP), Cockayne Syndrome (CS), Oculo-Facio-Skeletal syndrome (COFS) and rare UV-Sensitive Syndrome (UVSS). In similar to BER, NER is also included in the instability processes in trinucleotide repeat diseases (Y. Lin et al., 2006).

1.3.3 Mismatch Repair (MMR)

DNA mismatch repair system is the third and evolutionarily conserved post replicative repair SSB repair pathway that supports replication fidelity (Arana et al., 2010; T. A. Kunkel, 2009). Main substrates of MMR are base mismatches arises from replication and insertions and deletions loops (IDLs) localized in repetitive DNA sequences as a result of recombination events (Friedberg et al., 2005; Jiricny, 2006; G.-M. Li, 2008). Moreover, base changes arising from endogenous and exogenous DNA damaging agents are the target of MMR ((Hewish et al., 2010; Rowe & Glazer, 2010) It has been recently shown that Chromatin modifications facilitate accessing of the MMR proteins to the damaged DNA and initiation of repair (G.-M. Li, 2014; M. Li et al., 2013). Classical MMR pathway follows 4 main phases. The first step is detection of mismatched bases e.g A: G, T: C. Second step include determination of newly formed strand that contain mispaired nucleotide. The third step is for disruption or endo-/exonucleolytic digestion of the newly synthesized strand. Final step consists of the ligation and resynthesis of a misincorporated DNA sequence (Iyer et al., 2006). Parental DNA is used as a template for correction of the base sequence of the nascent DNA (Curtin, 2012; Martin, McCabe, et al., 2010). If

the errors are not corrected until the the end of the S phase, damaged products lead to microsatellite instability or frame-shift mutations shortly after cell division cycles (Guarné & Charbonnier, 2015; Kinsella, 2009)

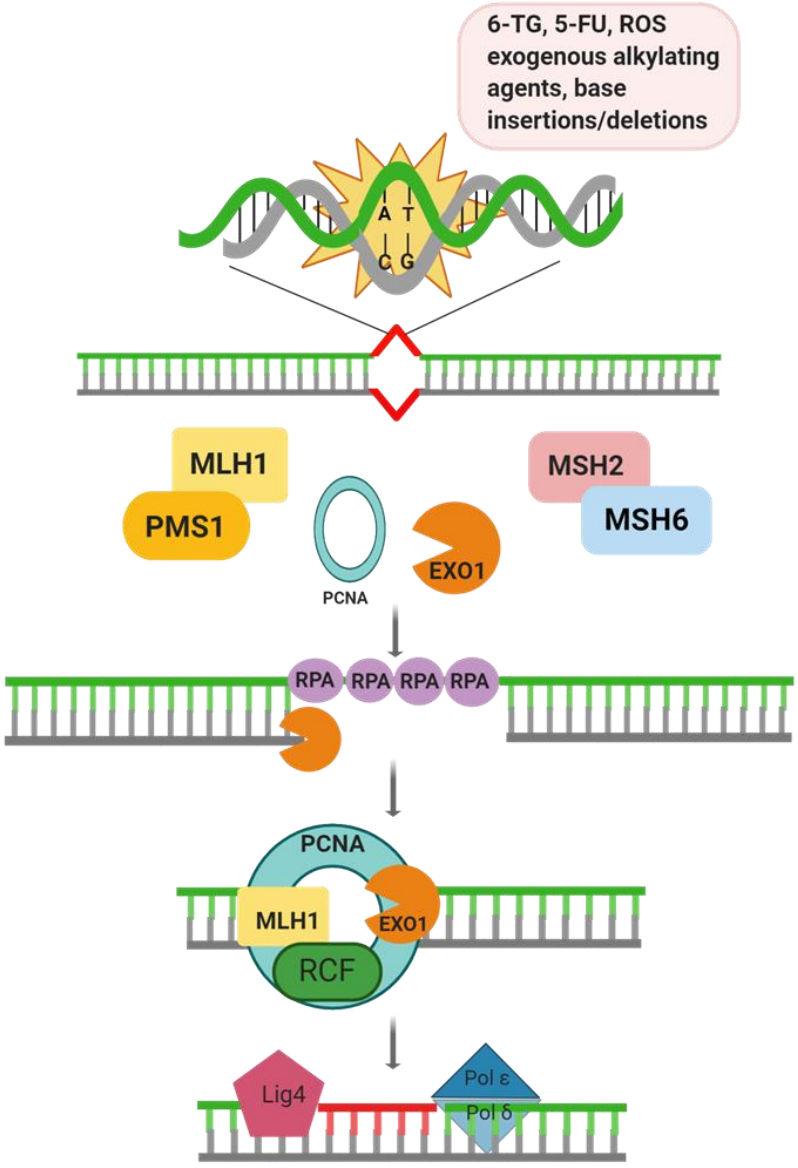

Figure 1.3.3.1: Schematic representation of the MMR pathway.

There are eight well defined MSH (MutS homolog) polypeptides in eukaryotes. In humans, MutSα heterodimer (MSH2/MSH6) functions in recognition of base mismatches and one or two nucleotide IDLs and the MutSβ heterodimer (MSH2/MSH3) takes role in detection of large IDLs up to 10 nucleotides (Thomas A. Kunkel & Erie, 2005; Sachadyn,

2010). Following damage recognition step, another MSH complex involving MutL homolog 1(MLH1) and its adaptors, PMS1 or PMS2 (postmeiotic-segregation increased protein) recruits to the damaged area.

The MSH and MLH complexes act as a sliding clamp and then slide over DNA until it comes across with any single-strand DNA gap (Martin, McCabe, et al., 2010). Afterwards, a replication protein A (RPA) behaves as a flagger and directs a different stabilizing protein (RFC) and PCNA for binding the damaged DNA and so protecting it. Assembly of these protein complexes into damaged areas creates an attractiveness for the incorporation of next complexes.

Once a MutL complex encounters the cluster at the single-strand gap, an error in the daughter strand is confirmed. With the identification of the gap by MutL, DNA exonuclease (Exo1) is recruited to repair the region and remove the damaged site. During the excision period, MLH: MSH complexes stay intact to the region and new DNA is synthesized by Pol δ in the excised region. PCNA stays over onto DNA as well as the MLH: MSH complex until the synthesis of new DNA is completed in which PCNA facilitates the sliding of the complex over the new sequence and so controls the progress. In the final step, Ligase I attach new DNA to the previous daughter strand (Martin, Lord, et al., 2010). Although the damage in the daughter strand is repaired by MMR, errors also might occur in template strands and these errors result in DSBs (Curtin, 2012).

Germline mutations of MMR genes cause Lynch syndrome (HNPCC) carrying familial susceptibility for various cancers (Peltomaki, 2001). Apart from the mismatch repair, MMR genes currently found to be suppressed against environmental stresses including

hypoxia, benzo[a]pyrene, inflammation and even tumor microenvironment (Bindra & Glazer, 2007; X. Chen et al., 2013; Edwards et al., 2009; Mihaylova et al., 2003; Nakamura et al., 2008).

1.3.4 Homologous Recombination Repair (HR)

DNA double strand breaks are extremely toxic damages caused by various chemical and physical damaging agents (Pfeiffer et al., 2000) and unrepaired DSBs are associated with many human diseases and cancers (Jackson & Bartek, 2009). Depending on the damage source, type of the damage and repair mechanism differs. DSBs are also formed naturally during physiological events: V(D)J recombination or meiosis in which DSBs occur in a particular site of the genome by well-defined processes (Schatz & Swanson, 2011; Stavnezer, 2008). In addition, studies show that DSBs occur as a result of intrinsic processes such as stalled or collapsed replication forks and also, extrinsic factors such as IR and chemotherapeutic agents (Schipler & Iliakis, 2013). Two main pathways have evolved to resolve DSBs in the organisms: homologous recombination (HR) and non-homologous end joining (NHEJ). As in SSBs, chromatin remodeling is the first event in the recording a DSB and is the initiating factor for the activation of a cascade involving ATM activation, addressed phosphorylation of H2AX, chromatin PARylation, MDC1 recruitment and lastly 53BP1 and BRCA1 recruitment (Rogakou et al., 1998; Rothkamm et al., 2003).

Homologous recombination repair (HRR) is one of the DSBs repair mechanisms which is highly conserved and well-defined (Xinjian Lin & Howell, 2006). HR includes many related sub-pathways that employ template-directed DNA repair and DNA strand

invasion in order to serve high-fidelity repair (X. Li & Heyer, 2008). HR pathway has two following processes, synthesis-dependent strand annealing (SDSA) and break-induced repair (BIR) different from classical DSBR-induced HR pathway (X. Li & Heyer, 2008). When it is compared with SSB-associated mechanisms, HR offers higher fidelity due to the accessibility of identical DNA copy. With the recognition and binding of The MRN (MRE11-RAD50-NBS1) complex to a DSB, HR is initiated and then ATM and TIP60 are directed to the DBS site (Stracker & Petrini, 2011; Sun et al., 2005). Upon activation of the ATM, H2AX phosphorylation occurs and then acts as an anchor for MDC1 (Bhatti et al., 2011). ATM further phosphorylates MDC1 and phosphorylated MDC1 serve as a platform for arrival of the ubiquitin E3 ligases RNF8 and RNF168 to the site (Altmeyer & Lukas, 2013). H2AX is then ubiquitinated by these E3 ligases and ubiquitinated H2AX functions as an anchoring site for binding of 53BP1 and BRCA1. Because HR is the primary pathway in the S/G2 phase, BRCA1 (recruited by ubiquitinated chromatin) has an advantage over 53BP1 and so, it starts the ubiquitination of the downstream CtIP (Chapman et al., 2012). Afterwards, other downstream factors, RecA, and RAD51 perform their function on the DNA.

Following the damage recognition and DSB processing, the next step of end resection consists of production of 3′ overhangs by a 5′-to-3′ nucleolytic degradation which moves forward the repair to the HR pathway. This process is highly orchestrated by multiprotein complexes which harbors helicase and nuclease activity. Accordingly, first resection performed by the endonuclease activity of MRN together with CtIP and then long-range resection is conducted by EXO1 or BLM with the help of DNA2 (L. Chen et al., 2008; Nimonkar et al., 2011). The initial step that RecA coats the 3′ overhangs is called pre-synapsis. During pre-synapsis, RecA/Rad51 protein monomers generate a helical

nucleoprotein filament by polymerizing onto ssDNA for the purpose of homology search. Following homology search, homologous and non-homologous connections are maintained until a homologous pairing between the RecA-ssDNA segment and dsDNA are found. Once the homologous pairing is established, strand exchange occurs and a joint molecule, D-loop is created. D-loop structure functions as a precursor for activation of subsequent pathways of HR and so, formation and resolution of D-loop are highly regulated with the help of mediator proteins (Heyer, 2015; Kanaar et al., 2008). Stability of the D-loop determines which HR sub-pathways go into action. If the nascent DNA synthesis stops after a particular distance during synthesis-dependent strand annealing (SDSA), the D-loop structure is dissolved and acts as an anti-crossover mechanism (Tham et al., 2016).

Branch migration occurs between the template and invading strand during the double strand break repair (DSBR) sub-pathway and so enlarges the heteroduplex region. Therefore, capture of the second 3'end and formation of a secondary D-loop is provided. Upon the ligation of these 3'ends by DNA ligase, recombination by-products are generated. Double holliday junction is one of the by-products and resolution of it by site-specific endonucleases creates crossover (CO) or non-crossover products depending on the cleavage position. During the SDSA process, the extended initial D-loop is dissolved rather than catching the second 3'end. Hence, strands between 3'ends of damaged DNA are annealed and missing information is restored by DNA synthesis. Crossover does not occur during this process. On the contrary, in the break-induced repair pathway (BIR), a second DNA molecule is utilized to copy missing information for an enlarged region; however, a second 3'end is not used at all (Tham et al., 2016).

1.3.5 Non-homologous end joining

Non-homologous end joining is an error-prone DNA repair system by which DNA DSBs are repaired imprecisely to maintain chromosomal integrity (Takata et al., 1998). 53BP1 plays a key regulatory role during the NHEJ pathway, recruits the NHEJ factors to the DSB site, induce checkpoint signaling and aids synapsis of the two ends (Panier & Boulton, 2014). Ku70, Ku80 a DNA-dependent protein kinase catalytic subunit (DNA-PKcs), XRCC4, DNA ligase IV, Artemis and XLF are the major components of NHEJ repair pathway (Lieber et al., 2010). The Ku (Ku70 and Ku80) heterodimer initiates NHEJ repair by sensing DSBs and binding to them. Binding of Ku heterodimer to DSBs occurs within the seconds to block end resection and facilitate recruitment of subsequent NHEJ factors by acting as a scaffold (P.-O. Mari et al., 2006; Mimitou & Symington, 2010; Pang et al., 1997; Evi Soutoglou et al., 2007). Current studies reported that the order of recruited components varies depending on the complexity of DNA damage. However, DNA-PKcs mainly binds to the Ku proteins after damage sensing and pushes Ku inwardly on the DNA to phosphorylate other close components involving auto auto phosphorylation itself (Gottlieb & Jackson, 1993; Weterings & Chen, 2008; Yoo et al., 1999) Ku proteins are subjected to an essential conformational change to make a stable complex with DNA-PKcs (Yaneva et al., 1997). XRCC4 is also assumed that contributes to the stabilization of NHEJ complex by binding to the ends and serving as a further platform together with Ku for recruitment of downstream components (Andres et al., 2012; Hammel et al., 2011; Malivert et al., 2010). DNA end processing is initiated by a series of proteins including Artemis, PNKP, APLF, WRN upon end bridging and stabilization. In the end processing events, groups blocking the ends are excised and the resulting naked strands are subjected to resection (Ahel et al., 2006; Bernstein et al., 2005;

Z. Li et al., 2011; Ma & Lieber, 2002; Perry et al., 2006; Roberts et al., 2010). The resultant gaps after end resection are fulfilled by family X polymerases depending on a template (POL μ) or independent from a template (POL λ)(Ramadan et al., 2004; Roberts et al., 2010). Finally, the ends are ligated by LIG4 and so, the NHEJ process is accomplished (Grawunder, 1997).

1.4 AUTOPHAGY

Every cell has a fate; death, but, for cytoplasmic organelles the fate is autophagy (Levine & Kroemer, 2008; Noboru Mizushima et al., 2008). Autophagy is a major conserved, intracellular degradation system which directs elimination of macromolecules in cytoplasm to provide sustainability for cell metabolism, to protect genomic stability and to support survival of cells (Antonioli et al., 2017; Deng et al., 2017; L.-T. Lin et al., 2010). While the destruction of damaging substances and continuation of healthful molecules are achieved by a natural regulatory role of autophagy in the body, removal of aggregated or wrongly folded proteins, elimination of injured organelles, proteins (Shah et al., 2018; Zhen Yang et al., 2015), carcinogenic molecules (Yun & Lee, 2018), and the eradication of external pathogens like viruses through lysosomal degradation are achieved by housekeeping role of autophagy (H. J. Kim et al., 2010; Levine & Kroemer, 2008; Sharma et al., 2018). Although there are various physiological roles of autophagy in the cell like removal of internal wastes and external substances to retain homeostasis, disturbing of the balance can give rise pathological consequences (Zhu et al., 2007). Normally, the primary role of autophagy is cleaning the body, it can exert this function via killing carcinogenic cells or degrading endogenous and exogenous cancerous agents, nonetheless, in cancer autophagy can act vice versa. In the resistance of stem cells to

radiotherapy and chemotherapy, metastasis and tumor recurrence autophagy maintains survival of the cell (Lei et al., 2017).

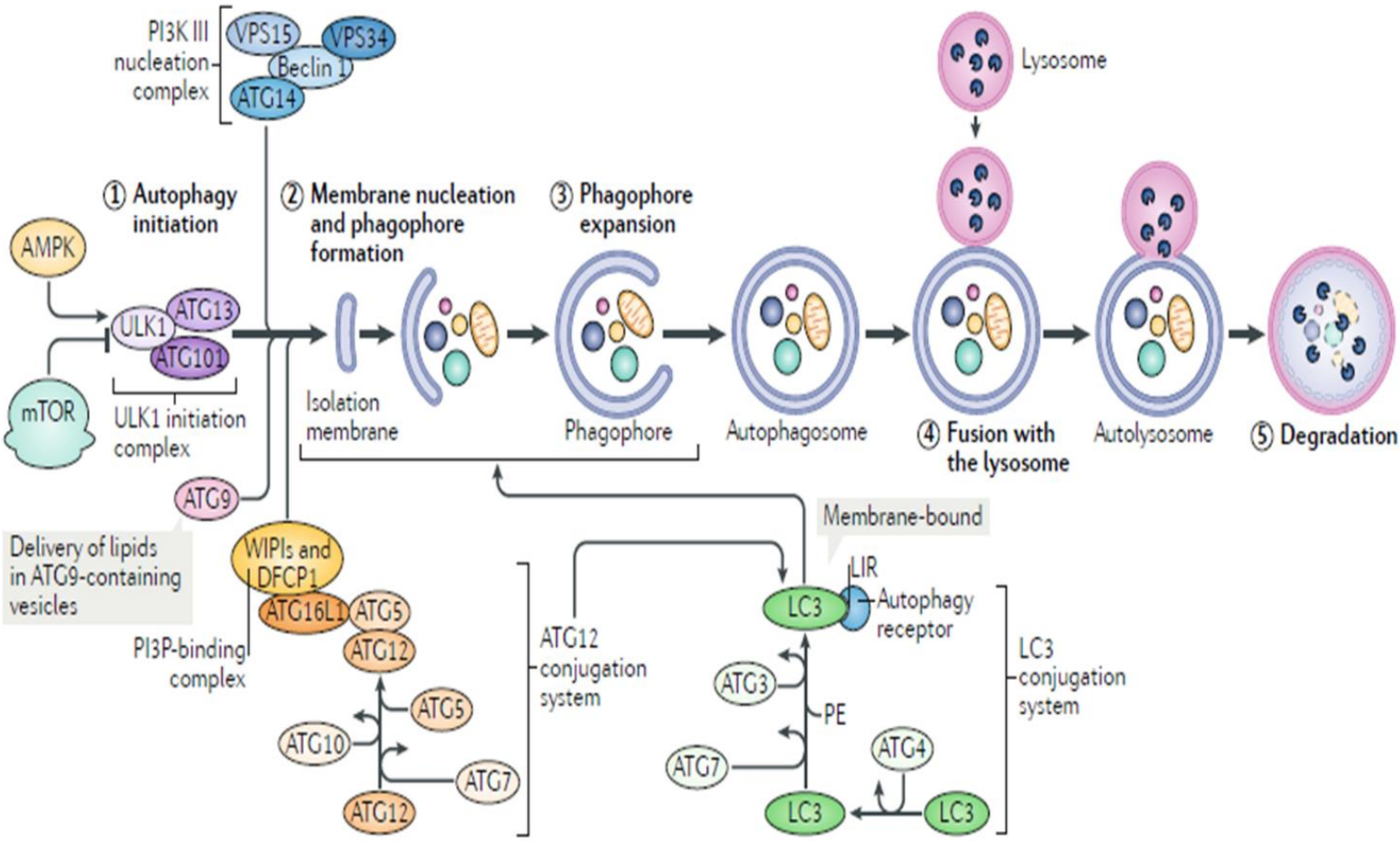

Figure 1.4.1: Schemtaic representation of autophagy pathway.

There are three distinct types of autophagy which have functioned in eukaryotic cells: macroautophagy, chaperon-mediated autophagy (CMA) and microautophagy(Orenstein & Cuervo, 2010). Although these three different autophagy processes differ from each other morphologically, lysosomal cargo degradation and recycling steps are shared among them (Yang & Klionsky, 2010). Macroautophagy (it will be referred to as shortly autophagy from here on) is a well-known and best characterized type of autophagy.

Macroautophagy is active at a basal level in the cells but it can be further stimulated by stressful conditions such as nutrient or energy deprivation to provide metabolites required for biosynthetic reactions and energy production (Yorimitsu & Klionsky, 2005). Macroautophagy is also known as a cytoprotective mechanism because of its role in cellular maintenance. Damaged organelles are eliminated by macroautophagy under basal conditions to ensure cellular homeostasis but excessive autophagy activation also can be lethal for the cell (Wirawan et al., 2012)

In macroautophagy, autophagic cargo is sequestered from the lysosome by double-membrane vesicles called autophagosome and then, cargo molecules are subsequently transferred to the lysosome (Yorimitsu & Klionsky, 2005) distinctly from Microautophagy and CMA pathway. Macroautophagy process is characterized by the formation of a double membrane structure which is known as autophagosome. Macro autophagy pathway composed of several ordered steps including: 1) Induction, 2) nucleation and phagophore formation, 3) phagophore expansion, 4) cargo selection and packaging, 5) Fusion with the lysosome, 6) degradation of autophagic cargo (Devenish et al., 2011).

Chaperon-mediated autophagy (CMA) is a second type of autophagy which is found only in mammalian cells. In contrast to non-selective autophagy pathways; macroautophagy and microautophagy, CMA is a highly selective process wherein all substrate molecules are chosen depending on a pentapeptide motif (KFERQ) that is harbored in the cargo molecules (Dice, 1990). In CMA pathway, cochaperones and the heat shock 70 kDa protein 8 (HSPA8/HSC70) detects the KFERQ consensus motif (Chiang et al., 1989). Then, substrate molecules were transferred directly across the lysosomal membrane by HSPA8. (Agarraberes & Dice, 2001). After the substrate molecule translocates into

lysosomal membrane where it binds to monomer of lysosomal-associated membrane protein 2A (LAMP2A) which is a CMA receptor for substrate molecules. Upon this binding, LAMP2A becomes multimerized and forms a translocation complex. With the help of a translocation complex and HSP90, the substrate is translocated into the lumenal side of lysosome (Cuervo & Dice, 1996).The translocation complex is then dissociated by cytosolic HSPA8. Therefore, multimerized LAMP2A disassembles and turns to its monomeric form which can bind new substrate molecules to start new translocation events (Parzych & Klionsky, 2014)

Microautophagy is a less understood type of autophagy in terms of mechanism and regulation of it. Similar to macroautophagy, microautophagy is a nonselective process where a part of cytoplasmic constituents is transported to the lysosome therefore, specific degradation of individual molecules cannot be achieved (Boya et al., 2013; Kaushik & Cuervo, 2012).

1.4.1 Mechanism of autophagy

Autophagic process is stimulated in the cell by numerous signaling pathways including shortage of nutrient (starvation) (Joy et al., 2018; Su et al., 2015), hypoxic conditions (Zhao Yang et al., 2015; Zhen Yang et al., 2015), oxidative stress (S.-J. Li et al., 2016; Tang et al., 2015), infection of the cell by pathogenic organisms (Ahmad et al., 2018; Fu et al., 2014), ER stress (Lee et al., 2015), proton concentration, metabolic perturbations (Shakeri et al., 2019). If there are enough nutrients and cytokines, mammalian target of rapamycin (mTOR) can direct cells to grow and act against to apoptosis (Kamada et al., 2010), but, in the absence of nutrient, starvation and stress direct inhibition of mTOR to trigger autophagy by different protein complexes: the unc-51-like kinase (ULK) including ULK-1, Atg13, Atg101, and FIP200 (FAK-family interacting protein); the

Phosphoinositide-3 kinase (PI3K) complex including Atg15; vacuolar protein sorting (VPS)15, VPS34, Beclin 1, and Beclin 1-regulated autophagy protein (AMBRA1) (Hara & Mizushima, 2009; M. G. Lin & Hurley, 2016); Atg9 and WIPI transmembrane protein complexes and ubiquitin-like systems (Atg12 and LC3) (Mercer et al., 2018; Noboru Mizushima & Komatsu, 2011).

ULK complex association firstly initiates the autophagic process by phosphorylating AMBRA1 and so, inducing PI3K complex (Mercer et al., 2018; Yu et al., 2010). Nucleation of autophagic membranes is accomplished by PI3K having a role also in tracking different membranes and Beclin1 proteins. Another important molecular event is maintained by recruitment of first ubiquitin like the Atg5-Atg12-Atg16 complex to pre-autophagosomal structure (PAS). Interaction of the complex with the outer membrane of phagophore blocks early premature formation of autolysosomes (Kaur & Debnath, 2015).

The other ubiquitin-like system exerts its function via triggering binding of microtubule-associated protein 1 light chain 3 (LC3) to phosphatidylethanolamine (PE) and so, lipidation of LC3. Because of the high affinity of LC3 for the lysosome in case of binding of it to the phagosome, captured pathogenic organisms can be destroyed or degradation of any pathogenic substance occurs at higher rate (Herb et al., 2020). Maturation of autophagosomes requires processing of LC3 into LC3-II by Atg4, Atg7 and Atg3. Conversion of LC3 to lipidated LC3-II is an indicator of autophagosome (Glick et al., 2010) and it localizes in either inner and outer surface of the autophagosome that is a requirement for the enlargement and closure of the autophagic membrane. Right after the completion of autophagosomal membrane second ubiquitin like Atg5-Atg12-Atg16 complex leaves from autophagosome. In the following step, Atg9 protein takes the role

for creating intraluminal vesicles and acidification of autolysosomes (Bader et al., 2015). Another important function of Atg9 protein is to enlarge the phagophore membrane during autophagosome formation by translocating to the autophagosome formation site (M. Mari et al., 2010). At the later period, autophagosome-lysosome fusion occurs to form autolysosomes under the control of lysosomal membrane proteins and cytoskeletal proteins (N. Mizushima, 2007). One of them is the LAMP-1/2 protein which regulates autophagosomal maturation and defects in the protein cause serious diseases (Maron, 2009). Inside the autolysosome, many digestive enzymes like hydrolytic enzymes break down the engulfed autophagic cargo and also internal autophagosome membrane. With the completion of the autophagic process, many building blocks like amino acids have been recycled after release to cytosol. Therefore, there is a close contact between autophagy and cell trafficking pathways (Holland et al., 2016).

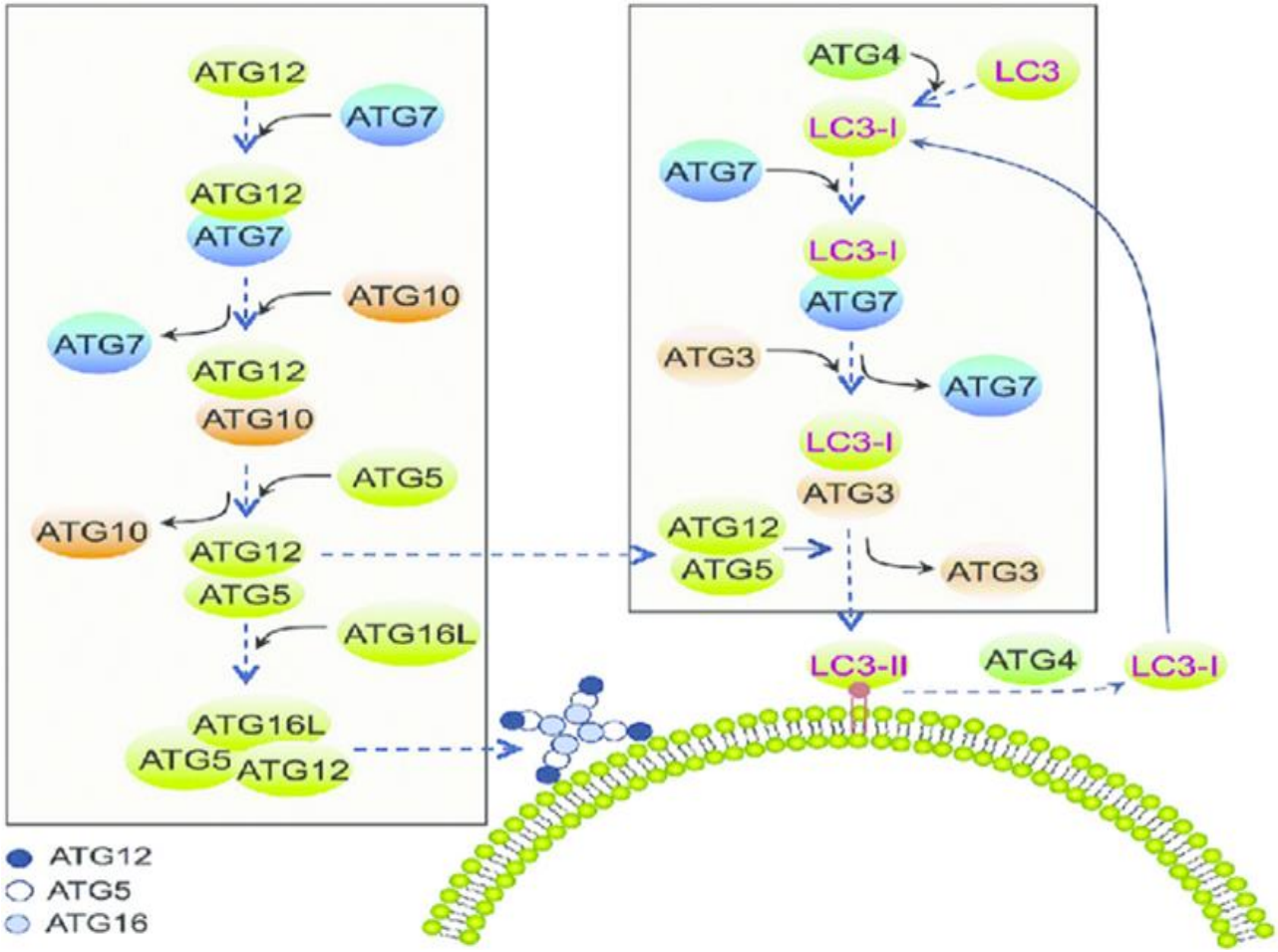

Figure 1.4.1.1 : Schematic representation of ATG5-ATG12-ATG16 conjugation system, (EMBO Reports: Vol 9, No 8, n.d.).

1.5 Crosstalk between Autophagy and DSB repair

Information about the crosstalk between autophagy and genome maintenance was recently enlarged with the data suggesting a more direct function of autophagy in DNA damage repair. The first of this research marked that valproic acid (VPA) caused histone deacetylases (HDACs) inhibition induce autophagy and elevated the degradation of the DNA endonuclease Sae2 by autophagy in yeast cells (Robert et al., 2011). Further on, these cells showed decreased levels of end-resection and cell survival against genotoxic stress. Additionally, it is noted that rapamycin induced autophagy activation also

decreases Sae2 levels underlining a potentially novel mechanism between DNA repair and autophagy in which Sae2 is acetylated and then degraded by autophagy. Different studies also noted that DSB might be repressed by rapamycin treatment (H. Chen et al., 2011). There is different data suggesting negative relation between autophagy and DNA damage repair but, there is also controversial data implying parallel interaction between these pathways. In some cases, autophagy inhibition causes decreased DNA damage repair but in other cases autophagy activation can lead to attenuated DNA damage repair (Bae & Guan, 2011; Hewitt et al., 2016; W. Lin et al., 2015; E. Y. Liu et al., 2015; Pollard & Curtin, 2018) As an example of positive interaction between autophagy and DNA repair, lack of autophagy in Atg7 knockout cells causes defective HR repair of DSB. And this deficiency in HR is associated with increased proteasome activity that also increases the autophagic elimination of the HR mediator checkpoint kinase 1 (CHK1) (E. Y. Liu et al., 2015). There is a compensatory mechanism between HR and another DSB repair system, NHEJ in case of impairment of one of them. Hence, HR defective Atg7 knockout cells are hyper-dependent to NHEJ for DSB repair and blockage of NHEJ in these cells results in rapid cell death. This type of relation between autophagy and HR or NHEJ is accepted as a synthetic lethal relationship and offers an exciting therapeutic way to eliminate autophagy-deficient cells that are a typical feature of age-related diseases in humans (Jiang & Mizushima, 2014)

Moreover, autophagy inhibition caused by lack of 200-kDa FAK-family-interacting protein (FIP200) which is a ULK1-interacting protein required for formation of autophagosome repressed the DNA repair and reduced cell viability after ionizing radiation and camptothecin treatment. It is also pointed out that knock-down of p62

diminishes the repair error and enhances cell survival (Bae & Guan, 2011). The further data indicated that inhibition of autophagy leads to p62 accumulation and so, increased p62 levels might have a key role in reducing DNA damage repair.

Accordingly, the study observing the nuclear–cytoplasmic shuttling of p62 suggests a relation between the cytoplasmic autophagy processes and the nucleus (Pankiv et al., 2010). Accumulated p62 caused by autophagic inhibition attenuates the damage stimulated chromatin ubiquitination. It is proposed that this phenotype is the result of the interaction between the LIM-binding (LB) domain of p62 and the MU1 domain of RNF168. As a result of this interaction, the E3 ligase function of RNF168 is inhibited and it leads to defective chromatin ubiquitination and impaired recruitment of the repair proteins after DNA damage. Autophagy inhibition also particularly suppresses DSB repair by HR but not by NHEJ via decreasing the recruitment of RAD51, RAP80, and BRCA1 proteins of the HR pathway (E. Y. Liu et al., 2015; Y. Wang et al., 2016). During this process CHK1 levels do not change in contrast to previous findings (E. Y. Liu et al., 2015) Because RNF168 takes place in the upstream region of HR and NHEJ, p62 related attenuation of chromatin ubiquitination results in disruption of both repair systems. In another model for autophagy related modulation of DNA repair, p62 inhibits DSB repair by HR via degradation of filamin A (FLNA in proteasome and RAD51 in the nucleus (Hewitt et al., 2016). FLNA takes a role in the HR pathway basically interacting with BRCA1/2 and recruiting RAD51 65-67.

Deficiency in HRR protein, BRCA2 which functions in loading of RAD51 monomers onto ssDNA sensitize cells against cisplatin and together with autophagy inhibition effect of cisplatin increase (Katsuki & Takata, 2016; Rytelewski et al., 2014; Sakai et al., 2008; Wan et al., 2018). In parallel, autophagy protein Beclin1 expression elevates in BRCA1

positive tumors and deletion of Beclin1 and BRCA1 genes are linked with breast and ovarian cancer development (Laddha et al., 2014; H. Li et al., 2010). Also, most of the autophagy-associated signaling molecules containing Akt or extracellular regulated protein kinases 1/2 (ERK1/2) cause the alteration in expression level of RAD51 which is a component of HR and adversely affect autophagy (Golding et al., 2009; K.-H. Kim et al., 2016; Ko et al., 2016). Moreover, decreased level of RAD51 is related with increased radiosensitivity following autophagy inhibition (Mo et al., 2014).

Micronuclei are extranuclear bodies which arises from damaged chromosomes, or the chromosomes are not integrated into the nucleus. Unrepaired DSBs basically give rise to micronuclei as a result of defective DSBs repair systems. Increased micronuclei formation depending on the impairment of the cell cycle is also shown to be a target for autophagic machinery and these micronuclei are also positive for the DNA damage marker γH2AX. Upon autophagy activation, micronuclei are enveloped by autophagy protein, LC3 and exposed to the degradation (Rello-Varona et al., 2012; Sagona et al., 2014). In this manner, autophagic removal of micronuclei might be considered to refer to the role of autophagy in genome maintenance and inhibition of autophagy leads to genomic instability due to increased γH2AX positive micronuclei. Sunitinib, is a multi-targeted receptor tyrosine kinase (RTK) inhibitor, also give rise to micronuclei and elevates autophagic degradation in renal cancer cells. Elimination of Sunitinib induced micronuclei requires DNA damage-associated proteins RAD51 and PARP1 activity. Besides, defects in these two proteins impairs sunitinib-induced autophagy and cause even basal nuclei (Yan et al., 2017). Another example for the role of autophagy in genomic stability is related to increased proteasomal degradation of checkpoint kinase 1

(CHK1) which causes perturbation of the HR pathway and hyperdependency on nonhomologous end joining (NHEJ).

Similar to HRR, autophagy is also associated with NHEJ in the repair of DBSs. NHEJ protein, 53BP1 increase due to the knock down of autophagy proteins Beclin1, UVRAG, and ATG5 but, HRR protein, RAD51 does not change upon radiation exposure (J. M. Park et al., 2014). Another NHEJ protein Ku70/XRCC6 increases the activity and expression of DNA-dependent repair kinase complex ATM-PRKDC (DNA-PKcs) together with PARP1 and TP53, by the way autophagy and apoptosis are regulated in hepatocytes (Z. Wang et al., 2013). Normally autophagy exhibits a pro-survival role upon IR exposure in hematopoietic stem cells (HSCs). Impairment of autophagy processes in HSCs was related with the absence or the lack of critical HRR and NHEJ proteins with the IR exposure, controversial to its cellular clearance role. In this manner, autophagy acts as a negative regulator of DNA damage inhibitory proteins by degrading them or preventing deprivation of them by causing the inhibition of their proteasomal degradation. For instance, XRCC4 and Ku80 levels increase with the inhibition of mTOR and decrease with the autophagy impairment underlining clearance role of autophagy is tightly related with IR-induced repair in HSCs (Xiang Lin et al., 2015). Chaperon-mediated autophagy (CMA) which is the special form of macroautophagy is also involved in DDR. In case of autophagic inhibition, CMA activity increases and degrades important DDR proteins, CHK1 (C. Park et al., 2015).

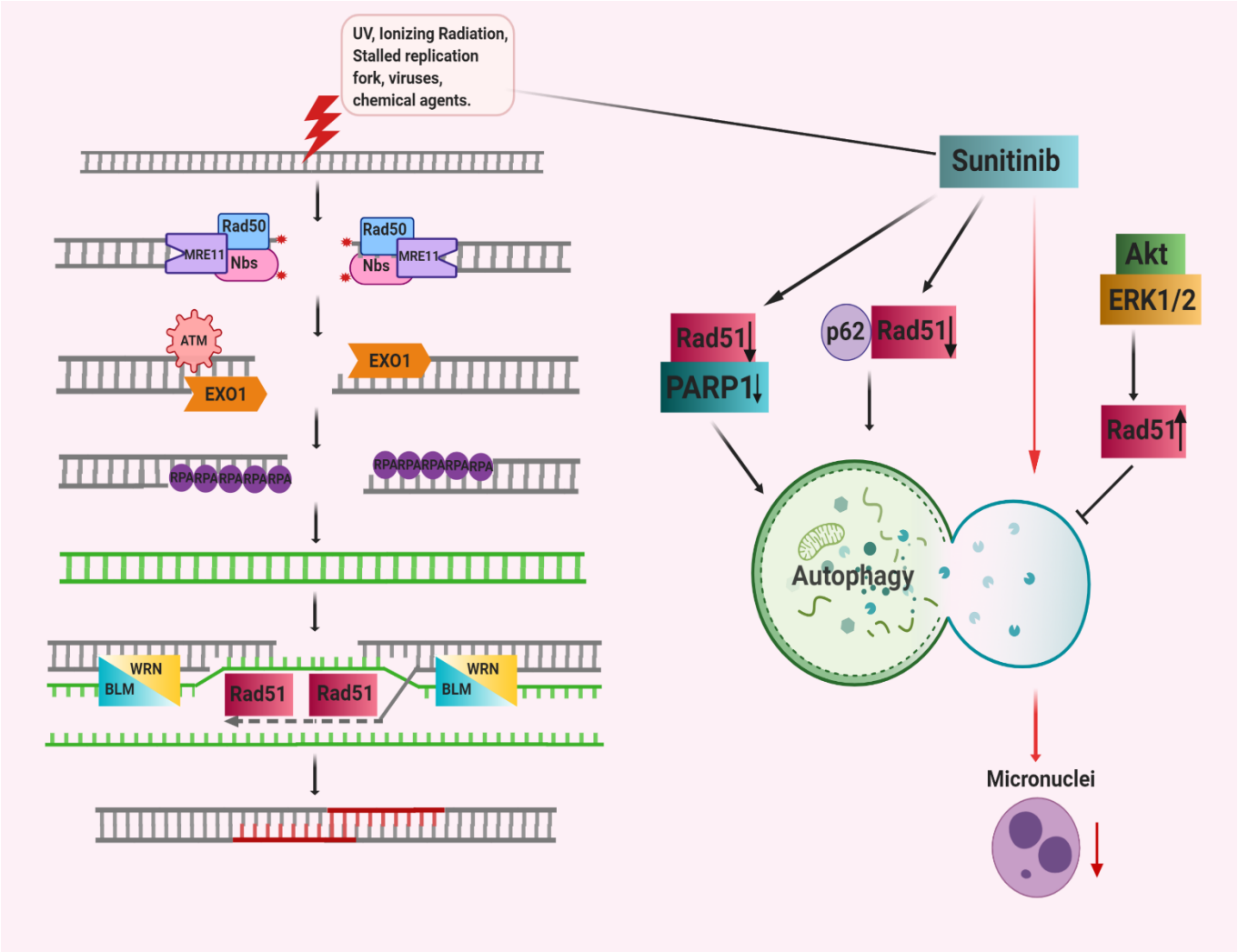

Figure 1.5.1: Schematic representation of the HR pathway and its crosstalk with the autophagy process.

Deficiency in HRR protein, BRCA2 which functions in loading of RAD51 monomers onto ssDNA sensitize cells against cisplatin and together with autophagy inhibition effect of cisplatin increase (Sakai et al., 2008; Rytelewski et al., 2014; Katsuki and Takata, 2016, Wan et al, 2018). In parallel, autophagy protein Beclin1 expression elevates in BRCA1 positive tumors and deletion of Beclin1 and BRCA1 genes are linked with the breast and ovarian cancer development (H. Li et al., 2010, Laddha et al., 2014). Also, most of the

autophagy-associated signaling molecules containing Akt or extracellular regulated protein kinases 1/2 (ERK1/2) cause the alteration in expression level of RAD51 which is a component of HR and adversely affect autophagy (Ko et al., 2016; Golding et al., 2009; Kim et al., 2016). Moreover, decreased level of RAD51 is related with increased radiosensitivity following autophagy inhibition (Mo et al., 2014).

Micronuclei are extranuclear bodies which arises from damaged chromosomes, or the chromosomes does not been integrated into the nucleus. Unrepaired DSBs basically give rise to micronuclei because of defective DSBs repair systems. Increased micronuclei formation depending on the impairment of the cell cycle is also shown to be a target for autophagic machinery and these micronuclei are also positive for the DNA damage marker γH2AX. Upon autophagy activation, micronuclei are enveloped by autophagy protein, LC3 and exposed to the degradation (Rello-Varona et al., 2012; Sagona et al., 2014). In this manner, autophagic removal of micronuclei might be considered to refer to the role of autophagy in genome maintenance and inhibition of autophagy leads to genomic instability due to increased γH2AX positive micronuclei. Sunitinib, is a multi-targeted receptor tyrosine kinase (RTK) inhibitor, also give rise to micronuclei and elevates autophagic degradation in renal cancer cells. Elimination of Sunitinib induced micronuclei requires DNA damage-associated proteins RAD51 and PARP1 activity. Besides, defects in these two proteins impairs sunitinib-induced autophagy and cause even basal nuclei (Yan et al., 2017). Another example for the role of autophagy in genomic stability is related to increased proteasomal degradation of checkpoint kinase 1 (CHK1) which causes perturbation of the HR pathway and hyperdependency on nonhomologous end joining (NHEJ).

Similar to HRR, autophagy also associated with NHEJ in the repair of DBSs. NHEJ protein, 53BP1 increase due to the knock down of autophagy proteins Beclin1, UVRAG, and ATG5 but, HRR protein, RAD51 does not change upon radiation exposure (Park et al., 2014). Another NHEJ protein Ku70/XRCC6 increases the activity and expression of DNA-dependent repair kinase complex ATM-PRKDC (DNA-PKcs) together with PARP1 and TP53, by the way autophagy and apoptosis are regulated in hepatocytes (Ziyan Wang et al., 2013). Normally autophagy exhibits a pro-survival role upon IR exposure in hematopoietic stem cells (HSCs). Impairment of autophagy process in HSCs was related with the absence or the lack of critical HRR and NHEJ proteins with the IR exposure, controversial to its cellular clearance role. In this manner, autophagy act as a negative regulator of DNA damage inhibitory proteins by degrading them or prevent deprivation of them by causing the inhibition of their proteasomal degradation. For instance, XRCC4 and Ku80 levels increase with the inhibition of mTOR and decrease with the autophagy impairment underlining clearance role of autophagy is tightly related with IR-induced repair in HSCs (Xiang Lin et al., 2015). Chaperon-mediated autophagy (CMA) which is the special form of macroautophagy is also involved in DDR. In case of autophagic inhibition, CMA activity increase and degrades important DDR proteins, CHK1 (Park et al., 2015).

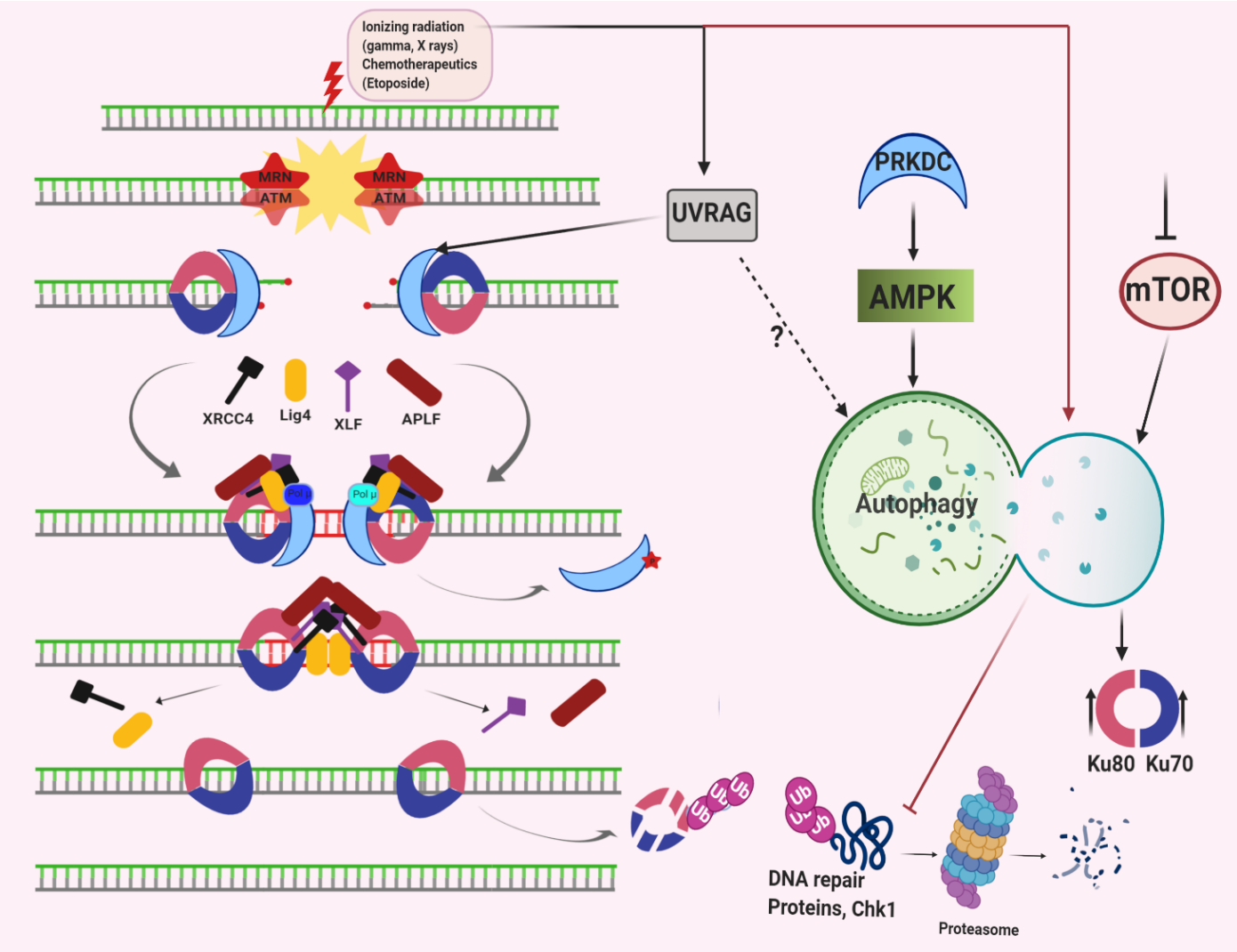

Figure 1.5.2: Schematic representation of the NHEJ pathway and its crosstalk with the autophagic process.

2. MATERIALS AND METHODS

2.1 PLASMIDS, CONSTRUCTS and SIRNAs

Myc-ddk-tagged human ATG5 (RC235557) plasmid was purchased from ORIGENE. Flag-GFP tagged human Ku70 (#46957), Ku80 (#46958) plasmids were obtained from Addgene. pEGFP-tagged LC3, and human ATG5 plasmids were kindly gift from Noboru Mizushima, pmCherry-tagged ATG5 plasmid kindly gift from Jae-Won Soh. The flag tagged 1-79, 80-192 and 193-275 inserts were generated by PCR directed cloning by adding particular restriction enzyme recognition sites to the primers and using Myc-ddk-tagged human ATG5 (RC235557) as a template. Primers that are used for the production of inserts were listed below. PCR amplified 1-79 inserts were expose to restriction enzyme cutting with HindIII and SalI. 1-79, 80-192 and 193-275 cDNA inserts were then cloned into pCMV-3Tag-6 vector that were cut with determined restriction enzymes.

The primers that were used for creation of ATG5 fragments:

For 1-79 fragment:	Fwd 5' ataaagcttgtcatgacgactgaacctttc 3'
	Rev 5' atagtcgactcaatctgttggctgtgg 3'
For 80-192 fragment:	Fwd 5' ataggatccagctacgaccgcgccatc 3'
	Rev 5' atactcgagtcactccaggaactcgcg 3'

For 193-275 fragment: Fwd 5' ataggatccagctacgaccgcgccatc 3'

Rev 5' atactcgagtcactccaggaactcgcg 3'

HindIII: AAGCTT

SalI: GTCGAC

2.2 CELL CULTURE

2.2.1 Cell Line Maintenance

HeLa cervix cancer cells, HEK293T human embryonic kidney cells and MCF-7 breast cancer cells were maintained in Dulbecco's modified Eagle's medium (DMEM; Biological Industries, BI01-050-1A) supplemented with 10% (v:v) fetal bovine serum (PAN, P30 3302), antibiotics (penicillin/streptomycin; Biological Industries, BI03-031-1B) and L-glutamine (Biological Industries, BI03-020-1B) in a 5% CO_2 humidified incubator at 37°C. ATG5 Crispr KO and ATG5 WT HeLa cell lines were cultured in DMEM additionally supplemented with 10µg/ml Puromycin (P9620, Sigma).

2.2.2 Cell Transfections

Transient transfection of HeLa and HEK293T cells were performed by using the standard calcium phosphate transfection protocol (Jordan, 1996).

2.2.3 DNA Damage Induction in Cell Culture

For induction of DNA damage, HEK293T cells were incubated in culture media containing Doxorubicin (1μM), Etoposide (50 μM, Sigma, E1383) and Cisplatin (30 μg/ml) that were dissolved in DMSO (Sigma, catalog no. VWRSAD2650) for 24h. For induction of DNA damage, HeLa and ATG5KO/WT HeLa cells were incubated in culture media containing Doxorubicin (100nM) and Etoposide (25 μM, Sigma, E1383) for 24h. After 24 h drug treatment cells were collected and exposed to further analysis steps.

2.2.4 DNA Damage Repair Induction (Recovery Experiment)

For recovery or DNA damage repair induction in HEK293T cells were incubated in culture media containing Etoposide (50 μM, Sigma, E1383) for 1h. For recovery or DNA damage repair induction, HeLa and ATG5KO/WT HeLa cells were incubated in culture media containing Etoposide (25 μM, Sigma, E1383) for 1h. After treatments, drug containing media were aspirated and cells were washed with PBS for two or three times and culture media was replenished. Cells were incubated in drug free media for different repair periods 0h, 3h, 6h ,24 h and 48. Following repair period cells were collected and exposed to further analysis steps.

2.2.5 Autophagy Induction in Cell Culture

For autophagy induction, cells were exposed to starvation within Earle's Balanced Salt solution (Biological Industries, BI02-010-1A) for 4 h, or exposed to torin1 (250 nM; Tocris, 4247) containing culture media for 3h. To observe autophagy inhibition in the cells, cells were treated with lysosomal protease inhibitors E64D (10μg/ml; Santa Cruz

Biotechnology, SC201280A) and pepstatin A (10μg/ml; Sigma, P5318) including culture media for 4 h. Then cells were collected, and further analysis were performed.

2.3 CELL FRACTINATION

Cell fractionation experiments were performed according to the previously reported protocol (Herrmann et al. 2017). For each condition, 4×10^7 HeLa cells (plated in two 15mm cell culture dishes as ~100% confluent) were harvested with ice-cold PBS and collected into the 15ml tube after treatment periods. Cell pellets were resuspended in hypotonic buffer (10 mM HEPES pH 7.9, 1.5 mM MgCl2, 10 mM KCl, 0.1 mM PMSF 0.5 mM DTT) and transferred into 2 ml Eppendorf tubes using P1000 pipette with the tip cut to prevent disruption of the cellular membranes. 25μl of the cell suspension were set aside in a new tube and labeled as 'cell fraction'. Remaining cell suspension was incubated on ice for 30 min. At this period, Dounce homogenizer and the pestle were pre-cooled on ice for 5 min at least. Then, the cell suspension was transferred to cold Dounce homogenizer using a transfer pipette and the cell membranes were disrupted by using 40 strokes of the tight-fitting pestle (paying attention to the formation of bubbles). Afterwards, the suspension was transferred to a new 2 ml tube and centrifuged for 5 min, at 1,500 × g, 4 °C. The supernatant was collected in another tube and labelled as 'cytosolic fraction'. And the pellet containing nuclei were labelled as 'nuclear fraction'.

2.4 PROTEIN ISOLATION

Protein isolations were performed following the transfection and treatment period of cells. Cells were then harvested with ice-cold PBS and collected into the Eppendorf or falcon

tubes on ice. Collected cells were exposed to centrifugation steps to remove remaining media from the cell pellets. Pellets were dissolved in RIPA buffer (25 mM Tris, 125 mM NaCl, 1% Nonidet P-40, 0.1% SDS, 0.5% sodium deoxycholate, 0.004% sodium azide, pH 8.0) supplemented with complete protease inhibitors (Sigma, P8340) and 1 mM PMSF (Sigma, P7626) considering percentages of them. Cell pellets were vortexed during 10 to 12 sec for each 5 minutes while they were incubated on ice for 30 minutes totally. Thereafter, cell lysates were exposed to centrifugation at 14.000 rpm during 15 min at 4°C. Protein samples were taken into new tubes and concentration measurements were determined by Bradford assay (Sigma, B6916). Afterwards, protein samples were mixed with 3X protein loading dye (6% SDS, 30% Glycerol, 16% β-Mercaptoethanol and 0.1% Bromophenol blue in 1 M Tris-HCl pH 6.8) and denatured at 95°C during 10 minutes.

2.5 IMMUNOBLOTTING TESTS

For immunoblotting, denaturated protein samples were separated in home-made SDS-PAGE gel. (for recipe of SDS-PAGE gel see Table 2.4.1 and 2.4.2). Then, gels were transferred onto nitrocellulose membrane (GE Healthcare, A10083108) under 250 mA for 75 to 120 minutes. For blocking of proteins, nitrocellulose membranes were incubated in 5% non-fat milk (Applichem, A0830,0500) in PBST (0.05% Tween 20 in PBS; 3.2 mM Na2HPO4, 0.5 mM KH2PO4, 1.3 mM KCl, 135 mM NaCl, pH 7.4) during 1h at RT on the shaker**.** Following the incubation, PBST washes were made for 3 times per 5 minutes on the shaker. After washing steps, the membranes were incubated with required primary antibodies diluted in red solution (5% BSA Cohn V Fraction, 0.02% Sodium Azide in PBST, pH 7.5, Phenol red) with different concentrations during 1h or overnight at 4°C depending on working protocol of used antibody. Antibody treated membranes

were washed again 3 times with PBST and incubated with HRP-conjugated secondary antibody diluted with 1.10000 ratio in 5% non-fat milk at RT for 1h. For imaging, secondary antibody treated membranes were washed in the same way and incubated with prepared homemade ECL solution (25 mM luminol, 9 mM coumaric acid, 70 mM Tris-HCl pH 8.8) including approximately 3µl of H2O2. While the membranes were exposed ECL solution completely, the chemical reaction initiated. In order to detect the signal, membranes were placed into cassettes and then blue films (Fujifilm, Blue Sensitive film 474107619289) put onto the membranes. After cassettes were incubated in dark room for 20 minutes, films firstly were developed and then fixed with manually prepared developer and fixer solutions. In case of two or more protein detection in the same membrane, after first signal detection, membranes were washed and incubated in stripping buffer (25mM Tris- HCl, 1% SDS pH 2.0) for 30 minutes at 60°C by shaking in every 5 minutes. Then, membranes were exposed to blocking and following steps as in previous imaging.

Table 2.5.1: The ingredients of home-made separating gel for SDS-PAGE

SEPERATING GEL	**15%**			**12%**			**10%**		
	5ml	10ml	20ml	5ml	10ml	20ml	5ml	10ml	20ml
ddH20	850 µl	1.75 ml	3.5 ml	1.35 ml	2.75 ml	5.5 ml	1.7 ml	3.4 ml	6.8 ml
50% Glycerol	400 µl	750 µl	1.5 ml	400 µl	750 µl	1.5 ml	400 µl	750 µl	1.5 ml
Lower Buffer	1.25 ml	2.5 ml	5 ml	1.25 ml	2.5 ml	5 ml	1.25 ml	2.5 ml	5 ml
Bis/Acrylamide	2.5 ml	5 ml	10 ml	2 ml	4 ml	8 ml	1.65 ml	3.35 ml	6.7 ml
10% APS	50 µl	100 µl	200 µl	50 µl	100 µl	200 µl	50 µl	100 µl	200 µl
Temed	5 µl	10µl	20 µl	5 µl	10µl	20 µl	5 µl	10µl	20 µl

STACKING GEL	**2.5 ml**	**5 ml**	**7.5 ml**	**12.5 ml**
ddH20	1.62 ml	3.25 ml	4.88 ml	8.13 ml
Lower buffer	625 ml	1.25 ml	1.87 ml	3.12 ml
Bis/Acrylamide	250 µl	500 µl	750 µl	1.25 µl
10% APS	20 µl	40 µl	60 µl	100 µl
Temed	5 µl	10 µl	15 µl	25 µl

2.6 IMMUNOPRECIPITATION ANALYSES

For the analysis of protein-protein interactions in cells, whole cell protein lysates were bound with Flag-beads (Anti-Flag M2 affinity gel; Sigma A2220) for Flag-tagged protein immunoprecipitation or bound with protein-A/G agarose beads (Santa Cruz Biotech., sc-2001 and sc-2002) which are pre-coupled with specific antibodies. For each bead coupling, 25 µl of beads were put on Eppendorf tubes and washed with 250 µl of PBS. Subsequently, beads were washed with 250 µl of RIPA buffer and then, with 250 µl of RIPA buffer supplemented by protease inhibitor centrifugating the tubes at 4°C, 6000g for 1 min. For endogenous Co-IP experiments 2.5 mg protein sample were loaded onto the pre-washed and antibody coupled agarose beads. For overexpressed proteins, 1 mg protein sample were loaded onto the pre-washed flag beads or pre-washed and antibody coupled agarose beads. Total volume of protein and bead solution was completed to 250 µl with RIPA buffer supplemented with protease inhibitors. Additionally, 100 µg of protein samples from each protein samples were taken into new tubes, mixed with 3X loading dye, boiled and labeled as input samples. Following bead and protein incubation over-night, at 4°C, unbound proteins were removed by 6 repeats of washing steps with 500 µl of homemade protease inhibitor (500X) and 1mM PMSF supplemented RIPA buffer and centrifugating at 4°C, 5000rpm. After washing, bead bound protein pellets were mixed with 3x loading dye and boiled at 95°C to elute bound proteins. In the last step, eluted proteins and input controls of them were expose to SDS-PAGE and immunoblotting as explained above.

2.7 IMMUNOFLUORESCENCE ANALYSES

In the immunofluorescence analysis, 12 well cell culture plates were used. Cover slides were placed into each well and them HeLa cells were directly plated onto cover slides covered wells. For each condition, 25000 cells were cultured per well. For HEK293T cells, autoclave sterilized cover slides were firstly coated with 100 µl of 0.01 % poly-L-lysine solution into 10 cm2 plates during 10 mins at RT. Poly-L-lysine solution was aspirated and cover slides were air-dried. Then, cover slides were washed with PBS and put into 12 well plate. 30.000 HEK293T cells were plated into each well.

After drug treatments and transfection periods, culture media was aspirated from incubated cells and PBS washes were performed. Cells were then fixed with 4% PFA (paraformaldehyde, ph 7.4, Sigma, P6148) during 30 minutes at dark on RT under the chemical hood. PFA was removed and cell were exposed to washings with PBS repeated three times. If fluorescence-tagged proteins will be analyzed, cover slides were directly placed over mounting solution (50% glycerol (Applichem, A4453) in PBS) added microscopy slides by providing cell surface meeting with the mounting solution. Next, excess mounting solution was removed by a kimwipes and the edges of the coverslips were coated with nail polish to stabilize fitted cover slide and microscopy slide. The slides were analyzed under confocal microscopy at 63X oil objective (Carl Zeiss, LSM710). by using laser filter suitable for fluorescence protein wavelength

If non-tagged endogenous proteins will be visualized, following fixation step, cells were placed onto the parafilm coated well of six well culture plate and 100 µl blocking solution (PBS with 0.1% BSA (Sigma, A4503) and 0.1% saponin (Sigma, 84510)) were added on

to the cells. Therein, cells were permeabilized for 30 minutes at 4°C in an orbital shaker. Then, blocking solution were aspirated and samples were treated with 60 µl of suitable primary antibody solution diluted in blocking solution (the dilution ratio were determined depending on IF protocol of each antibody) by shaking for 1h, RT. Following primary antibody treatment, PBS washes were made three times and samples were treated with suitable fluorescence dye conjugated secondary antibody diluted in blocking solution (1:500 ratio) for 1h, at RT. If the primary antibody were produced in mouse: Alexa Fluor 488 goat anti mouse IgG (Thermo Fisher Scientific, 982245) and Alexa Fluor 568 goat anti-mouse IgG (Thermo Fisher Scientific, A11004) were used as secondary antibody. If the primary antibody were produced in rabbit: Alexa Fluor 488 goat anti- rabbit IgG (Thermo Fisher Scientific, 948490) and Alexa Fluor 568 goat anti-rabbit IgG (Thermo Fisher Scientific, A11011) were used as secondary antibodies.Finally, secondary antibody solution was removed and 3 times PBS washes were made. Cover slides were mounted as explained in detailed before and image analysis were performed under confocal microscopy.

2.8 GEL FILTRATION (FPLC) ANALYSES

Gel filtration chromatography is a method in order to separate molecules based on their size and shape. Separation of the molecules through the column generally correlate with their molecular weights. With the help of this technique the molecular weight of an unknown protein can be analytically determined. In the gel filtration experiment, a Superdex-200 10/300 GL column (GE healthcare, 17-5175-01) with a separation range of 10-600 kDa was used as a porous matrix that allows separation. The column firstly was connected and fitted to the ÄKTA Pure FPLC system (ÄKTA Pure 150L FPLC & Frac-

950 Fraction Collector, GE Healthcare). The column wash was performed with filtered and sonicated 36 ml deionized water (as wash volume is 3-fold greater than column bed volume) and then, washing was made using 0,05% glycerol/RIPA buffer ((1:1) without protease inhibitors) until all the parameters (pressure: 1.5 MPa, flow rate: 0,5 ml/min., fraction volume: 0,5 ml, sample loop volume: 500 µl) are stabilized which were can be followed real-time by UNICORNTM software of the AKTA system. The last washing step before protein loading was made with 24 ml of sonicated RIPA buffer supplemented by protease inhibitors. The marker calibration was done by loading 250 µl of molecular weight marker to the column as a sample (Sigma, MWGF-1000).

After marker calibration, for each condition, 500 µl protein samples containing 7mg protein were passed through the column and separated protein fractions were collected automatically for each 0.5 ml volume into fraction collector tubes. Between each different protein loading, the column was washed with sonicated water, equilibration buffer and RIPA buffer supplemented with protease inhibitor orderly. After the collection of all fractions, each fraction was mixed with 250 µl of 3X loading dye, boiled at 95^0C and stored at -20°C for further use. SDS-PAGE and immunoblotting were then performed as explained in detail above.

2.9 RNA ISOLATION and RT-PCR ANALYSIS

In order to perform RT-PCR analysis, firstly total RNA was isolated from the HeLa cells by using TRIzol reagent (Sigma, T9424) according to the manufacturer's protocols. Total RNA of the cells was treated DNase 1 (Thermo Fischer Scientific, EN0521) to get rid of DNA fragments from the samples. Then, DNase 1 treated RNA samples were reverse

transcribed by using M-MuLV reverse transcriptase (Fermentas, EP0351) and random hexamers (Invitrogen, 48190-011) to obtain cDNAs. Real time quantification of mRNA levels was made with applying the SYBR Green Quantitative RT-PCR kit (Roche, 04-913-914-001) protocol and using LightCycler 480 (Roche) for the analysis. The SYBR green protocol were used as following:

Initial cycle: 95°C, 10 min

PCR amplification: 95°C, 15 sec
60°C, 1 min. } 40 cycles

Subsequently, the thermal denaturation protocol was applied to the samples in order to obtain a dissociation curve for the checking of amplification specificity as following:

95°C, 60 sec
55°C, 60 sec } 1 cycle

55°C, 10 sec } 80 cycles

Differences in mRNA levels were quantified by the $2^{\Delta\Delta CT}$ method. GAPDH (glyceraldehyde-3-phosphate dehydrogenase) mRNA were used as control for all the samples. Primer pair used were:

ATG5 primers: 5'-AGTGAATCTGTGCCATCGAGT -3'

5'-AGTAGAGCTGCTGCCAAACC -3'

DNA-PKcs primers: 5'-CTGTGCAACTTCACTAAGTCCA -3'

5'-CAATCTGAGGACGAATTGCCT -3'

KU70 primers: 5'-GCTAGAAGACCTGTTGCGGAA -3'

5'-TGTTGAGCTTCAGCTTTAACCTG-3'

KU80 primers: 5'-GTGCGGTCGGGGAATAAGG -3'

5'-GGGGATTCTATACCAGGAATGGA -3'

2.10 STATISTICAL ANALYSES

Statistical analyses were performed using Paired t-test or ANOVA using Graph Pad Prism 8.01 software. Data were represented as means of ±SD of n independent experiments (biological replicates). Values of $p<0.05$ were considered as significant.

3. RESULTS

3.1 CLONING STUDIES OF ATG5

ATG5 protein is required for the formation of autophagosomes and increases susceptibility through apoptotic stimuli. The role of ATG5 about apoptosis was found to be related with calpain-mediated cleaved domain of ATG5, which covers 1 to 192 aa. In order to understand the role of either calpain cleaved domain, remaining cleavage product of it and putative signal sequence of ATG5, construct designs were planned as in Fig. 3.1.1

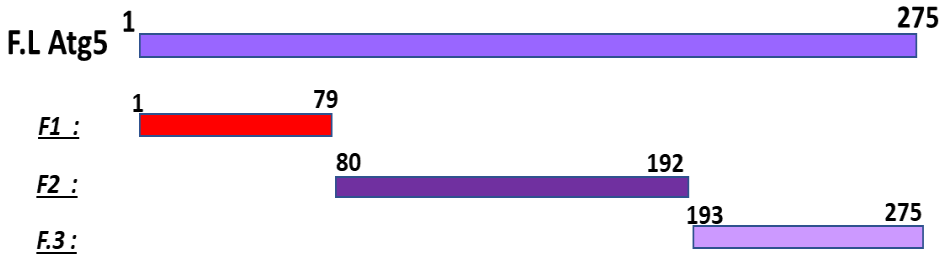

Figure 3.1.1: Schematic representation of ATG5 fragments sizes. F.L: Full length, F1: 1-79 fragment, F2: 80-192 fragment, F3: 193-275 fragment.

Cloning experiments of determined constructs; 1-79, 80-192 and 193 were performed by following the procedure as it is shown in Fig.3.1.2.

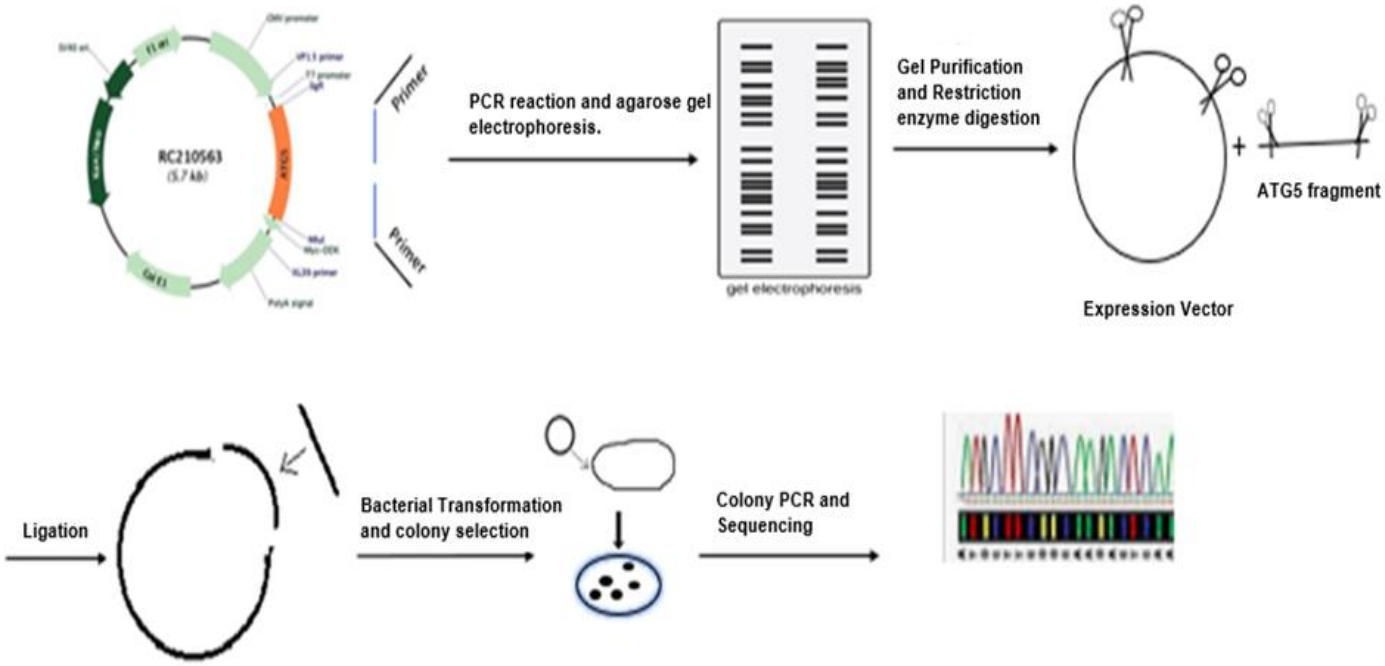

Figure 3.1.2: Schematic representation of cloning steps of ATG5 fragments.

Created ATG5 constructs sequences were verified with the sequencing analysis and rightly incorporated inserts into the plasmid DNA were selected as positive clones. Transfection experiments were performed by using these positive clones in HEK293T cells. To check any protein products for further function analysis of ATG5 fragments, immunoblotting experiments were performed and results were shown in Fig. 3.1.3. According to the results, 8-192 and 193-275 fragments were detected succesfully in expected size with flag antibody but there was no any protein band for N-terminal ATG5 fragment; 1-79.

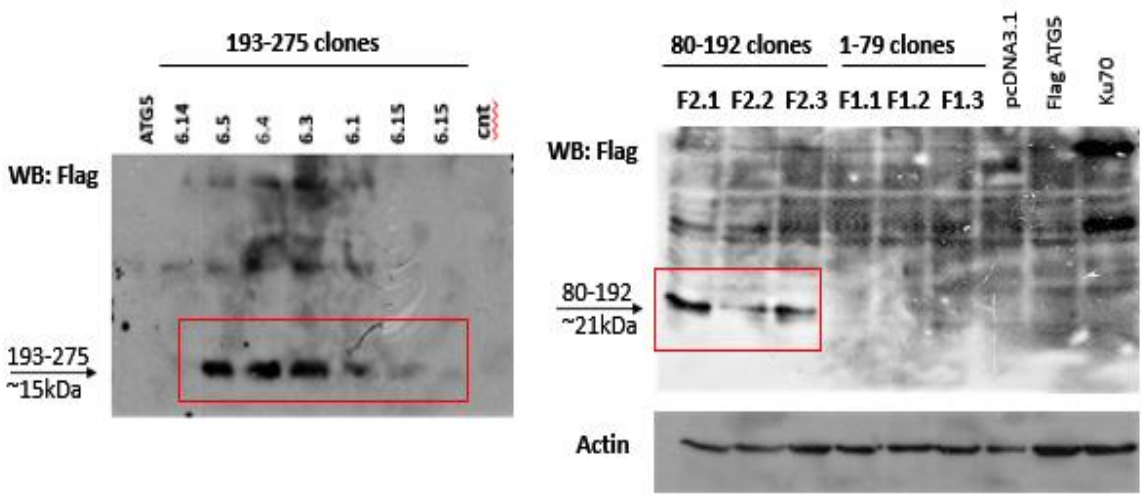

Figure 3.1.3: a. Immunoblotting results of different 193-275 clones. HEK293T cells were transfected with 193-275 fragment inserted plasmids. Following 48 h cells were collected and immunoblotting was performed. 193-275 fragment expression detected with C-terminal ATG5 antibody. **b.** Immunoblotting results of different 1-79 and 80-192 clones. HEK293T cells were transfected with 1-79 and 80-192 fragments inserted plasmids. Following 48 h cells were collected and immunoblotting was performed. 1-79 and 80-192 fragments expression detected with N-terminal ATG5 antibody. Actin was used as loading control.

To understand the functional roles of 80-192, 193-275 and calpained cleaved domain, 1-192 fragments under DNA DSB inducing conditions over p-H2AX formation, immunoblotting experiments were performed. The results were obtained as in **Fig. 3.1.4** p-H2AX accumulation in 193-275 fragment overexpression is higher than the others in control condition compare to Full length Flag-ATG5, however, in etoposide conditions, calpain cleaved domain (1-192) and its subdomain (80-192) overexpression caused to higher p-H2AX accumulation compare to C-terminal domain (193-275) and Full length-Flag ATG5. It can be concluded that calpained cleaved domain and its subdomain increases the gentoxic stress in HEK293T cells.

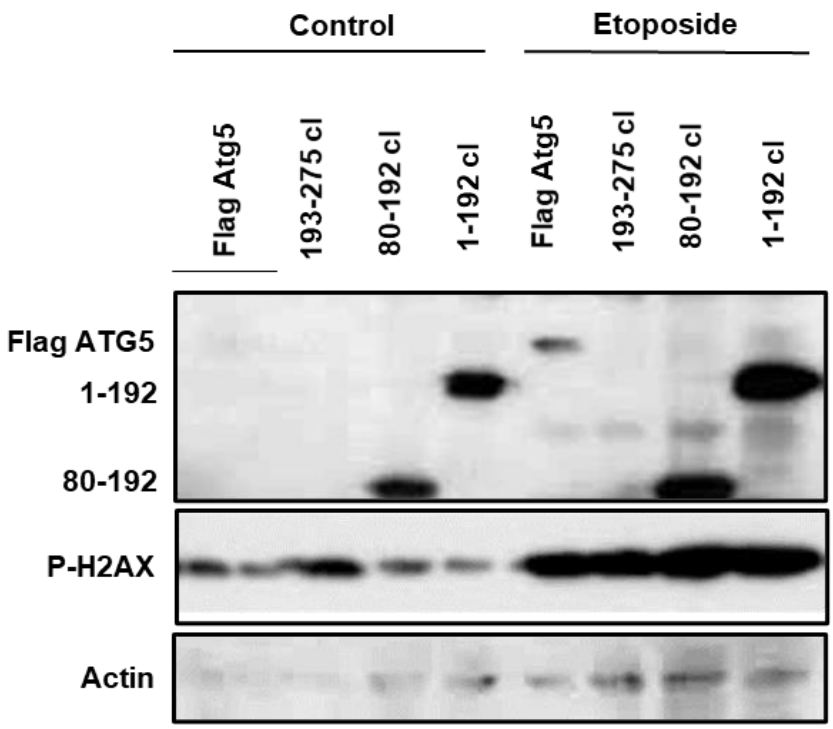

Figure 3.1.4: Immunoblotting experiment result of ATG5 fragments overexpressed cells under Etoposide treatment. HEK293T cells were transfected with Flag tagged ATG5, flag tagged 1-79, 80-192 and 193-275 fragments. After transfection cells were treated with DMSO (control) and 50μM Etoposide during 24 h. Following treatment cells were collected, phospho-protein isolation and immunoblotting was performed. For immunoblotting Flag, p-H2AX antibodies were used. Actin was used as loading control.

3.2 PRELIMINARY DATA PRIOR TO PROJECT DESIGN

Prior to the project preliminary data were obtained from Tri-SLAC-based LC-MS/MS analysis of HEK293T and HeLa cells. Enrichment of Ku70, Ku80 and DNA-PKcs proteins compared with beads alone were represented as a graph, respectively in Fig.3.2.1. According to the data, ATG5-K70, ATG5-KU80 and ATG5 DNA-PKcs fold change were found three times more than the control at least, thus, these complex formations were identified.

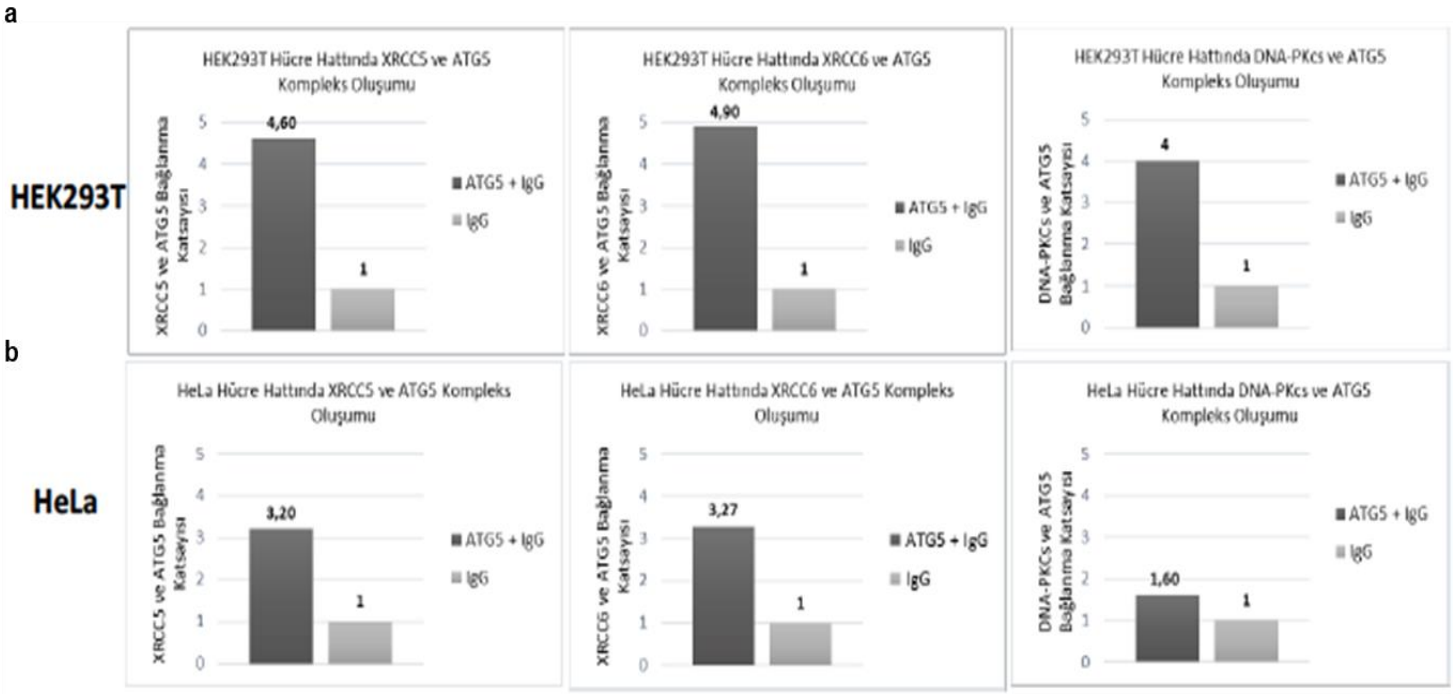

Figure 3.2.1: SILAC-based LC-MS/MS analysis results of HEK/293T and HeLa cells. SILAC labelled cells were transfected with Flag tagged ATG5 plasmid for 48 h. Following transfection, cell lysates were used for FLAG immunoprecipitation tests. After mixing all conditions, following gel electrophoresis, samples were subjected to LC-MS/MS analysis. Enrichment of Ku70, Ku80 and DNA-PKcs compared with beads alone were represented as a graph, respectively. (n=1). (This experiment was performed by former graduate Seçil Erbil)

In addition to LC-MS/MS data, ATG5-KU70 and ATG5-KU80 interaction were further analyzed by co-immunoprecipitation experiments in HEK293T and HeLa cells. Non tagged ATG5 and Flag tagged KU70 co-overexpressed HEK293T and HeLa cell lysates were subjected to the immunoprecipitation with Flag antibody. The results that are shown in Fig.3.2.2 displayed that ATG5 interacted with KU70 and KU80 physically. Therefore, formation of these complex that were observed in LC-MS/MS data were confirmed. (these Co-IP experiments were performed by former graduate Yunus Akkoç.)

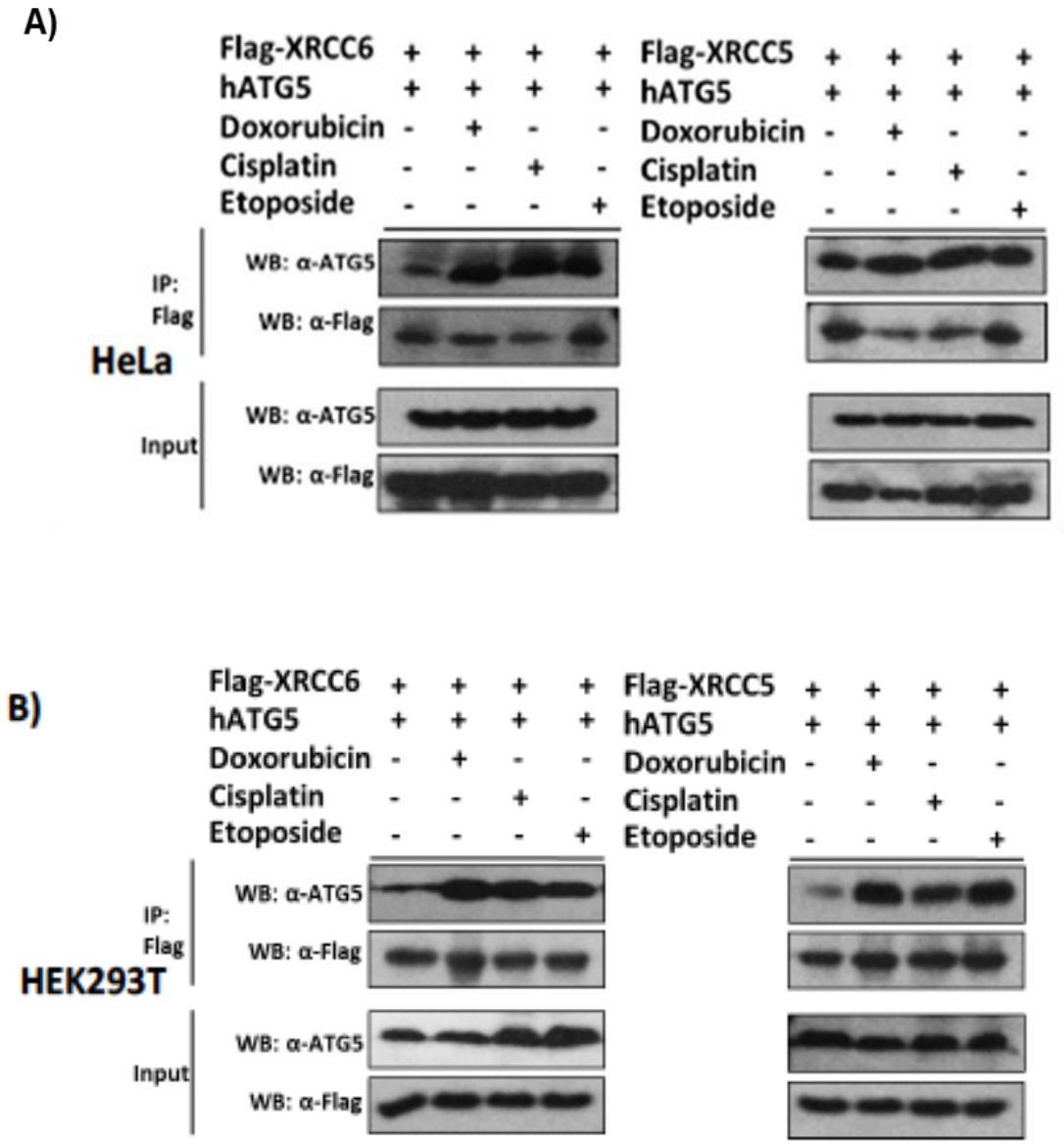

Figure 3.2.2: ATG5 immunoprecipitation experiments to test ATG5-KU70 and ATG5-KU80 binding in **A)** HeLa and **B)** HEK/293T cells. (IP-FLAG, Flag immunoprecipitation and Input, protein lysate control). The experiments were performed by former graduate, Yunus Akkoç)

3.3 CONFIRMATION AND CHARACTERIZATION OF ATG5-KU70 AND ATG5-KU80 INTERACTION IN CONTROL AND DNA DAMAGE INDUCED CONDITIONS

LC-MS/MS data and Co-IP data were further confirmed with repeated Co-IP experiments in HEK293T cells. The results were shown in Fig.3.3.1.

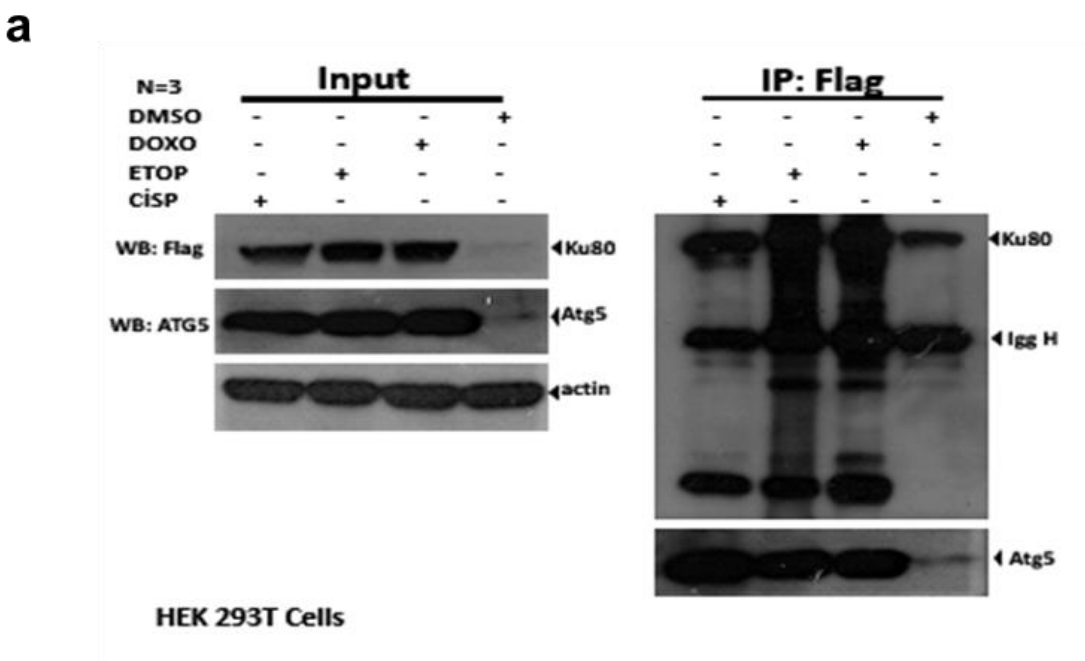

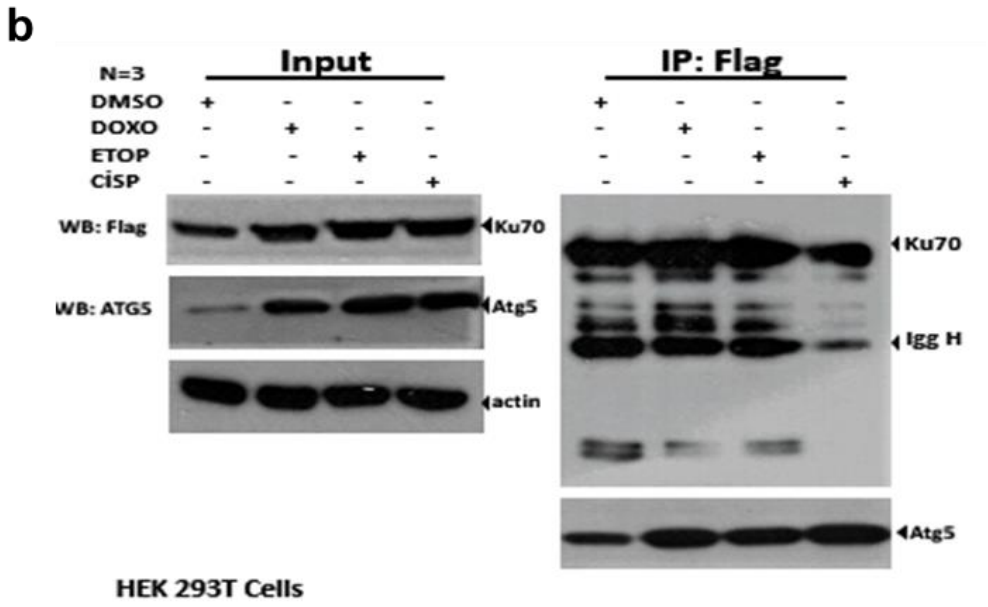

Figure 3.3.1: ATG5 immunoprecipitation experiment results to confirm Ku70 and Ku80 bindings. **a.** HEK/293T cells were grown in 10 cm2 plates for overnight prior to Flag tagged KU80 and non-tagged full length ATG5 construct co-transfection to the cells. **b.** HEK/293T cells were grown in 10 cm2 plates for overnight prior to Flag tagged KU80 and non-tagged full length ATG5 construct co-transfection to the cells. Following 24 h transfection, cells were treated with DMSO, Doxorubicin (1μM), Etoposide (50 μM) and Cisplatin (12.5 μg/ml) during 24 h. After treatments with these drugs, cells were harvested, and proteins were isolated. Cell lysates were incubated with Flag-beads overnight at 4°C. Immunoprecipitants were extracted with 3X loading dye by boiling for 10 minutes, at 95°C. Samples were subjected to SDS-PAGE analysis. Anti-ATG5 and anti-FLAG antibodies were used for immunoblotting. Input, total cell extract. Molecular FLAG-IP, Flag immunoprecipitation (n=3 independent experiment performed in HEK/293T cells).

3.4 ANALYSIS OF THE DYNAMICS OF ATG5-KU70 INTERACTION

In order to further analyze ATG5-KU70 protein complex, in a closest to native structure, gel filtration experiments were performed. Etoposide and Doxorubicin treated HeLa cells were separated through the chromatography column (Superdex 200 column with a

separation range of 10 to 600 kDA). Collected fractions were analyzed by immunoblotting using anti-ATG5 and anti-Ku70 antibodies. Based on the obtained results shown in Fig. 3.4.1, it was found that there have been three different protein complexes containing ATG5 and KU70 proteins and decreased overlapping fractions of ATG5-KU70 protein.

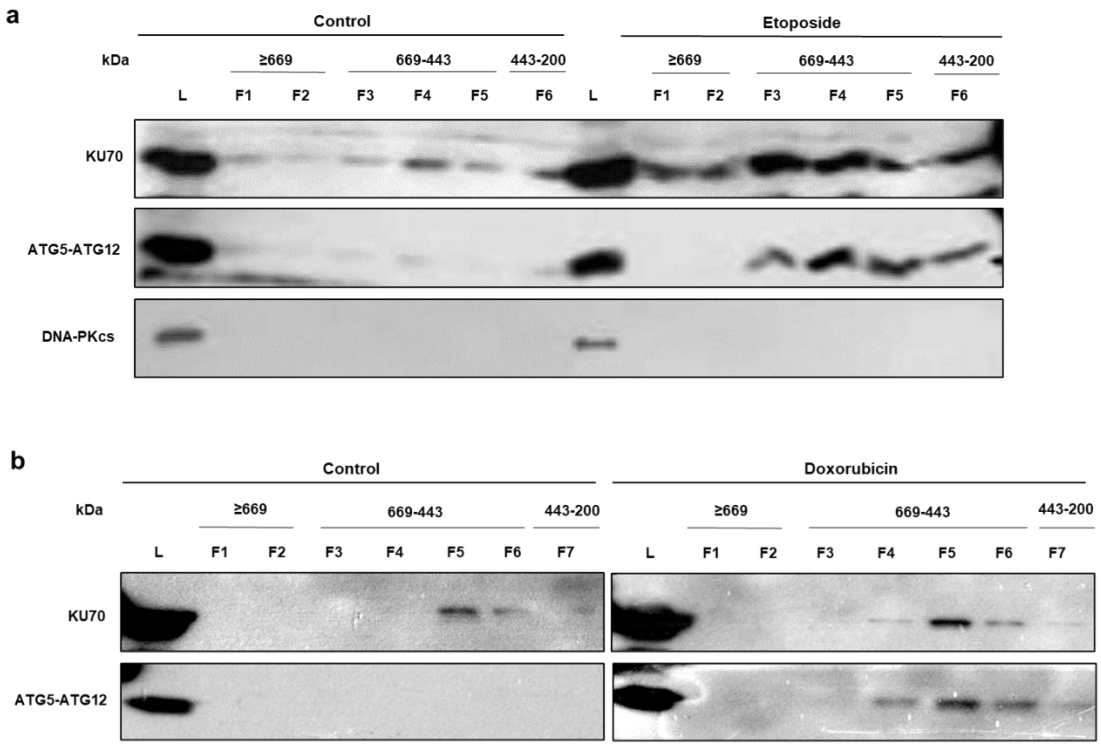

Figure 3.4.1: Gel filtration tests of HeLa cell-derived total lysates. HeLa cells treated with **a.** Etoposide (50 μM) and **b.** Doxorubicin (1μM). 5-10 mg of total cell lysates were applied to the calibrated Superdex 200 10/300 GL (GE Healthcare, 17-5175-01) and 20 fractions collected for each condition. Fractions were separated through SDS-PAGE and Anti-ATG5, anti-Ku70 and DNA-PKcs antibodies used for immunoblotting. L, Lysate control and kDA, kilodaltons (left panel).

The FPLC results also could be interpreted that ATG5-KU70 interaction is the part of a bigger protein complex in size of approximately 443-669 kDa. Moreover, Etoposide and Doxorubicin induced genotoxic stress induced the formation of KU70 and ATG5

containing complex (please see the 3,4,5 and 6 in Etoposide treatment, and 4,5,6 and7 in Doxorubicin treatment).

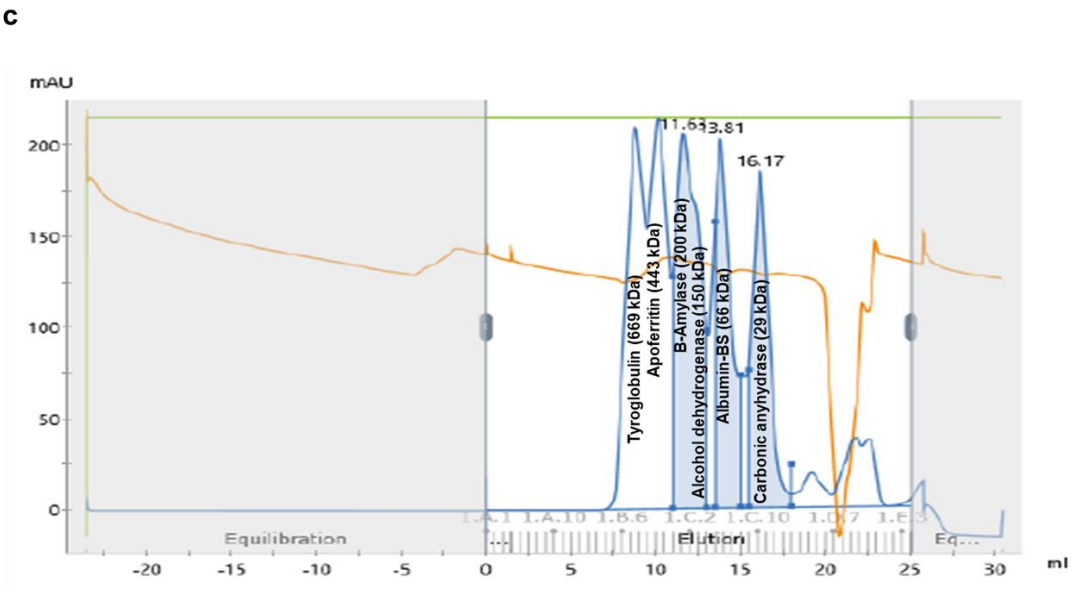

Figure 3.4.2: Representative chromatogram showing peaks of the molecular weight marker mix.

Before the loading of protein samples, commercial molecular marker mix was loaded into the column and the marker proteins were observed in different peaks on the chromatogram.

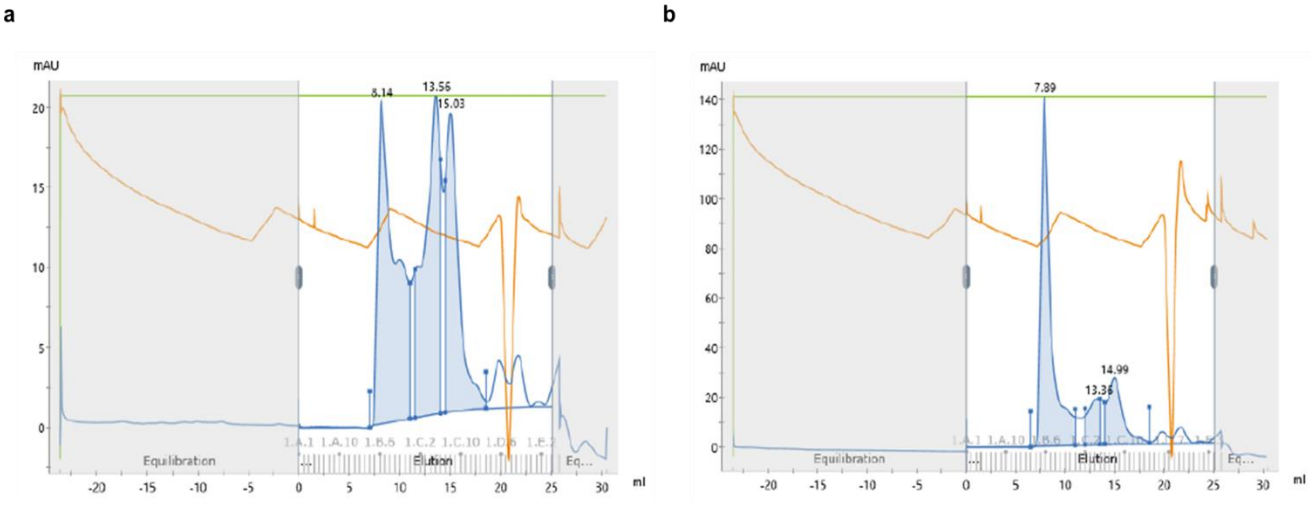

Figure 3.4.3: Representative chromatograms of DMSO treated control cell lysates **a.** and Etoposide treated cell lysates **b**. of HeLa cells through the FPLC separation.

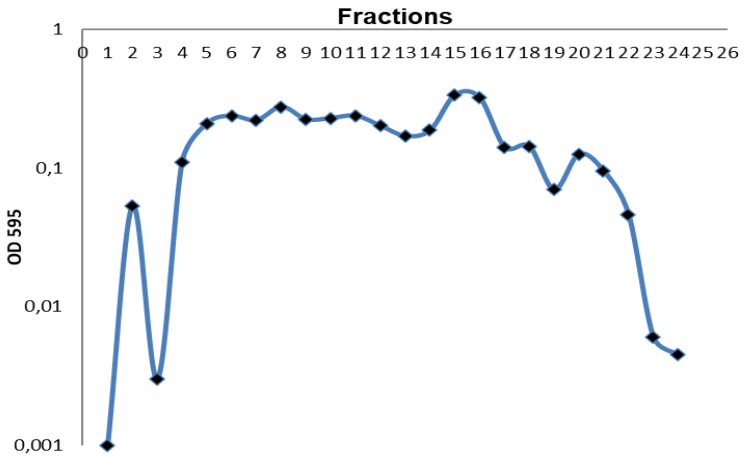

Figure 3.4.4: OD595 absorbance confirmation of the marker peaks of the gel filtration over Superdex 200 column.

After the test presence of protein complex including ATG5 and KU70 protein in FPLC experiments, endogenous dual protein-protein interaction between KU70 and ATG5 was analyzed with Endogenous Co-IP experiments in HEK293T and HeLa cells. Experiment was performed by following different methodologies.

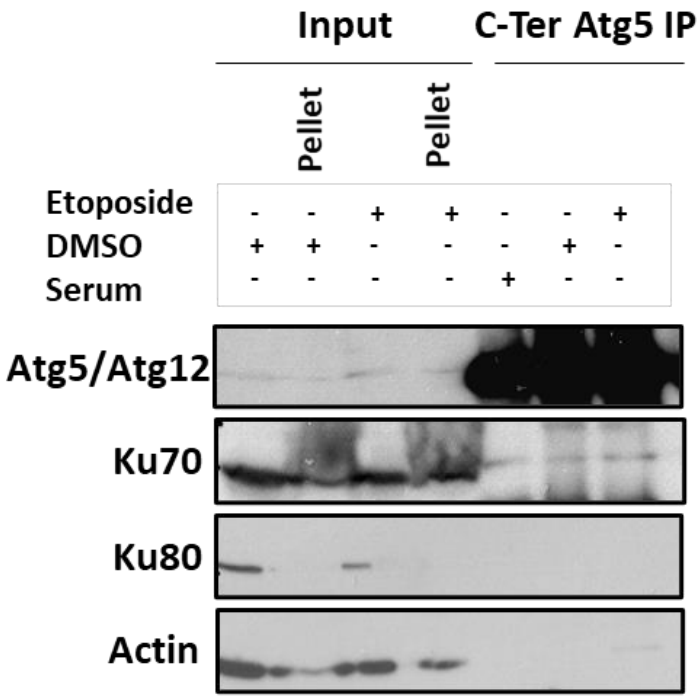

Figure 3.4.5: Endogenous ATG5-Immunoprecipitation experiments performed in HEK293T cells. Cells were treated with 50 µM Etoposide for 24 h and DMSO as control.

After treatments, cell lysates were incubated with anti-ATG5 coated agarose beads for overnight at 4°C. Then, SDS-PAGE analysis and immunoblotting were performed. C terminal Anti-ATG5, anti-KU70, anti-KU80 and anti-b-actin antibodies were used for immunoblotting. Pellet; cellular pellet obtained during protein isolation. Input, control cell lysate; IP, Immunoprecipitation. Serum; Control rabbit serum.

In Fig 3.4.5, HEK293 cells were used for obtaining endogenous whole protein lysates under etoposide induced and control conditions. ATG5 Co-IP experiment were performed with the lysates. To understand whether KU70 and ATG5 protein interaction depends on DNA or not, DNA containing pellet of cell debris were also loaded onto SDS gel and immunoblotting was performed. The result in Fig 3.4.5 revaled that ATG5-KU70 interaction occurs in control conditions and increasing upon DNA DSB damage. Also, a particular amount of ATG5 and KU70 protein also remaining in the pellet during protein isolation and level of these proteins were increasing upon genotoxic stress in the pellet as well. In contrast to overexpression IP results, endogenous Co-IP experiments showed that there was no any KU80 protein in the IP part implying there was no direct endogenous KU80-ATG5 interaction. Similar data were obtained from different endogenous Co-IP experiments represented in Fig 3.4.6, Fig 3.4.7 and Fig.3.4.8.

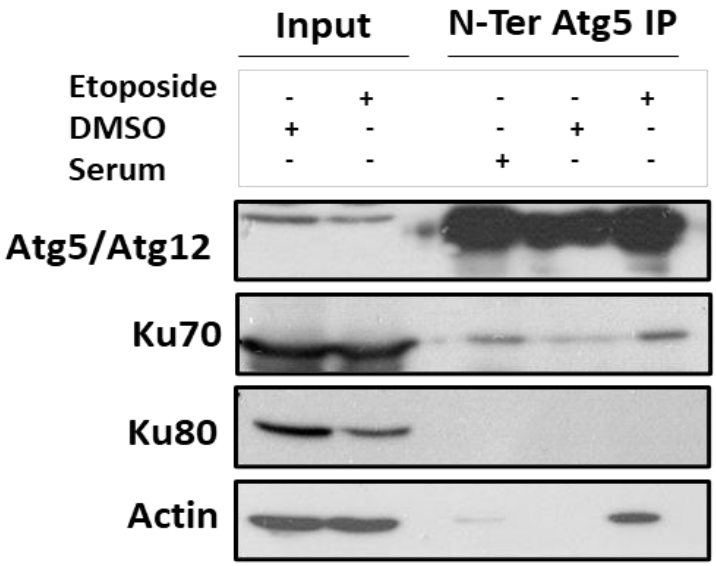

Figure 3.4.6: Endogenous ATG5-Immunoprecipitation experiments performed in HEK/293T cells. Cells were treated with 50 μM Etoposide for 24 h and DMSO as control. After treatments, cell lysates were incubated with anti-ATG5 coated agarose beads for overnight at 4°C. Then, SDS-PAGE analysis and immunoblotting were performed. N-terminal Anti-ATG5, anti-KU70, anti-KU80 and anti-b-actin antibodies were used for immunoblotting. Pellet; cellular pellet obtained during protein isolation. Input, control cell lysate; IP, Immunoprecipitation. Serum; Control rabbit serum.

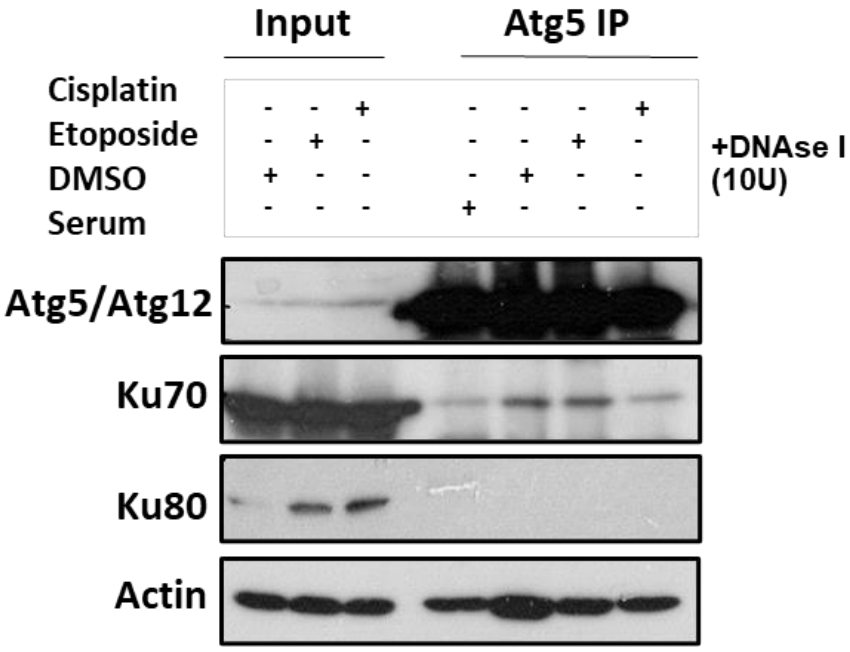

Figure 3.4.7: Endogenous ATG5-Immunoprecipitation experiments performed in HeLa cells. Cells were treated with 25 μM Etoposide and 1 μg/ml Cisplatin for 24 h and DMSO

as control. After treatments, protein isolation was performed in the presence of DNAse I, 10U. Then cell lysates were incubated with anti-ATG5 coated agarose beads for overnight at 4°C. Then, SDS-PAGE analysis and immunoblotting were performed. N-terminal Anti-ATG5, anti-KU70, anti-KU80 and anti-b-actin antibodies were used for immunoblotting. Input, control cell lysate; IP, Immunoprecipitation. Serum; Control rabbit serum.

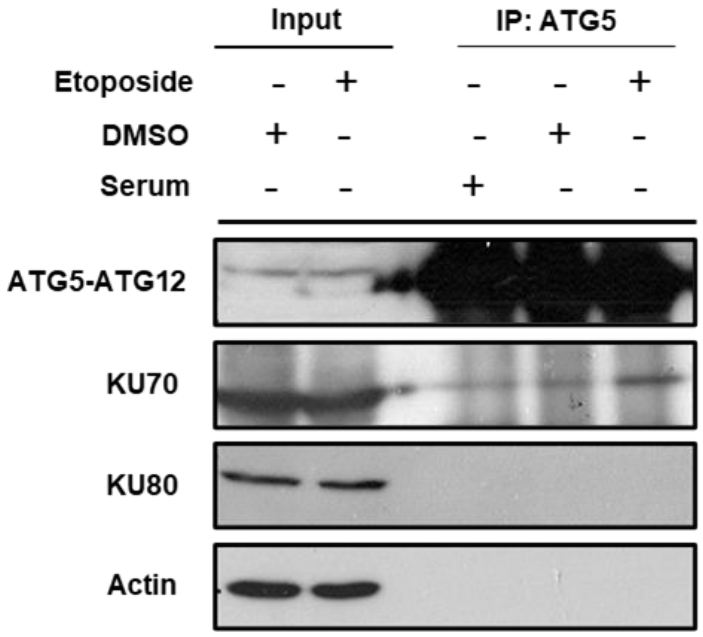

Figure 3.4.8: Endogenous ATG5-Immunoprecipitation experiments performed in HeLa cells. Cells were treated with 25 μM Etoposide for 24 h and DMSO as control. Protein isolation was performed with gluteraldehyde added (1:5 molar ratio) extraction buffer. Obtained cell lysates were incubated with anti-ATG5 coated agarose beads for overnight at 4°C. Then, SDS-PAGE analysis and immunoblotting were performed. N-terminal Anti-ATG5, anti-KU70, anti-KU80 and anti-b-actin antibodies were used for immunoblotting. Input, control cell lysate; IP, Immunoprecipitation. Serum; Control rabbit serum.

ATG5-KU70 interaction was confirmed with different experimental data as it explained above, but the data was related with ATG5 which is conjugated with ATG12 (endogenous free ATG5 protein is not detected in HEK293T cells). To clarify whether the interaction

was occurring between ATG5-ATG12 complex and KU70 or free ATG5 and KU70, it was designed overexpression Co-IP experiment by overexpressing Full Length non-tagged ATG5 protein in HEK293T cells. Immunoblotting results in Fig. 3.4.9 proved that free ATG5 protein also was interact with KU70 but not KU80 in control and DNA DSB induced conditions.

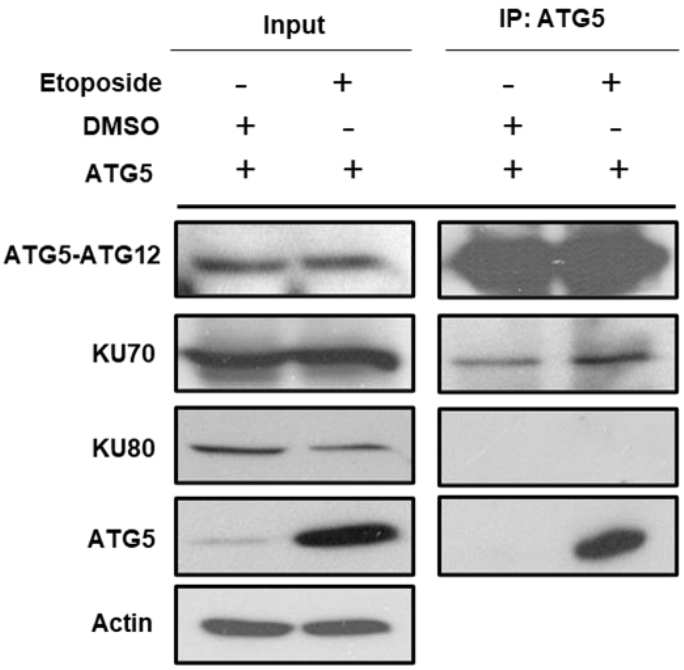

Figure 3.4.9: Endogenous ATG5-Immunoprecipitation experiments performed in HEK293T cells. Cells were transfected with non tagged full length ATG5 construct. Following 24h transfcetion, cells were treated with 25 μM Etoposide for 24 h and DMSO as control. Obtained cell lysates were incubated with anti-ATG5 coated agarose beads for overnight at 4°C. Then, SDS-PAGE analysis and immunoblotting were performed. N-terminal Anti-ATG5, anti-KU70, anti-KU80 and anti-b-actin antibodies were used for immunoblotting. Input, control cell lysate; IP, Immunoprecipitation.

As an alternative way to check protein-protein interaction and to see subcellular localization of the interaction, colocalization experiments were designed in HEK293T cells. Cherry tagged ATG5 and GFP tagged KU70 construct were transfected into the

HEK293T cells and colocalization of these two proteins were analyzed by overlapping of red and green signals into the nucleus. Confocal microscopy analysis of the cells was shown in Fig.3.4.10. According to the data, under basal and genotoxic stress induced condition, KU70 and ATG5 colocalized in the nucleus. And colocalization of these proteins were significantly increasing upon DNA DSB induction as it shown in the data Fig.3.4.11.

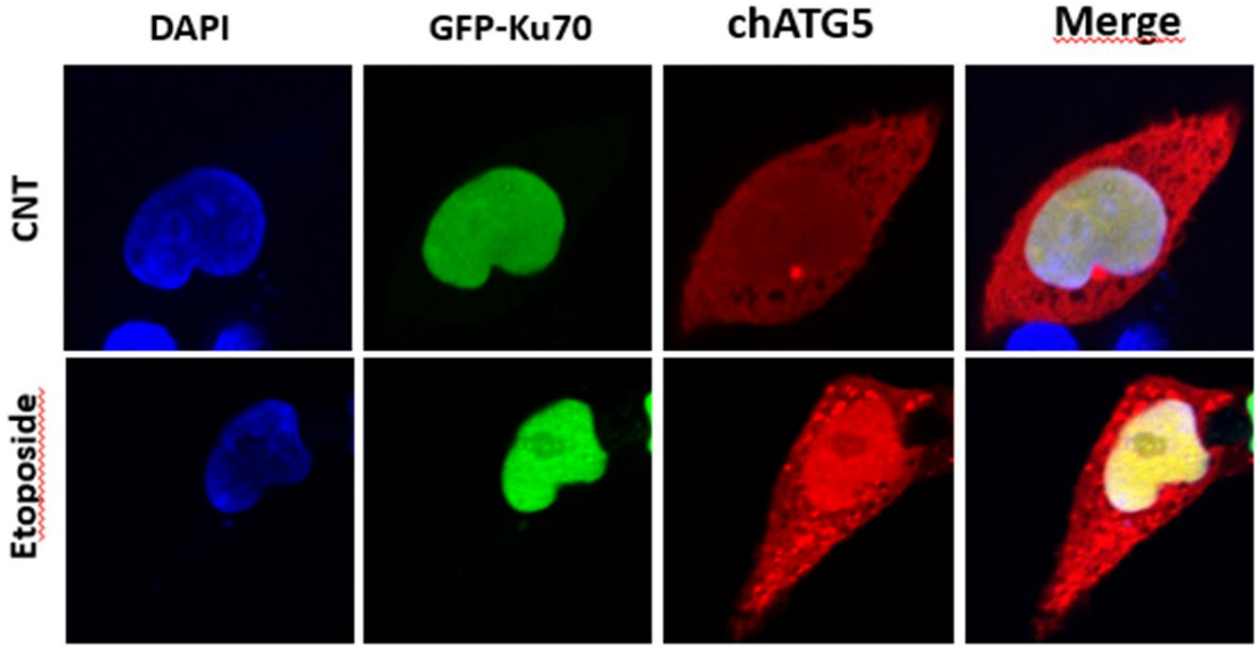

Figure 3.4.10: Colocalization experiments of KU70 and ATG5 under DNA DSB damage induction by etoposide in HEK293T cells. HEK293T cells were splitted on coverslides and 16 h after splitting co-transfected with mCherry-tagged ATG5 and GFP-tagged Ku70. Following 24 h transfection, cells were treated with 25μM etoposide for 24 h and DMSO as a control. Cells, then fixed with 4%PFA and visualized under confocal microscope at 63x magnification. Nuclei were stained with Hoechst (blue). Merge, overlay of green and red signals.

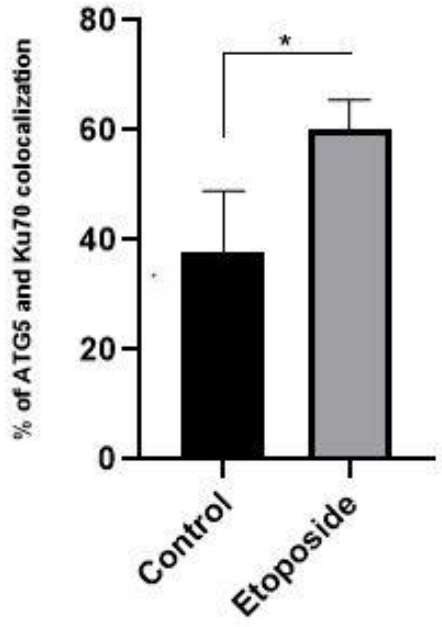

Figure 3.4.11: Quantification of confocal microscopy analysis in HEK293T cells.. Confocal images were analyzed and ATG5-Ku70 colocalization in nucleus were represented in the graph (mean ± S.D. of independent experiments, n = 3, *, $p<0.05$).

In the colocalization data, it was seen that nuclear colocalization of ATG5 and KU70. Because autophagy process occurs in cytoplasm, we want to test the presence of ATG5-ATG12 complex in the nucleus as well as KU70 and to test whether the protein levels in the nucleus is changing upon genotoxic stress. To answer these questions, cell fractionation was performed in HEK293T cells with the control and doxorubicin treated cell lysates. Depending on the cellular fractionation results which is represented in Fig. 3.4.12, it was concluded that ATG5-12 complex also found in the nucleus as well as KU70 and KU80 and protein levels of these proteins were increasing upon DNA DSB damage induction in the nucleus but not in cytosol.

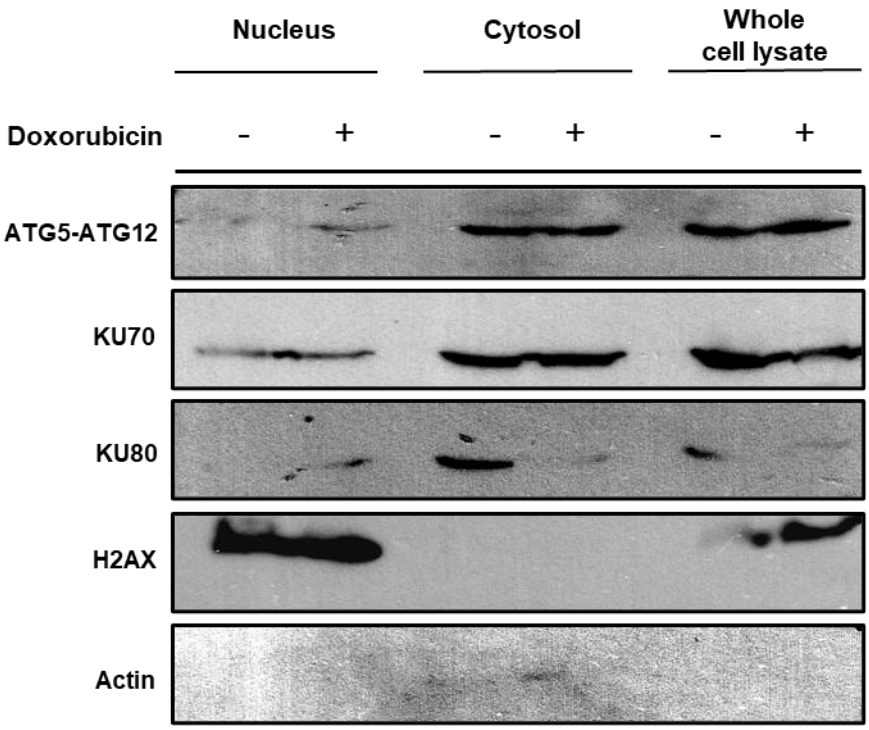

Figure 3.4.12: Cellular fractionation were performed after Doxorubicin treatment. (+), Doxorubicin; (-), DMSO in HEK293T cells. Nucleus, nuclear fraction; Cytosol, cytosolic fraction; Lysate, whole cell lysate were subjected to immunoblotting. Anti-ATG5, anti-Ku70, anti-Ku80, anti-H2AX and anti-β-Actin were used as a nuclear and cytosolic fractionation control, respectively

3.5 KU70 INTERACTS WITH N-TERMINAL PART OF ATG5

In order to map KU70-ATG5 interaction to understand which domain of ATG5 protein is responsible for the interaction, overexpressed Co-IP experiments were performed in HEK293T cells. Cells were co-transfected with N-terminal calpain cleaved fragment of ATG5 and KU70 or full-length Flag tagged ATG5 and KU70. Transfected cell lysates were subjected to Co-IP analysis and the results of the immunoblotting were represented

in Fig.3.5.1. According to Co-IP results, it can be noted that ATG5 and KU70 interaction occurs through N- terminal 1-192 part of ATG5 under basal conditions.

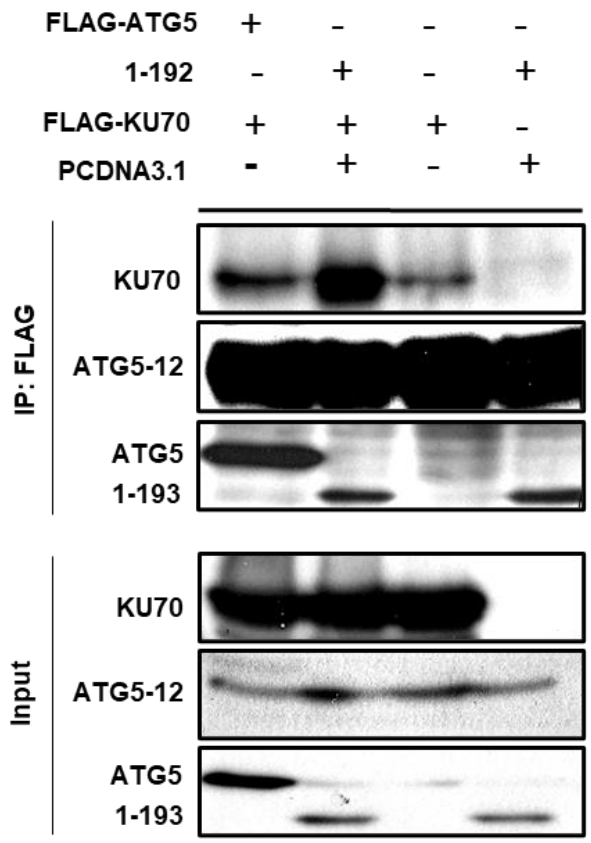

Figure 3.5.1: ATG5 immunoprecipitation analysis in HEK293T cells. HEK293T cells were co-transfected with FLAG-tagged Ku70 and/or non-tagged full length ATG5 construct or 1-192 construct. Cells were exposed either Etoposide 50μM for 24 h or DMSO as a vehicle after 24 h post-transfection and IPs were performed using Flag beads. Anti-ATG5, anti-Ku70, anti-Ku80 and anti-FLAG antibodies were used for immunoblotting. Input, total cell extract.

3.6 ANALYSIS OF THE EFFECT OF AUTOPHAGIC STIMULI ON DNA DSB INDUCTION

To understand the crosstalk between autophagy and DNA damage responses, we analyzed the effect the autophagy activation on DNA DSB accumulation through p-H2AX foci formation. Confocal microscopy analysis was conducted in MEF cells under autophagy induction with starvation and DNA damage induction with H202 (as a positive control of accumulated p-H2AX). The results that were represented in 3.6.1 pointed that starvation caused remarkably increased p-H2AX foci which can be seen as green dots in the STV condition and in the positive control. Increased p-H2AX foci formation also quantified with the p-H2AX dot counting analysis which is displayed in Fig.3.6.2. To conclude, autophagy activation caused genotoxic stress remarkably through increasing DNA DSB damage marker, p-H2AX foci.

The effect of autophagy induction on DNA damage also was identified with immunoblotting experiment. Starved, H202 treated and control MEF cells were subjected to immunoblotting and DNA DSB marker, p-H2AX protein levels were analyzed. The data obtained from the p-H2AX immunoblotting was represented in Fig.3.6.3. Depending on the results, it was concluded that autophagy activation causes markedly DNA damage accumulation in the cells through increased p-H2AX protein level.

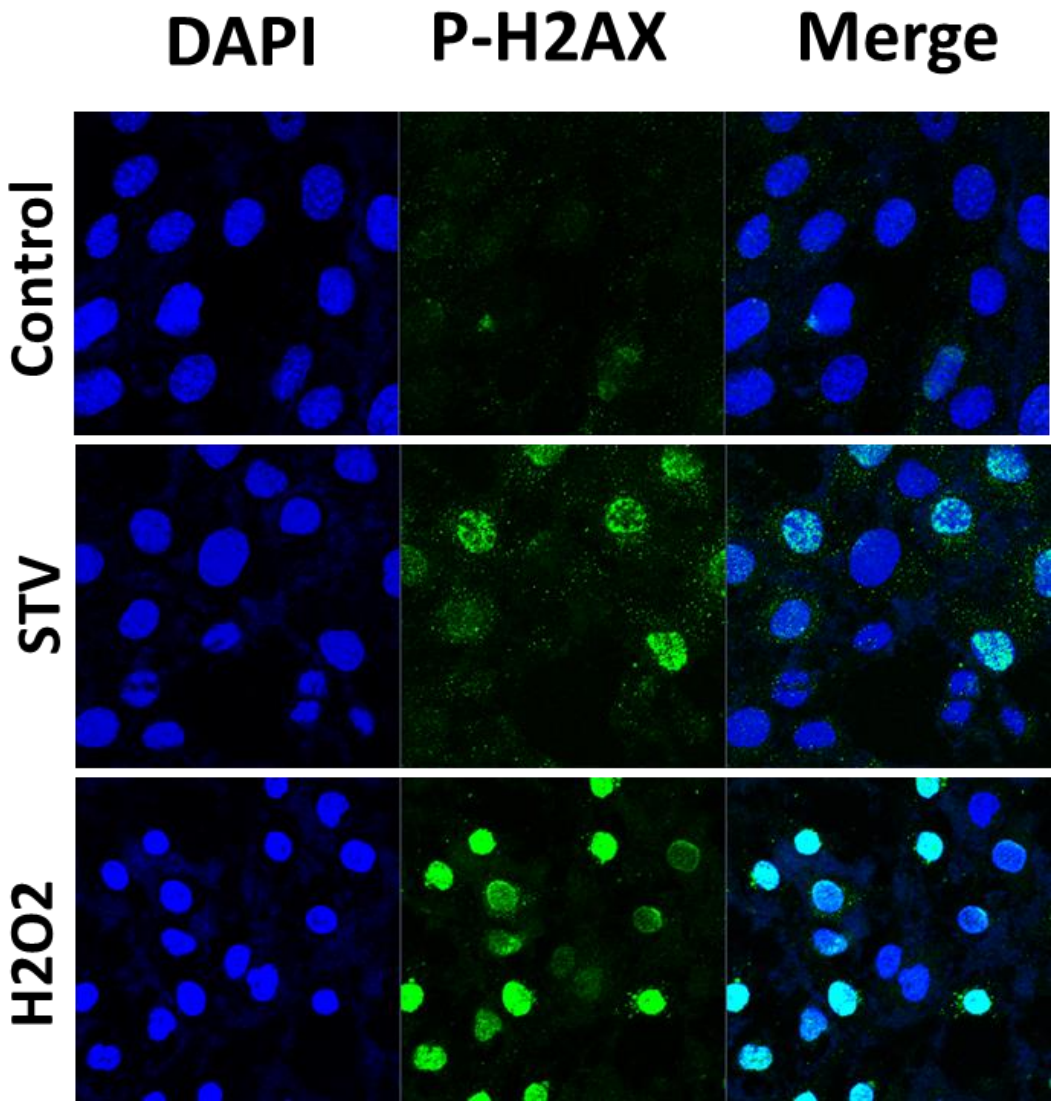

Figure 3.6.1: The effect of autophagic activity on p-H2AX foci formation in MEF cells. Cells were treated with EBSS (4h), H2O2 (1mM, 4h) and DMSO as a vehicle. Following treatment, cells were fixed with 4% PFA and permeabilized with BSA/saponin solution. Then permeabilized cells were incubated with Anti-p-H2AX primary antibody and Alexa Fluor-488 (Green) secondary antibody. After washes, stained with DAPI (Blue) and analyzed under confocal microscope at 63x. (Merge, overlay of green and blue signals, STV; Starvation, H2O2; hydrogen peroxide)

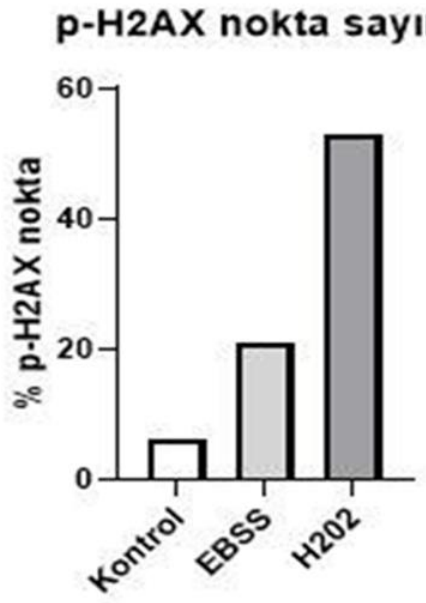

Figure 3.6.2: Quantification of confocal microscopy analysis in MEF cells.. Confocal microscopy images of EBSS (4h), H2O2 (1mM, 4h) and DMSO as a vehicle treated cells were analyzed and p-H2AX foci formation counted in the nucleus. P-H2AX foci formation in the nucleus of 50 cells were counted per condition. The cells that have nuclear p-h2AX foci more than the average was shown as p-H2AX positive.cells and the percentage of positive cells were represented in the graph.

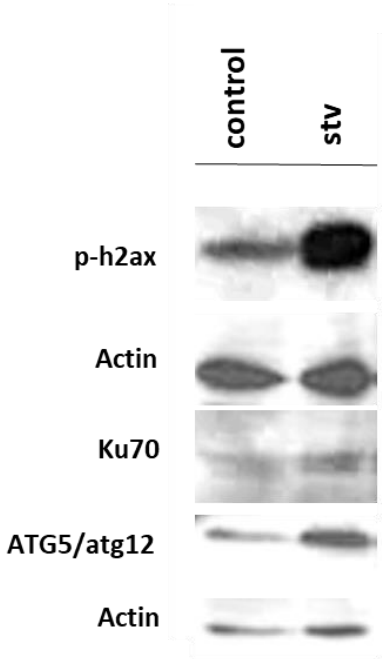

Figure 3.6.3: Immunoblotting results of EBSS treated MEF cells. Cells were treated with EBSS (4h) and DMSO as a vehicle. Following the treatment, SDS-PAGE analysis and

immunoblotting were performed. N-terminal Anti-ATG5, anti-KU70, anti-p-H2AX and anti-b-actin antibodies were used for immunoblotting. (STV; starvation).

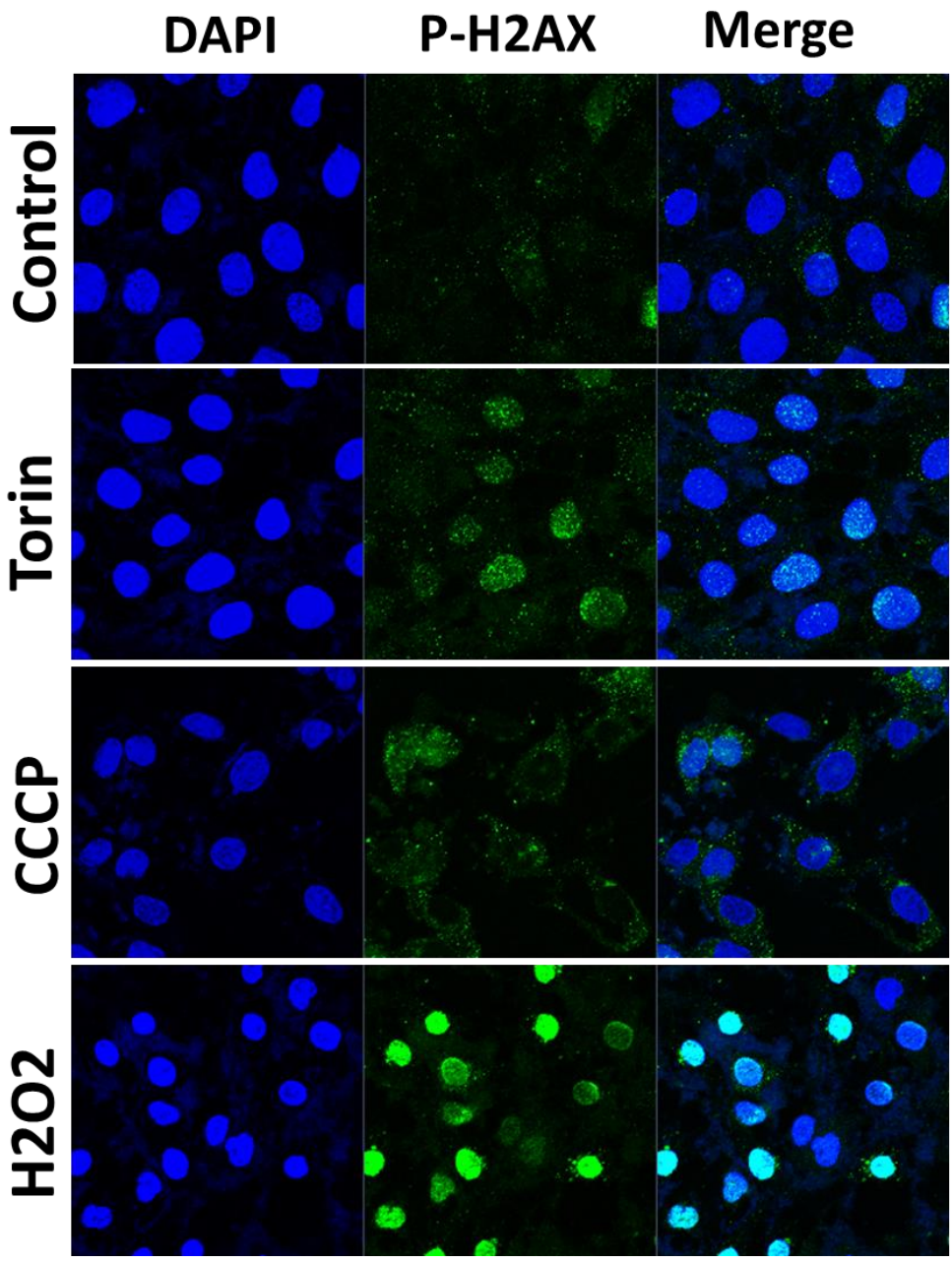

Figure 3.6.4: Analysis of the effect of autophagic activation on DNA DSB damage in MEF cells. Cells were treated with Torin 1 (250nM, 3h), CCCP (10µM, 24h), H2O2 (1mM, 4h) and DMSO as a vehicle. Following treatment, cells were fixed with 4% PFA and permeabilized with BSA/saponin solution. Then permeabilized cells were incubated with Anti-p-H2AX primary antibody and Alexa Fluor-488 (Green) secondary antibody.

After washes, stained with DAPI (Blue) and analyzed under confocal microscope at 63x. (Merge, overlay of green and blue signals, STV; Starvation, H2O2; hydrogen peroxide, Torin; Torin 1)

To further check the effect of autophagic stimulation over DNA damage, another confocal microscopy analysis was performed by using MEF cells. The cells were treated with autophagy activator; Torin 1, mitophagy inducer; CCCP and DNA damage inducer H202 (as a positive control) and then subjected to confocal microscopy analysis. According to the data obtained from confocal microscopy images, it was observed that p-H2AX formation was increasing upon autophagy and mitophagy activation compared to control. Same results were obtained in p-H2AX dot counting as in Fig 3.6.5. Additionally, p-H2AX immunoblotting results shown in Fig.3.6.6 implicated that upon autophagy and mitophagy leads to DNA damage accumulation in the cell.

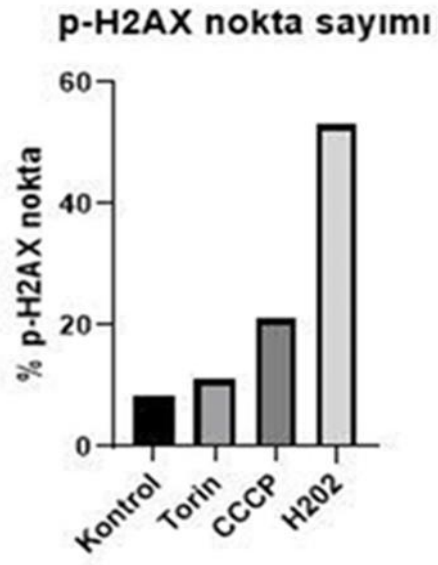

Figure 3.6.5: Quantification of confocal microscopy analysis in MEF cells.. Confocal microscopy images of Torin 1 (250nM, 3h), CCCP (10μM, 24h), H2O2 (1mM, 4h) and DMSO as a vehicle treated cells were analyzed and p-H2AX foci formation counted in the nucleus. P-H2AX foci formation in the nucleus of 50 cells were counted per condition.

The cells that have nuclear p-h2AX foci more than the average was shown as p-H2AX positive.cells and the percentage of positive cells were represented in the graph.

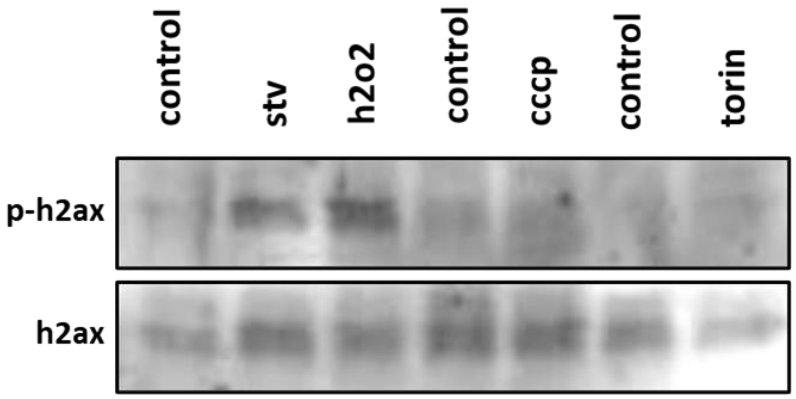

Figure 3.6.6: The effect of autophagy activation on DNA DSB damage in MEF cells. Cells were treated with EBSS Torin 1 (250nM, 3h), CCCP (10μM, 24h), H2O2 (1mM, 4h) and DMSO as a vehicle. Following the treatment, SDS-PAGE analysis and immunoblotting were performed. Anti-p-H2AX and p-H2AX were used for immunoblotting. (STV; starvation, H2O2; hydrogen peroxide, Torin; Torin1).

3.7 ANALYSIS OF THE EFFECT OF AUTOPHAGY ACTIVATION AND INHIBITION ON KU70 TURNOVER

To understand the relationship between autophagy and DNA damage response in further, or to clarify whether the interaction between ATG5 and KU70 is related with autophagic turnover of KU70, immunoblotting experiment was designed under autophagy inducing and autophagy inhibiting conditions. For this purpose, MEF cells were treated with autophagy inducer STV and Torin 1 with or without lysosomal inhibitors E64D, Pepstatin A and Hydroxychloroqine and then subjected to the immunoblot analysis. The data acquired from the immunoblotting experiment in Fig.3.7.1 revealed that upon autophagy activation with STV and Torin, autophagic activity increased in the cells which was

understood from autophagy markers; p62 degradation and LC3 1 to LC3 II shift. And inhibited autophagic activity was confirmed in STV+E+P, STV+HQ and Torin1 +E+P, Torin 1+HQ conditions through accumulation of LC3 II and degradation of p62. KU70 level did not decrease with autophagy activation or did not increase autophagy inhibition remarking that KU70 is not the autophagy target under these conditions. Therefore, KU70-ATG5 interaction might have a different role than the autophagy.

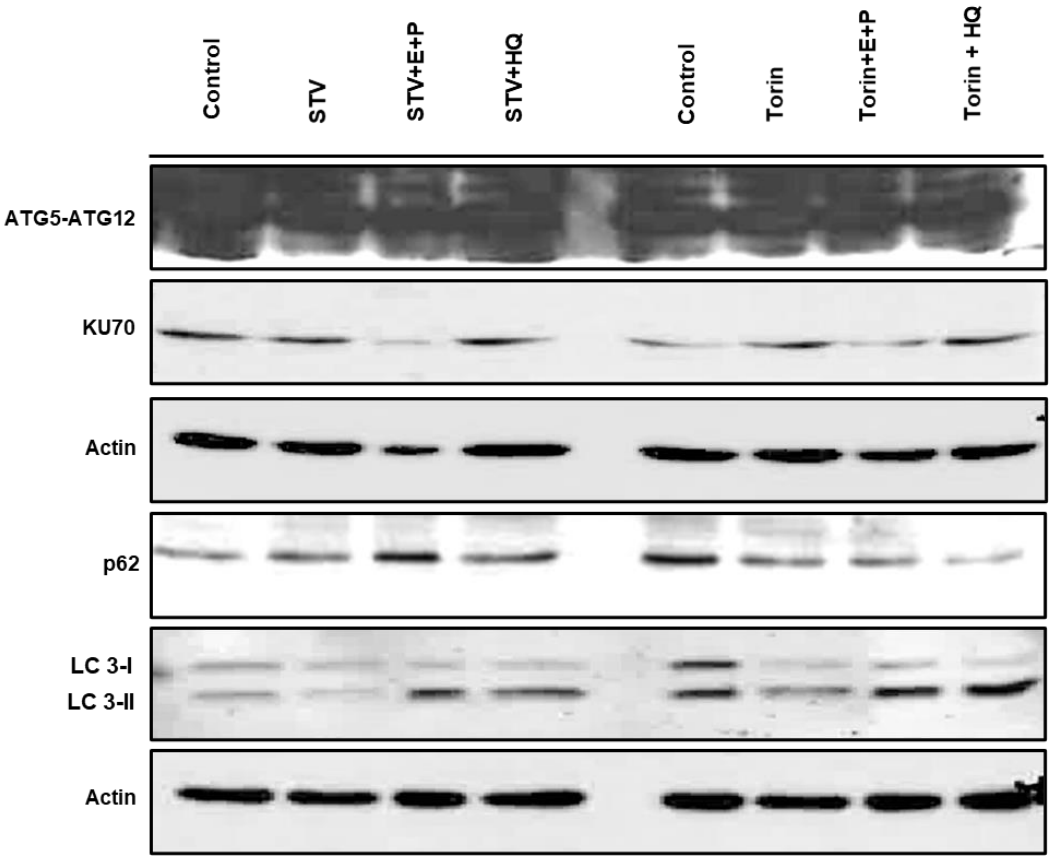

Figure 3.7.1: The effect of autophagy activation and inhibition on KU70 degradation in MEF cells. Cells were treated with EBSS (4h) +/- E+P (E64D (10µg/ml) and pepstatin A (10µg/ml)) and +/- HQ (10µM, 1h), Torin 1 (250nM, 3h) +/- E+P and +/- HQ (10µM, 1h) and DMSO as a vehicle. Following the treatment, SDS-PAGE analysis and immunoblotting were performed. Anti-ATG5, anti-Ku70, anti-p62 and anti-LC3 were used for immunoblotting. b-Actin used for loading control (STV; starvation, H2O2, Torin; Torin1, HQ; hydroxychloroquin).

3.8 ANALYIS OF THE EFFECT OF DNA DSB DAMAGE RESPONSE ON AUTOPHAGY ACTIVATION

In order to understand the molecular crosstalk between autophagy and DNA damage response, autophagic activity was examined under DNA DSB damage and DSB repair conditions. HeLa cells were treated with etoposide and left for repair during different periods. Then cell lysates were subjected to the immunoblotting process. Acquired data from immunoblotting experiment determined that autophagic activity was not remarkably active during DNA damage period, and 3h-6h recovery periods but, it was increasing after 24h recovery of DSB DNA damage.

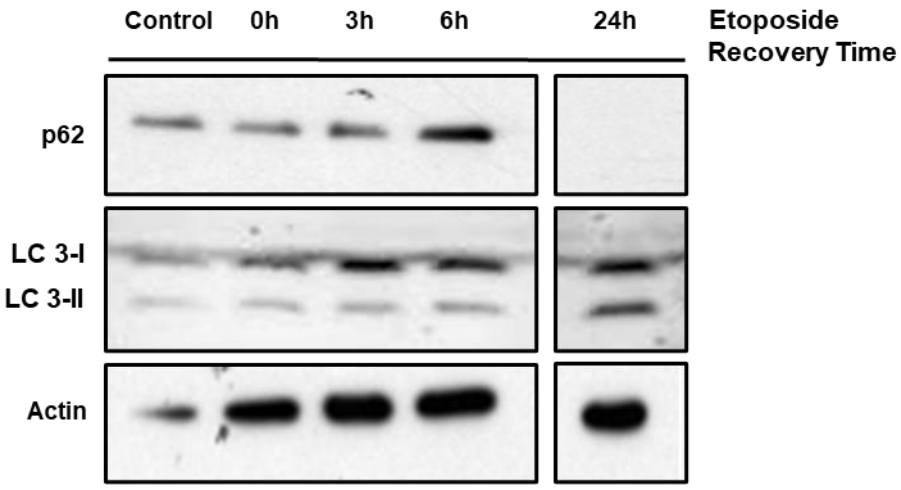

Figure 3.8.1: The effect of Etoposide induced DNA damage and repair on autophagy activation. Hela cells treated with Etoposide (25μM, 1h) and the drug was removed 1h after from the cells. Culture media was replenished and cells were incubated for 0h, 3h, 6h and 24h. After incubation, cell lysates were subjected to SDS-PAGE analysis and immunoblotting. Anti-p62 and anti-LC3 were used for immunoblotting. b-Actin used for loading control.

3.9 THE FUNCTIONAL ROLE OF ATG5-KU70 INTERACTION IN DNA DAMAGE REPAIR

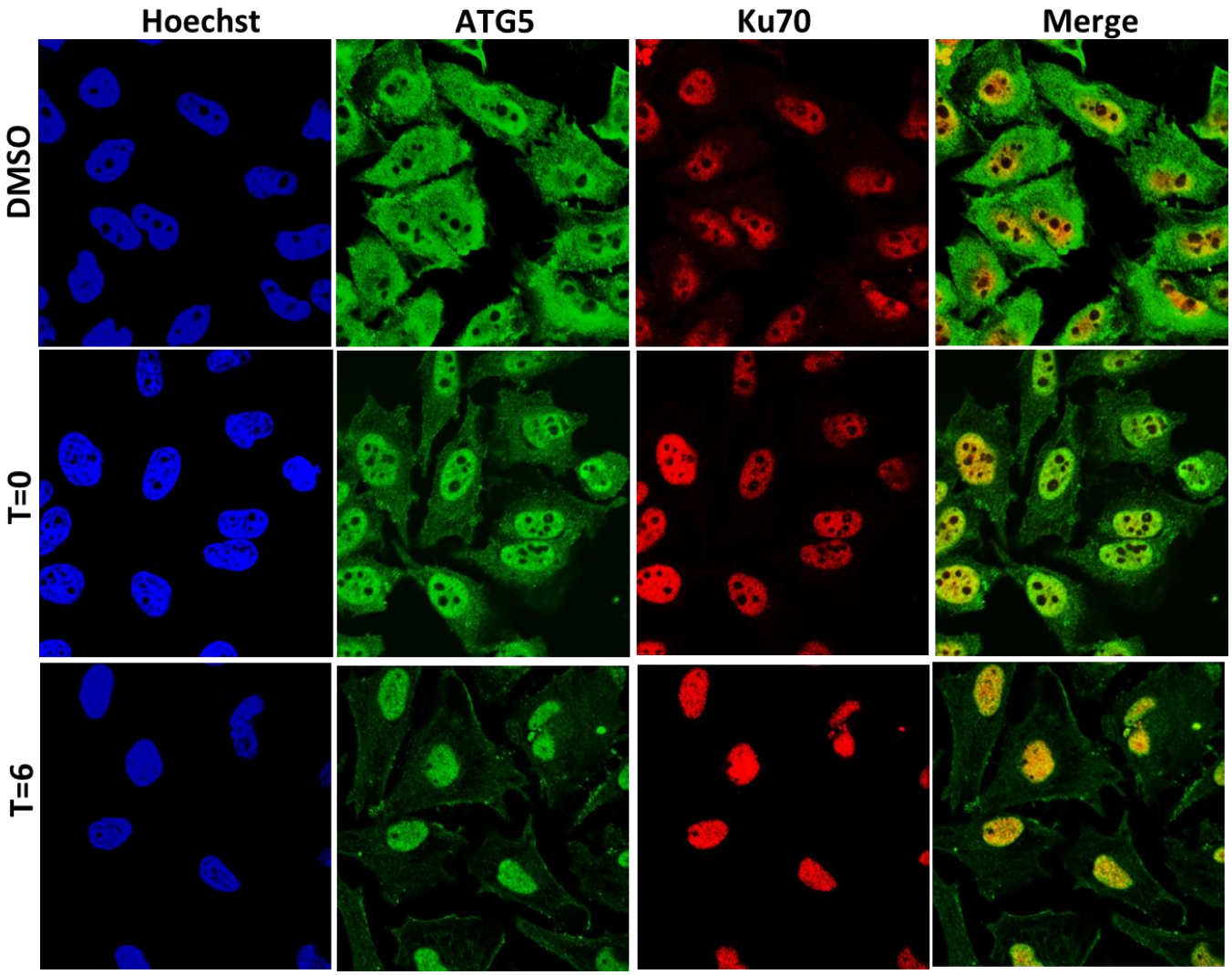

Figure 3.9.1: Colocalization analysis between ATG5 and KU70 under DNA damage and repair inducing conditions in HeLa cells. Hela cells treated with Etoposide (25μM, 1h) and the drug was removed 1h after from the cells. Culture media was replenished and cells were incubated for 0h, 6h and 24h for recovery. After treatments, cells were fixed with 4% PFA and permeabilized with Triton-X. Then permeabilized cells were incubated with Anti-ATG5 and anti-Ku70 primary antibodies and Alexa Fluor-488 (Green) and alexa-568 (red) secondary antibodies. After washes, fixed cells were stained with DAPI (Blue) and analyzed under confocal microscope at 63x. (Merge, overlay of green and red signals)

To discover the role ATG5-KU70 interaction in DNA DSB repair, colocalization analysis were performed under DNA DSB damage stimulation and the repair conditions. ATG5 Crispr KO HeLa (ATG5KO) cells and ATG5WT cells were exposed to 1h etoposide treatment and then left for recovery during 0h or 6h. Treated cells were subjected to immunofluorescence analysis and examined under confocal microscopy. Quantification of ATG5-KU70 nuclear colocalization based on the confocal microscopy images were shown also in Fig.3.9.2. These results which were represented in Fig. 3.9.1 and Fig.3.9.2 indicated that nuclear colocalization of ATG5 and KU70 depending on overlapping signals was significantly increased during DNA DSB damage compare to undamaged conditions and further increased at 6h recovery period. To conclude, ATG5-KU70 interaction has a functional role in DNA damage and DNA DSB repair possibly by NHEJ pathway.

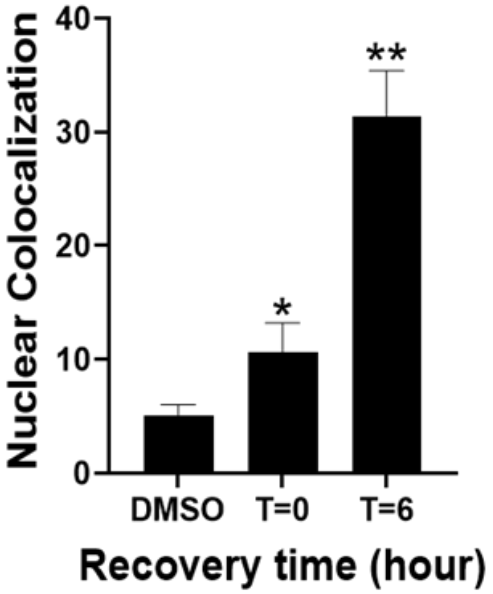

Figure 3.9.2: Quantification of DNA damage and repair induced ATG5-KU70 colocalization in HeLa cells. Confocal microscopy images of Etoposide (25μM, 1h) treated and recovered cells were analyzed and colocalization of ATG5 (green) and KU70 (Red) signal was calculated based on the overlapping coefficient of these signals in the nucleus. KU70-ATG5 colocalization signals that have the overlapping coefficient higher

than 0.5 were accepted as colocalized and represented in the graph as percentage. graph (mean ± S.D. of independent experiments, n = 3, *, p<0.05).

3.9.1 Analysis of the effect of ATG5 over etoposide induced DNA DSB damage and following repair process

To further clarify functional role of ATG5-KU70 interaction in DNA DSB damage and repair, the immunoblotting experiments were designed under DNA DSB and repair inducing conditions in ATG5KO and ATG5WT HeLa cells.

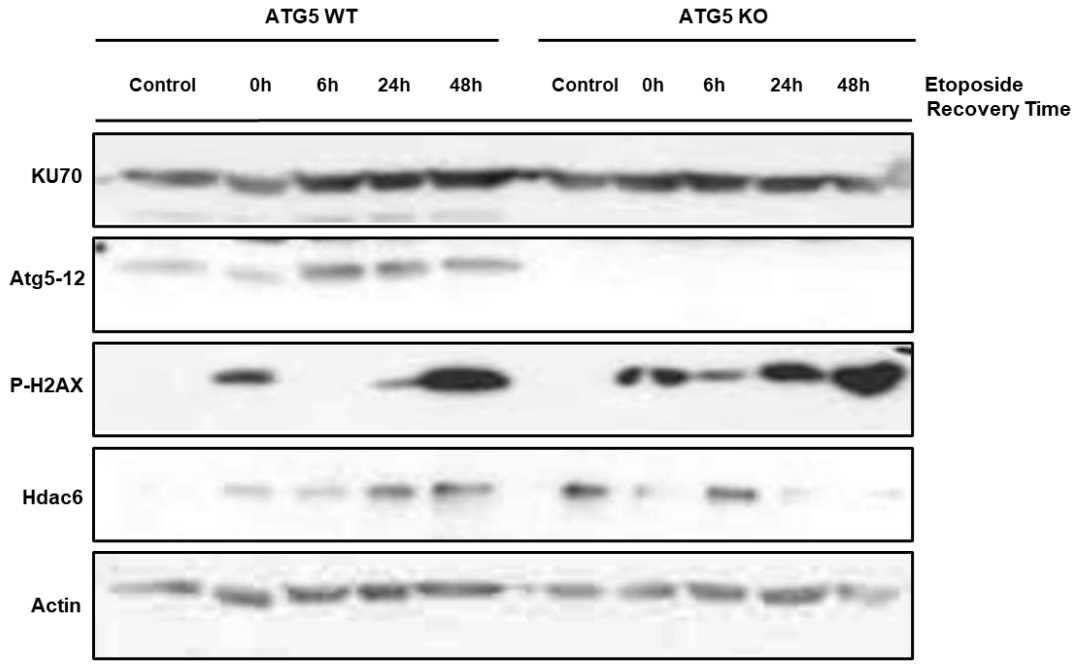

Figure 3.9.1.1: The effect of ATG5 deprivation on DNA DSB damage and repair periods in ATG5KO and ATG5WT HeLa cells. ATG5KO and ATG5WT HeLa cells treated with Etoposide (25μM, 1h) and the drug was removed 1h after from the cells. Culture media was replenished and cells were incubated for 0h, 6h and 24h. After the treatments, cell lysates were subjected to SDS-PAGE analysis and immunoblotting. Anti-p62, anti-KU70, anti-ATG5, anti-p-H2AX and anti-Hdac6 were used for immunoblotting. b-Actin used for loading control.

Examination of DNA DSB damage and resolution was demonstrated in immunoblotting experiments represented in Fig. 3.9.1.1 and 3.9.1.2. According to results which is shown in Fig. 3.9.1.1, DNA DSB damage accumulated in ATG5KO cells higher than the ATG5WT cells through the level of p-H2AX. The damage in ATGWT cells were repaired after 6h but, ATG5KO cells was still have DNA damage accumulation after 6h. ATG5-ATG12 complex and KU70 protein levels was increased also during repair periods; 6h, 24h and 48h in ATG5WT cells. Moreover, Hdac 6 protein levels was found differently changed in WT and KO cells which indicating free KU70 related with apoptosis.

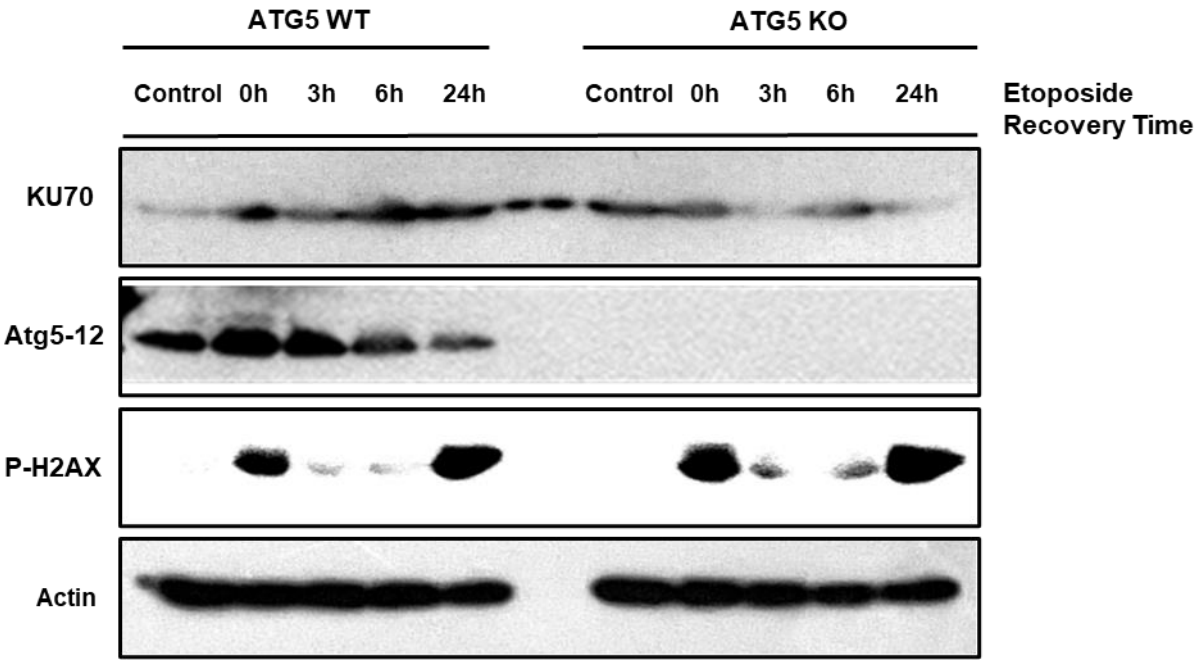

Figure 3.9.1.2: The effect of ATG5 deprivation on DNA DSB damage and repair periods in ATG5KO and ATG5WT HeLa cells. ATG5KO and ATG5WT HeLa cells were treated with Etoposide (25µM, 1h) and the drug was removed 1h after from the cells. Culture media was replenished and cells were incubated for 0h, 3h, 6h and 24h. After the treatments, cell lysates were subjected to SDS-PAGE analysis and immunoblotting. Anti-p62, anti-KU70, anti-ATG5 and anti-p-H2AX were used for immunoblotting. b-Actin used for loading control.

Similar results were obtained from represented data in Fig.3.9.1.2. The Lack of ATG5 caused increased p-H2AX accumulation for 3h and 6h repair periods in ATG5KO cells. Also ATG5KO cells had higher p-H2AX accumulation in 0h and 24h than ATG5KO cells.

3.9.2 ATG5 rescue recovers the delay in DNA DSB repair induced by etoposide

In order to check whether enhanced DNA damage accumulation which was identified as p-H2AX protein level was depended on ATG5 protein, it was planned a rescue experiment in ATG5KO HeLa cells. ATG5KO cells were transfected with full length nontagged ATG5 construct and then treated with Etoposide and left for recovery for 3h, 6h and 24h. Following treatments, cells were subjected to immunoblotting analysis and the results were shown in Fig. 3.9.2.1. As it was argued, replenishment of ATG5 protein in KO cells were rescued resolution of p-H2AX accumulation at 6h which is implying absence of ATG5 caused persistent DNA DSB damage in HeLa cells.

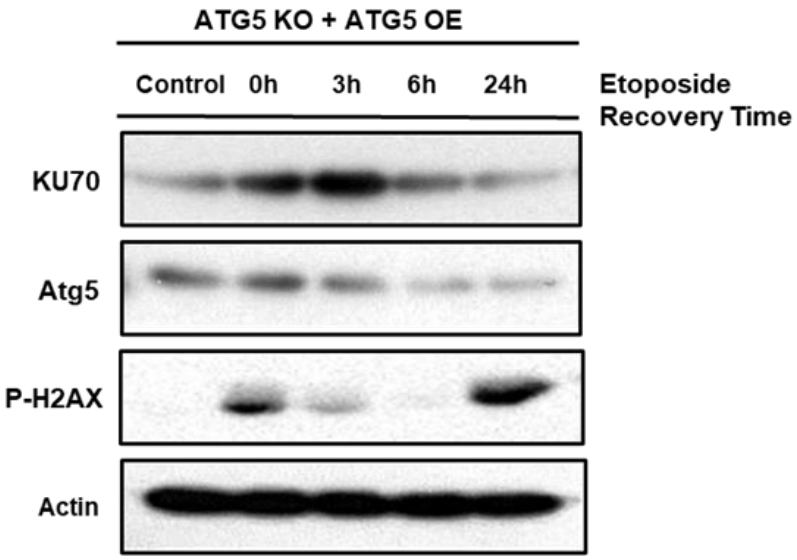

Figure 3.9.2.1: The effect of ATG5 rescue on DNA DSB damage and DSB repair process in ATG5KO HeLa cells. ATG5KO cells were transfected with non-tagged full length ATG5 construct. Following 24h transfection, cells were treated with Etoposide (25μM, 1h) and the drug was removed 1h after from the cells. Culture media was replenished and cells were incubated for 0h, 3h, 6h and 24h. After the treatments, cell lysates were subjected to SDS-PAGE analysis and immunoblotting. Anti-KU70, anti-ATG5 and anti-p-H2AX were used for immunoblotting. b-Actin used for loading control.

3.9.3 ATG5 is not included in p-H2AX foci formation upon DNA DSB induction by Etoposide.

ATG5 and K70 interaction was established in previous experiments under DNA DSB damage stimulation but, it was not known whether KU70-ATG5 complex includes DSB marker protein p-H2AX or whether this interaction occurs onto chromatin in concerted with p-H2AX. For the purpose of it, confocal microscopy analysis was designed to check colocalization between ATG5 and p-H2AX under DNA DSB stimulation. HeLa cells were treated with etoposide during 24h and then immunofluorescence experiment was performed. Colocalization analysis in Fig 3.9.3.1 and quantification data in Fig. 3.9.3.2 demonstrated that ATG5 and p-H2AX colocalized partially but not significantly.

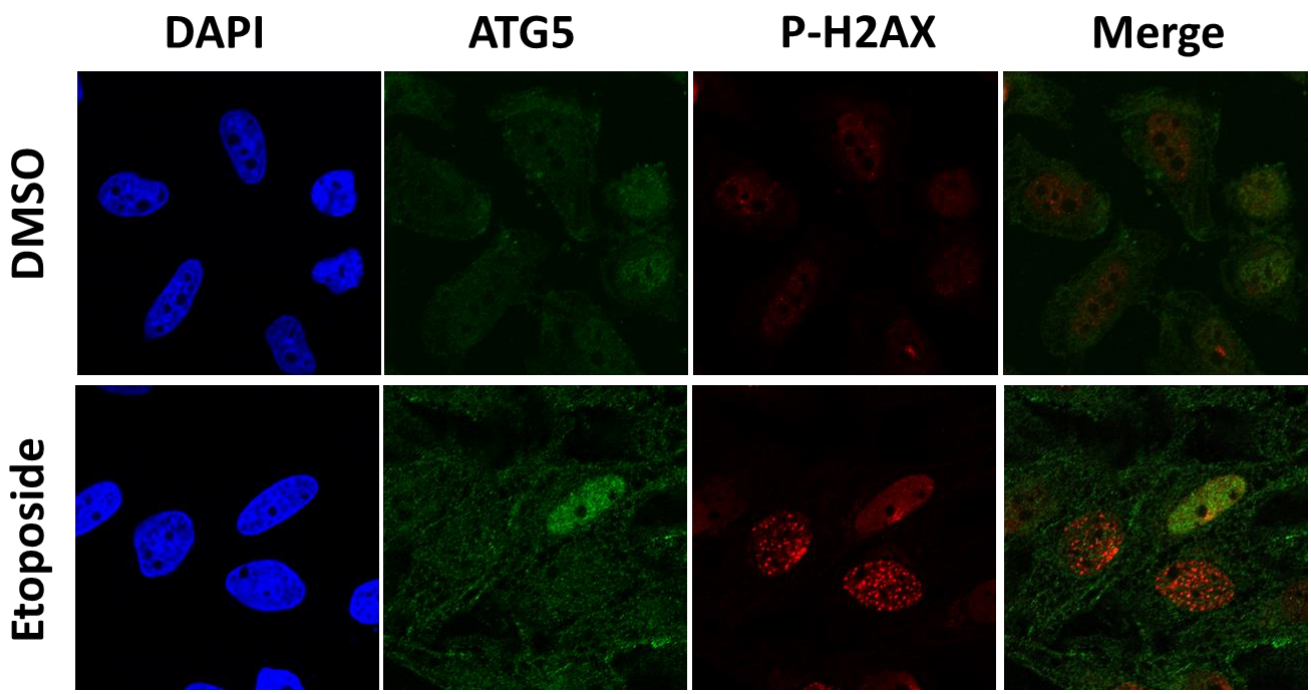

Figure 3.9.3.1: Colocalization analysis between ATG5 and p-H2AX under DNA damage induction by etoposide in HeLa cells. Hela cells treated with Etoposide (25µM, 24h). After the treatment, cells were fixed with 4% PFA and permeabilized with Triton-X. Then permeabilized cells were incubated with Anti-p-ATG5 and anti-p-H2AX primary antibodies and Alexa Fluor-488 (Green) and alexa-568 (red) secondary antibodies. After washes, fixed cells were stained with DAPI (Blue) and analyzed under confocal microscope at 63x. (Merge, overlay of green and red signals)

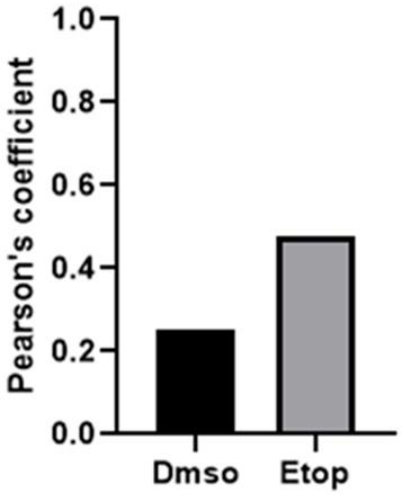

Figure 3.9.3.2: Colocalization analysis of ATG5 and p-H2AX under the DNA DSB damage inducing condition in HeLa cells. Confocal microscopy images of Etoposide (25µM, 24h) treated cells were analyzed and colocalization of ATG5 (green) and p-H2AX (Red) signal was calculated based on the pearson's coefficient of these signals in the nucleus by using image J, JACoP plug in. p-H2AX-ATG5 colocalization signals based on the pearson's coefficient were represented in the graph.

3.9.4: Loss of ATG5-Ku70 interaction enables recovery of genotoxic stress induced by etoposide.

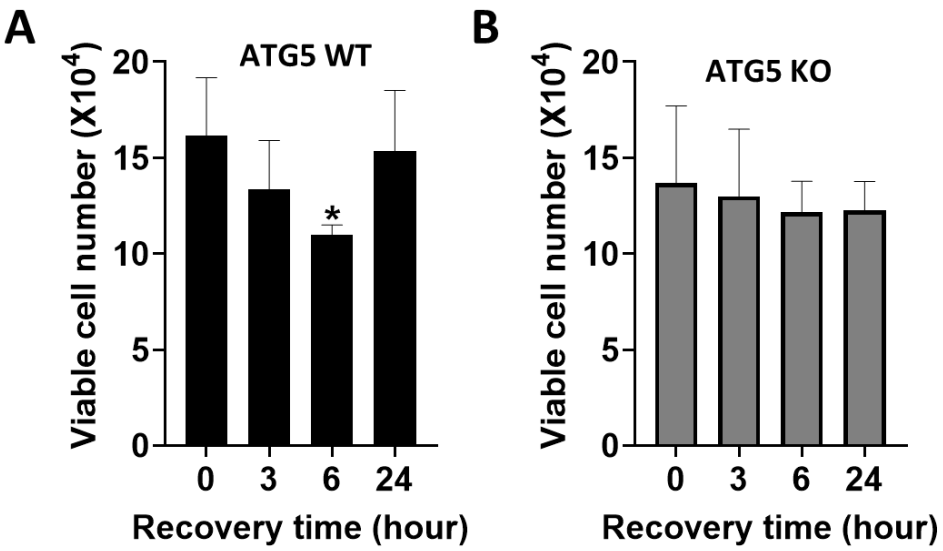

Figure 3.9.4.1: Cellular viability of ATG5WT and ATG5 KO cells under the DNA DSB damage and repair conditions. Cells were treated with etoposide (25µM, 1h) After the

treatment, culture media was replenished and cells were incubated for 0h, 3h, 6h and 24h. for recovery. Then cell viability were assessed by trypan blue exclusion assay (mean ± S.D. of independent experiments, n = 3, *, $p<0.05$).

3.10 ANALYSIS OF THE EFFECT OF DNA DAMAGE ON ATG5 AND DNA REPAIR GENE EXPRESSION LEVEL

ATG5-KU70 interaction at protein levels were established in previous analysis, to test whether gene expression of ATG5 and KU70 was affected during DNA DSB damage induced by Etoposide and Cisplatin, RT-PCR experiments were performed by using ATG5, KU70, KU80 and DNA-PKcs genes specific primers in HeLa cells. mRNA expression levels were normalized to GAPDH mRNA and representative graphs were shown in Fig. 3.10.1, Fig.3.10.2, Fig.3.10.3 and Fig.3.10.4. According to the results, it was observed that upon Etoposide treatment, gene expression level of ATG5, KU70, KU80 and DNA-PKcs significantly decreased. There was no significant change in gene expression levels of these genes in cisplatin treated cells.

In order to analyze, whether decrease in gene expression levels of ATG5, KU70, KU80 and DNA-PKcs reflects the changes in protein levels, it was performed immunoblotting experiment in the same conditions. According to the results which is shown in Fig 3.10.5, there was no any decrease in protein levels of ATG5, KU70 and KU80 in etoposide treated samples which implies etoposide causes increased protein levels related with increasing protein stability rather than increasing expression of the genes.

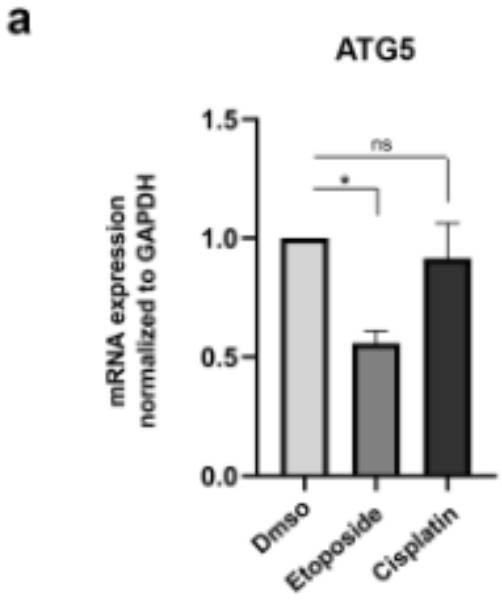

Figure 3.10.1: Effect of DNA damage induced by etoposide and cisplatin on ATG5 mRNA levels. ATG5 mRNA expression levels were quantified by RT-qPCR in HeLa cells treated with etoposide (25μM, 24h) and cisplatin (1μg/ml, 24h). ATG5 specific primer set was used for analysis. Data were normalized to *GAPDH* (mean ±SD of n=3 independent experiments, *p<0.02, ns p>0.05).

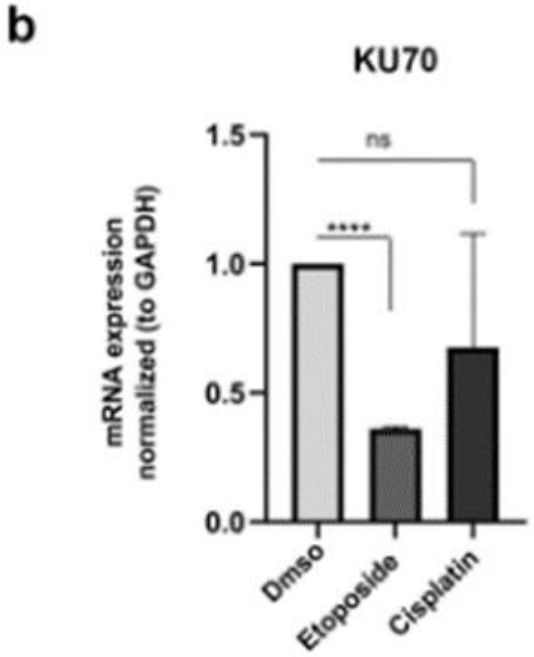

Figure 3.10.2: Effect of DNA damage induced by etoposide and cisplatin on KU70 mRNA levels. KU70 mRNA expression levels were quantified by RT-qPCR in HeLa

cells treated with etoposide (25µM, 24h) and cisplatin (1µg/ml, 24h). KU70 specific primer set was used for analysis. Data were normalized to GAPDH (mean ±SD of n=3 independent experiments, ****p<0.0001, ns p>0.05).

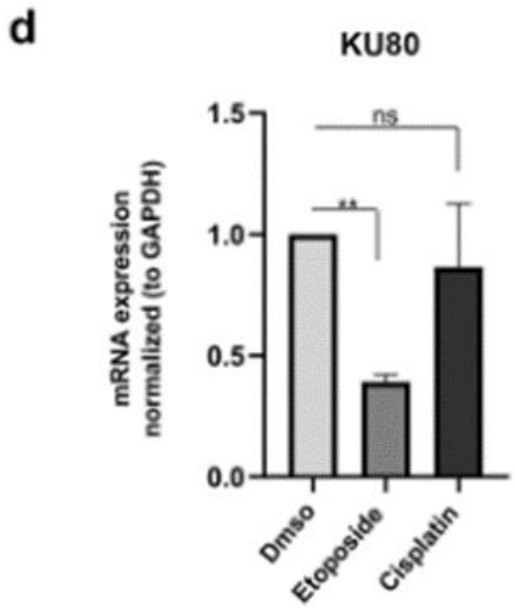

Figure 3.10.3: Effect of DNA damage induced by etoposide and cisplatin on KU80 mRNA levels. KU80 mRNA expression levels were quantified by RT-qPCR in HeLa cells treated with etoposide (25µM, 24h) and cisplatin (1µg/ml, 24h). KU80 specific primer set was used for analysis. Data were normalized to GAPDH (mean ±SD of n=3 independent experiments, **p<0.01, ns p>0.05).

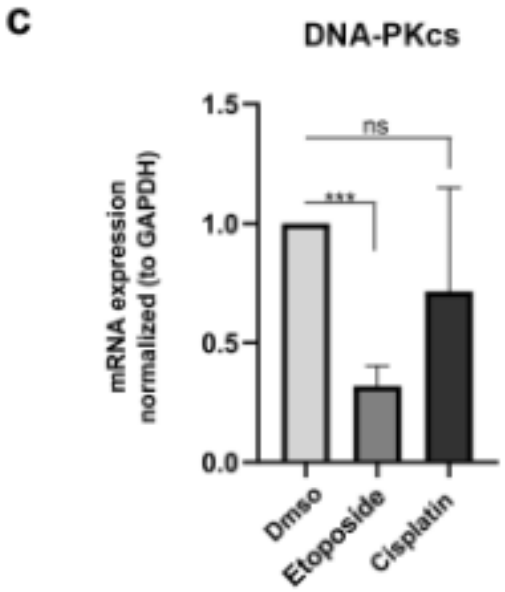

Figure 3.10.4: Effect of DNA damage induced by etoposide and cisplatin on DNA-PKcs mRNA levels. DNA-PKcs mRNA expression levels were quantified by RT-qPCR in HeLa cells treated with etoposide (25µM, 24h) and cisplatin (1µg/ml, 24h). DNA-PKcs specific primer set was used for analysis. Data were normalized to GAPDH (mean ±SD of n=3 independent experiments, ***p<0.001, ns p>0.05).

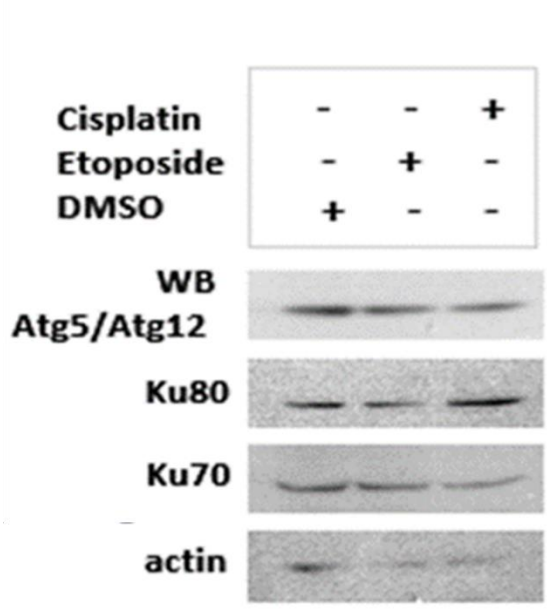

Figure 3.10.5: The effect of DNA damage on ATG5, KU70 and KU80 protein levels. HeLa cells treated with etoposide (25µM, 24h) and cisplatin (1µg/ml, 24h). After treatment, cell lysates were subjected to SDS-PAGE and immunoblotting. Anti-KU70,

anti-ATG5 and anti-KU80 were used for immunoblotting. b-Actin used for loading control.

4. DISCUSSION

Autophagy and DNA repair systems are evolutionarily conserved and well-defined cellular mechanisms. Although the autophagy and DNA repair have different players that are responsible for specific tasks, these two processes act in a harmony with each other in regulating the response to chemotherapy or radiation in order to provide genomic stability of a cell.

Emerging data related with the crosstalk between autophagy and genome maintenance was also enlarged with the studies dissecting the more detailed role of autophagy in DNA repair. Autophagy controlled ROS production mitigates DNA damage, autophagy can also recycle main DNA repair proteins included in the operation of lesions so, change the dynamics of the DNA repair process (Robert et al., 2011). Therapeutic implications in autophagy deficient cells results in attenuation of DNA damage responses including suppression of checkpoint kinase-1 activation, aberrant DNA DSB repair by HRR and more reliance on NHEJ repair for cell survival (Gillespie & Ryan, 2016). Moreover, autophagy impaired cells exhibit defective NHEJ repair depending on decreased chromatin recruitment of Ku70, Ku80, DNA-PKcs and XLF proteins (Sharma et al., 2020). Therefore, in case of autophagy deficiency, suppression of NHEJ following DNA damage leads to persistent genomic lesions and rapid cell death (Liu et al., 2015).

In this thesis study, we discovered that: autophagy marker protein ATG5 is found within a complex with major NHEJ repair proteins; Ku70, Ku80 and DNA-PKcs. Moreover, we showed a direct protein-protein interactions between ATG5-Ku70 and

ATG5-Ku80 also we showed that these interactions were increasing with the DNA DSB damage induction. for the first time we showed that NHEJ component Ku70 in the same complex with ATG5-12 and it is dynamic enhanced upon genotoxic stress; iv, ATG5 nuclear translocation-induced by genotoxic stress and its interaction with Ku70 predominantly occurs in the nuclei; v, ATG5-Ku70 interaction in nucleus is more significant during recovery from the DNA-damage was observed; vi, loss of ATG5 was abolished the repair capacity of cells and enable proliferation following recovery.

Utilizing Tri-SILAC-LC-MS/MS, co-immunoprecipitation, confocal microscopy and gel filtration analyses, we demonstrated that ATG5 interacted with NHEJ components including DNA-PKcs, Ku70 and Ku80. A novel and direct interaction with endogenous ATG5 validated with Ku70 in nucleus under basal condition. Our data revealed that these interactions were highly dynamic and enhanced following genotoxic stress by DNA damage causing agents.

Protective role of autophagy upon genotoxic stress was previously described (Karantza-Wadsworth et al., 2007). Several studies indicated that ATG5 exerts an alternative function during genotoxic stress independently from its role in autophagy (Maskey et al., 2013; Pyo et al., 2005; Sun et al., 2021; Yousefi et al., 2006). Nuclear ATG5 was shown to interact with survivin and blocked its association with Aurora B, a chromosomal passenger complex protein (CPC) regulating mitosis (Maskey et al., 2013). In another study, nuclear ATG5 has also been associated with increased drug resistance and microsatellite instability-high (MSI-H) phenotype in colorectal cancer (Sun et al., 2021). In our system, nuclear translocation of ATG5 was increased upon DNA damage and it was more prominent during repair after post-damage. Although several studies

reported the nuclear role of ATG5, yet the role of nuclear ATG5 during repair was not reported.

The role of autophagy proteins in DDR and repair mechanisms have been studied previously (J. M. Park et al., 2014; Zhao et al., 2012). Although some autophagy-related proteins have been addressed in the NHEJ mechanisms, no study documented the involvement of ATG5 in NHEJ. Ionizing-radiation (IR)-induced damage caused by the accumulation of UVRAG, an autophagy-related protein, facilitates the activation of DNA-PKcs by monitoring the recruitment of DNA-PKcs for the recognition of DSBs (Zhao et al., 2012). Of note, Loss of UVRAG or attenuation of autophagic activity resulted in impaired repair (Zhao et al., 2012).

Therefore, in addition to involvement of individual autophagy-related proteins in the orchestration of DNA repair, autophagy capacity of cells may be important. Cellular clearance of NHEJ complex proteins may be regulated by two major cellular catabolic processes, UPS, and autophagy (Kocaturk & Gozuacik, 2018). Rather than engulfment of cargo by autophagosomes in autophagy, UPS involves the poly-ubiquitination of target proteins and their degradation in the proteasomes (Ciechanover, 1998).

Although they were shown to act individually on different targets, in some contexts, they were co-regulated (Korolchuk et al., 2009). Increased autophagic activity following mTOR-inhibition has been associated with reduced UPS and led to the accumulation of Ku80 and XRCC4 in IR-induced DNA damage in hematopoietic stem cells (HSCs) (Lin et al., 2015). In another study, DDR protein, checkpoint kinase 1 (Chk1)

which plays a critical role in the decision between Homologous repair (HR) and NHEJ was found to be degraded by CMA. Of note, another autophagic degradation system called chaperone mediated autophagy (CMA) was shown to be enhanced upon inhibition of autophagy (C. Park et al., 2015). SQSTM1/p62 is a well-known autophagy receptor protein which is degraded upon autophagic activity. p62 was reported to be accumulated on DNA lesions upon genotoxic stress. Following IR-induced damage, p62 was shown to be interacted with Filamin A following nuclear translocation. This interaction facilitated the degradation of both Filamin A and RAD51 by proteasomes into nucleus which favors NHEJ over HR (Hewitt et al., 2016).

HR is another major repair mechanism responsible for the repair of DSBs (Takata et al., 1998). Loss of autophagic activity was reported to cause a shift in between these two major DSBs repair mechanisms. IR-induced DNA damage activates autophagy which in turn degrades USP14, deubiquitinase of Ku70. Inhibition of IR-induced autophagy causes accumulation of USP14 on DSBs that enables recruitment of NHEJ components on IR-induced foci. Autophagy deficient cells were identified as insufficient to recruit NHEJ components on DSBs and accumulate more IR-induced foci which was associated with diminished repair capacity (Sharma et al., 2018).

Deregulation of DNA-PKcs activity or disintegration of Ku70/Ku80 heterodimer may cause severe defects in NHEJ and lead to an unrepairable genomic instability. For instance, levels of NHEJ complex components including DNA-PKcs, Ku70 and Ku80, were reported to be upregulated in several cancer cells following radio- and chemotherapy which hampered the efficacy of the anti-cancer therapy (Begg et al., 2011). Therefore, targeting NHEJ may serve as a key role to sensitize cancer cells against

therapeutics. Anti-cancer drugs were generally designed to target rapidly dividing cancer cells through introducing DNA damage. Unrepaired damages were found to be associated with mitotic catastrophe (MC) and subsequent cell death to avoid genomic instability (Vitale et al., 2011). Previous studies reported that intact autophagic activity was important for cell death following mitotic catastrophe (Maskey et al., 2013; Sorokina et al., 2017; Vitale et al., 2011). Anti-cancer drug-induced MC was reduced in autophagy incompetent cells. Of note, in some cases, MC was found to be induced upon autophagic activation (Sorokina et al., 2017). In contrast, nuclear ATG5-induced mitotic catastrophe was not found to be linked with elevated cell death (Maskey et al., 2013). Our data suggested that cells are more sensitive to anti-cancer drugs when autophagy is intact during recovery. Strikingly, we discovered that loss of ATG5 resulted in attenuation of recovery following post-damage.

Altogether, our study revealed an important interaction between autophagy machinery and NHEJ repair during genotoxic stress. There has been no published data showing that ATG5 is involved in NHEJ. We discovered for the first time that ATG5-Ku70 interaction is required for the efficacy of repair following genotoxic stress. Hence, we proposed a new role of autophagy protein ATG5 in DNA-damage repair following genotoxic stress.

Table 3.2.1: The list of studies in the literature conducted on the association between autophagy and DNA repair systems (Sarıkaya et al, 2021)

Cell line/Tissue And Organism	**Drug/Genetic modification**	**Repair Mechanism**	**DNA Repair-associated Target**	**Autophagy Status**	**Quantification of DNA Damage**	**Reference**
Ampk -/- and WT MEFs	UVB	NER	XPC	N.D.	Slot blot assay of CPD and 6-4PP	(C. L. Wu et al. 2013)
Atg5 -/- ; Atg7 -/- and WT MEFs, HaCaT	UVB	NER	XPC	Inhibited	Slot blot assay of CPD and 6-4PP	(L. Qiang et al. 2016)

Hs294T, A2058	Cisplatin	NER	XPA	Activated	PARP1 activity	(Ge et al. 2016)
Primary human Fibroblast	XPA-/-	NER	XPA, PARP1	Inhibited	PARP1 activity	(Fang et al. 2014)
Parp1 -/- and WT MEFs, MCF7	Starvation	BER	PARP1	Inhibited	PARP1 activity	(José M. Rodríguez-Vargas et al. 2016)

HL1 mouse cardiomyocyte	Serum and Glucose deprivation	BER	OGG1	Activated	Detection of γH2AX, p-ATM, NBS1 and 8-oxoG	(Siggens et al. 2012)
MLE-12	Hyperoxia	BER	OGG1	Inhibited	Comet tail length, OGG1 activity	(Ye et al. 2017)
U2OS	5-FU	BER	MSH2	Activated	PARP1 activity	(P. Sengupta et al. 2013)
C.elegans	5-FU	BER	MSH2, MSH6	Activated	RPA-1 filament formation, CHK-1 phosphorylation	(P. Sengupta et al. 2013)

AGS, NCI-N87	5-FU, AT101	BER	APE1	Activated	N.D.	(Wei, Duan, et al. 2016)
HCT116, HEC59	6-thioguanine (6-TG)	MMR	MLH1, MSH2	Activated	PARP1 activity	(X. Zeng et al. 2007)
HCT116	6-thioguanine (6-TG) and 5-fluorouracil (5-FU)	MMR	MLH1	Activated	CHK-1 phosphorylation	(J.-R. Zeng et al. 2013)

CAOV-3	Cisplatin	HR	BRCA2	Activated	Comet tail length	(Wan et al. 2018)
786-O	Sunitinib	HR	RAD51	Activated	Micronuclei formation	(Yan et al. 2017)
Mouse Oocytes	Rad51 RNAi	HR	RAD51	Activated	Comet tail length	(K.-H. Kim et al. 2016)
CNE-1, CNE-2	Ionizing radiation (IR)	HR	RAD51	Activated	Detection of γH2AX	(Mo et al. 2014)

HT-29, DLD-1	Ionizing radiation (IR)	NHEJ	UVRAG	Activated	Detection of γH2AX, nuclear foci positivity of 53BP1	(J. M. Park et al. 2014)
TLR4mut liver	Diethylnitrosamine (DEN)	NHEJ	Ku70	Inhibited	Detection of γH2AX and 8-oxoG	(C. Wang and Lees-Miller 2013)
Sqstm1 -/- and WT MEFs	Ionizing radiation (IR)	NHEJ	FLNA and RAD51	Activated	Detection of γH2AX and TP53BP1	(Hewitt et al. 2016)
Bone marrow, Hematopoietic cells	Ionizing radiation (IR)	HR, NHEJ	N.D.	Activated	Detection of γH2AX, Comet tail length	(Y.-H. Lin et al. 2015)

L2A -/-; Atg7 -/- and WT MEFs	Etoposide	HR, NHEJ	CHK1	Inhibited	Detection of γH2AX, Comet tail length	(S.-Y. Park et al. 2015)
Atg7-/- and WT MEFs	Ionizing radiation (IR)	HR, NHEJ	CHK1	Activated	Detection of γH2AX, Comet tail length, Plasmid-based NHEJ and HR assay	(M. Liu et al. 2015)

5. REFERENCES

Abbotts, R., & Wilson, D. M., 3rd. (2017). Coordination of DNA single strand break repair. *Free Radical Biology & Medicine*, *107*, 228–244.

Agarraberes, F. A., & Dice, J. F. (2001). A molecular chaperone complex at the lysosomal membrane is required for protein translocation. Journal of Cell Science, 114(Pt 13), 2491–2499.

Ahel, I., Rass, U., El-Khamisy, S. F., Katyal, S., Clements, P. M., McKinnon, P. J., Caldecott, K. W., & West, S. C. (2006). The neurodegenerative disease protein aprataxin resolves abortive DNA ligation intermediates. Nature, 443(7112), 713–716.

Ahmad, L., Mostowy, S., & Sancho-Shimizu, V. (2018). Autophagy-Virus Interplay: From Cell Biology to Human Disease. In Frontiers in Cell and Developmental Biology (Vol. 6). https://doi.org/10.3389/fcell.2018.00155

Akbari, M., Peña-Diaz, J., Andersen, S., Liabakk, N.-B., Otterlei, M., & Krokan, H. E. (2009). Extracts of proliferating and non-proliferating human cells display different base excision pathways and repair fidelity. DNA Repair, 8(7), 834–843.

Akbari, M., Visnes, T., Krokan, H. E., & Otterlei, M. (2008). Mitochondrial base excision repair of uracil and AP sites takes place by single-nucleotide insertion and long-patch DNA synthesis. DNA Repair, 7(4), 605–616.

Almeida, K. H., & Sobol, R. W. (2007). A unified view of base excision repair: lesion-dependent protein complexes regulated by post-translational modification. DNA Repair, 6(6), 695–711.

Altmeyer, M., & Lukas, J. (2013). Guarding against Collateral Damage during Chromatin Transactions. In Cell (Vol. 153, Issue 7, pp. 1431–1434). https://doi.org/10.1016/j.cell.2013.05.044

Andres, S. N., Vergnes, A., Ristic, D., Wyman, C., Modesti, M., & Junop, M. (2012). A human XRCC4–XLF complex bridges DNA. Nucleic Acids Research, 40(4), 1868–1878.

Antonioli, M., Di Rienzo, M., Piacentini, M., & Fimia, G. M. (2017). Emerging Mechanisms in Initiating and Terminating Autophagy. Trends in Biochemical Sciences, 42(1), 28–41.

Arana, M. E., Holmes, S. F., Fortune, J. M., Moon, A. F., Pedersen, L. C., & Kunkel, T. A. (2010). Crystal Structure of N terminal domain of a DNA repair protein. Worldwide Protein Data Bank. https://doi.org/10.2210/pdb3h4l/pdb

Bader, C. A., Shandala, T., Ng, Y. S., Johnson, I. R. D., & Brooks, D. A. (2015). Atg9 is required for intraluminal vesicles in amphisomes and autolysosomes. In Biology Open (Vol. 4, Issue 11, pp. 1345–1355). https://doi.org/10.1242/bio.013979

Bae, H., & Guan, J.-L. (2011). Suppression of autophagy by FIP200 deletion impairs DNA damage repair and increases cell death upon treatments with anticancer agents. Molecular Cancer Research: MCR, 9(9), 1232–1241.

Begg, A. C., Stewart, F. A., & Vens, C. (2011). Strategies to improve radiotherapy with targeted drugs. Nature Reviews. Cancer, 11(4), 239–253.

Bennetzen, M. V., Larsen, D. H., Bunkenborg, J., Bartek, J., Lukas, J., & Andersen, J. S. (2010). Site-specific phosphorylation dynamics of the nuclear proteome during the DNA damage response. Molecular & Cellular Proteomics: MCP, 9(6), 1314–1323.

Bergink, S., & Jentsch, S. (2009). Principles of ubiquitin and SUMO modifications in DNA repair. Nature, 458(7237), 461–467.

Bernstein, N. K., Williams, R. S., Rakovszky, M. L., Cui, D., Green, R., Karimi-Busheri, F., Mani, R. S., Galicia, S., Koch, C. A., Cass, C. E., Durocher, D., Weinfeld, M., & Glover, J. N. M. (2005). The molecular architecture of the mammalian DNA repair enzyme, polynucleotide kinase. Molecular Cell, 17(5), 657–670.

Bhatti, S., Kozlov, S., Farooqi, A. A., Naqi, A., Lavin, M., & Khanna, K. K. (2011). ATM protein kinase: the linchpin of cellular defenses to stress. Cellular and Molecular Life Sciences: CMLS, 68(18), 2977–3006.

Bindra, R. S., & Glazer, P. M. (2007). Co-repression of mismatch repair gene expression by hypoxia in cancer cells: role of the Myc/Max network. Cancer Letters, 252(1), 93–103.

Bonilla, C. Y., Melo, J. A., & Toczyski, D. P. (2008). Colocalization of sensors is sufficient to activate the DNA damage checkpoint in the absence of damage. Molecular Cell, 30(3), 267–276.

Boya, P., Reggiori, F., & Codogno, P. (2013). Emerging regulation and functions of autophagy. Nature Cell Biology, 15(7), 713–720

Brown, E. J., & Baltimore, D. (2000). ATR disruption leads to chromosomal fragmentation and early embryonic lethality. Genes & Development, 14(4), 397–402.

Brown, E. J., & Baltimore, D. (2003). Essential and dispensable roles of ATR in cell cycle arrest and genome maintenance. Genes & Development, 17(5), 615–628.

Byun, T. S., Pacek, M., Yee, M.-C., Walter, J. C., & Cimprich, K. A. (2005). Functional uncoupling of MCM helicase and DNA polymerase activities activates the ATR-dependent checkpoint. Genes & Development, 19(9), 1040–1052.

Cadet, J., & Wagner, J. R. (2013). DNA Base Damage by Reactive Oxygen Species, Oxidizing Agents, and UV Radiation. In Cold Spring Harbor Perspectives in Biology (Vol. 5, Issue 2, pp. a012559–a012559). https://doi.org/10.1101/cshperspect.a012559

Carusillo A, Mussolino C. (2020). DNA Damage: From Threat to Treatment. Cells. 10;9(7):1665. doi: 10.3390/cells9071665.

Chapman, J. R., Sossick, A. J., Boulton, S. J., & Jackson, S. P. (2012). BRCA1-associated exclusion of 53BP1 from DNA damage sites underlies temporal control of DNA repair. Journal of Cell Science, 125(Pt 15), 3529–3534.

Chatterjee, N., & Siede, W. (2013). Replicating damaged DNA in eukaryotes. Cold Spring Harbor Perspectives in Biology, 5(12), a019836.

Chatterjee, N., & Walker, G. C. (2017). Mechanisms of DNA damage, repair, and mutagenesis. Environmental and Molecular Mutagenesis, 58(5), 235–263.

Chatterjee, P., Choudhary, G. S., Alswillah, T., & Xiong, X. (2015). The TMPRSS2–ERG gene fusion blocks XRCC4-mediated nonhomologous end-joining repair and radiosensitizes prostate cancer cells to PARP inhibition. Molecular Cancer. https://mct.aacrjournals.org/content/14/8/1896.short

Chen, H., Ma, Z., Vanderwaal, R. P., Feng, Z., Gonzalez-Suarez, I., Wang, S., Zhang, J., Roti Roti, J. L., Gonzalo, S., & Zhang, J. (2011). The mTOR inhibitor rapamycin suppresses DNA double-strand break repair. Radiation Research, 175(2), 214–224.

Chen, L., Nievera, C. J., Lee, A. Y.-L., & Wu, X. (2008). Cell cycle-dependent complex formation of BRCA1.CtIP.MRN is important for DNA double-strand break repair. The Journal of Biological Chemistry, 283(12), 7713–7720.

Chen, X., Zhao, Y., Li, G.-M., & Guo, L. (2013). Proteomic analysis of mismatch repair-mediated alkylating agent-induced DNA damage response. Cell & Bioscience, 3(1), 37.

Chiang, H. L., Terlecky, S. R., Plant, C. P., & Dice, J. F. (1989). A role for a 70-kilodalton heat shock protein in lysosomal degradation of intracellular proteins. Science, 246(4928), 382–385.

Chu, G., & Chang, E. (1988). Xeroderma pigmentosum group E cells lack a nuclear factor that binds to damaged DNA. In Science (Vol. 242, Issue 4878, pp. 564–567). https://doi.org/10.1126/science.3175673

Ciccia, A., & Elledge, S. J. (2010). The DNA damage response: making it safe to play with knives. Molecular Cell, 40(2), 179–204.

Ciechanover, A. (1998). The ubiquitin–proteasome pathway: on protein death and cell life. The EMBO Journal, 17(24), 7151–7160.

Cimprich, K. A., & Cortez, D. (2008). ATR: an essential regulator of genome integrity. Nature Reviews. Molecular Cell Biology, 9(8), 616–627.

Compe, E., & Egly, J.-M. (2012). TFIIH: when transcription met DNA repair. In Nature Reviews Molecular Cell Biology (Vol. 13, Issue 6, pp. 343–354). https://doi.org/10.1038/nrm3350

Cuervo, A. M., & Dice, J. F. (1996). A receptor for the selective uptake and degradation of proteins by lysosomes. Science, 273(5274), 501–503.

Curtin, N. J. (2012). DNA repair dysregulation from cancer driver to therapeutic target. Nature Reviews. Cancer, 12(12), 801–817.

D'Andrea, A. D. (2015). DNA Repair Pathways and Human Cancer. In The Molecular Basis of Cancer (pp. 47–66.e2). https://doi.org/10.1016/b978-1-4557-4066-6.00004-4

Demirbağ-Sarıkaya, S., Çakir, H., Gözüaçık, D., & Akkoç, Y. (2021). Crosstalk between autophagy and DNA repair systems, Turkish Journal of Biology, 45, 235-252.

Deng, Z., Purtell, K., Lachance, V., Wold, M. S., Chen, S., & Yue, Z. (2017). Autophagy Receptors and Neurodegenerative Diseases. Trends in Cell Biology, 27(7), 491–504.

de Souza-Pinto, N. C., Mason, P. A., Hashiguchi, K., Weissman, L., Tian, J., Guay, D., Lebel, M., Stevnsner, T. V., Rasmussen, L. J., & Bohr, V. A. (2009). Novel DNA mismatch-repair activity involving YB-1 in human mitochondria. DNA Repair, 8(6), 704–719.

Devenish, R., Mijaljica, D., Carlos, & Prescott. (2011). Biosensors for Monitoring Autophagy. In Biosensors - Emerging Materials and Applications. https://doi.org/10.5772/17177

Dianov, G. L., & Hübscher, U. (2013). Mammalian base excision repair: the forgotten archangel. Nucleic Acids Research, 41(6), 3483–3490.

Dice, J. F. (1990). Peptide sequences that target cytosolic proteins for lysosomal proteolysis. Trends in Biochemical Sciences, 15(8), 305–309.

Edwards, R. A., Witherspoon, M., Wang, K., Afrasiabi, K., Pham, T., Birnbaumer, L., & Lipkin, S. M. (2009). Epigenetic repression of DNA mismatch repair by inflammation

and hypoxia in inflammatory bowel disease-associated colorectal cancer. Cancer Research, 69(16), 6423–6429.

EMBO reports: Vol 9, No 8. (n.d.). https://doi.org/10.1002/embor.v9.8

Fagbemi, A. F., Orelli, B., & Schärer, O. D. (2011). Regulation of endonuclease activity in human nucleotide excision repair. In DNA Repair (Vol. 10, Issue 7, pp. 722–729). https://doi.org/10.1016/j.dnarep.2011.04.022

Fousteri, M., Vermeulen, W., van Zeeland, A. A., & Mullenders, L. H. F. (2006). Cockayne Syndrome A and B Proteins Differentially Regulate Recruitment of Chromatin Remodeling and Repair Factors to Stalled RNA Polymerase II In Vivo. In Molecular Cell (Vol. 23, Issue 4, pp. 471–482). https://doi.org/10.1016/j.molcel.2006.06.029

Friedberg, E. C., Lehmann, A. R., & Fuchs, R. P. P. (2005). Trading places: how do DNA polymerases switch during translesion DNA synthesis? Molecular Cell, 18(5), 499–505.

Fu, Q., Shi, H., Ren, Y., Guo, F., Ni, W., Qiao, J., Wang, P., Zhang, H., & Chen, C. (2014). Bovine viral diarrhea virus infection induces autophagy in MDBK cells. In Journal of Microbiology (Vol. 52, Issue 7, pp. 619–625). https://doi.org/10.1007/s12275-014-3479-4

Gasser, S., & Raulet, D. (2006). The DNA damage response, immunity and cancer. Seminars in Cancer Biology, 16(5), 344–347.

Gillespie, D. A., & Ryan, K. M. (2016). Autophagy is critically required for DNA repair by homologous recombination. Molecular & Cellular Oncology, 3(1), e1030538.

Gillet, L. C. J., & Schärer, O. D. (2006). Molecular mechanisms of mammalian global genome nucleotide excision repair. Chemical Reviews, 106(2), 253–276.

Glick, D., Barth, S., & Macleod, K. F. (2010). Autophagy: cellular and molecular mechanisms. In The Journal of Pathology (Vol. 221, Issue 1, pp. 3–12). https://doi.org/10.1002/path.2697

Golding, S. E., Morgan, R. N., Adams, B. R., Hawkins, A. J., Povirk, L. F., & Valerie, K. (2009). Pro-survival AKT and ERK signaling from EGFR and mutant EGFRvIII enhances DNA double-strand break repair in human glioma cells. In Cancer Biology & Therapy (Vol. 8, Issue 8, pp. 730–738). https://doi.org/10.4161/cbt.8.8.7927

Goldstein, M., & Kastan, M. B. (2015). The DNA damage response: implications for tumor responses to radiation and chemotherapy. Annual Review of Medicine, 66, 129–143.

Gottlieb, T. M., & Jackson, S. P. (1993). The DNA-dependent protein kinase: requirement for DNA ends and association with Ku antigen. Cell, 72(1), 131–142.

Grawunder, U. (1997). A complex of RAG-1 and RAG-2 proteins persists on DNA after single- strand cleavage at V(D)J recombination signal sequences. In Nucleic Acids Research (Vol. 25, Issue 7, pp. 1375–1382). https://doi.org/10.1093/nar/25.7.1375

Guarné, A., & Charbonnier, J.-B. (2015). Insights from a decade of biophysical studies on MutL: Roles in strand discrimination and mismatch removal. Progress in Biophysics and Molecular Biology, 117(2-3), 149–156.

Hammel, M., Rey, M., Yu, Y., Mani, R. S., Classen, S., Liu, M., Pique, M. E., Fang, S., Mahaney, B. L., Weinfeld, M., Schriemer, D. C., Lees-Miller, S. P., & Tainer, J. A. (2011). XRCC4 protein interactions with XRCC4-like factor (XLF) create an extended grooved scaffold for DNA ligation and double strand break repair. The Journal of Biological Chemistry, 286(37), 32638–32650.

Hara, T., & Mizushima, N. (2009). Role of ULK-FIP200 complex in mammalian autophagy: FIP200, a counterpart of yeast Atg17? In Autophagy (Vol. 5, Issue 1, pp. 85–87). https://doi.org/10.4161/auto.5.1.7180

Harper, J. W., & Elledge, S. J. (2007). The DNA damage response: ten years after. Molecular Cell, 28(5), 739–745.

Herb, M., Gluschko, A., & Schramm, M. (2020). LC3-associated phagocytosis - The highway to hell for phagocytosed microbes. In Seminars in Cell & Developmental Biology (Vol. 101, pp. 68–76). https://doi.org/10.1016/j.semcdb.2019.04.016

Hewish, M., Lord, C. J., Martin, S. A., Cunningham, D., & Ashworth, A. (2010). Mismatch repair deficient colorectal cancer in the era of personalized treatment. Nature Reviews. Clinical Oncology, 7(4), 197–208.

Hewitt, G., Carroll, B., Sarallah, R., Correia-Melo, C., Ogrodnik, M., Nelson, G., Otten, E. G., Manni, D., Antrobus, R., Morgan, B. A., von Zglinicki, T., Jurk, D., Seluanov, A., Gorbunova, V., Johansen, T., Passos, J. F., & Korolchuk, V. I. (2016). SQSTM1/p62 mediates crosstalk between autophagy and the UPS in DNA repair. Autophagy, 12(10), 1917–1930.

Heyer, W.-D. (2015). Regulation of recombination and genomic maintenance. Cold Spring Harbor Perspectives in Biology, 7(8), a016501.

Holland, P., Knævelsrud, H., Søreng, K., Mathai, B. J., Lystad, A. H., Pankiv, S., Bjørndal, G. T., Schultz, S. W., Lobert, V. H., Chan, R. B., Zhou, B., Liestøl, K., Carlsson, S. R., Melia, T. J., Di Paolo, G., & Simonsen, A. (2016). HS1BP3 negatively regulates autophagy by modulation of phosphatidic acid levels. Nature Communications, 7, 13889.

Hossain, M. A., Lin, Y., & Yan, S. (2018). Single-Strand Break End Resection in Genome Integrity: Mechanism and Regulation by APE2. International Journal of Molecular Sciences, 19(8). https://doi.org/10.3390/ijms19082389

Huffman, J., Sundheim, O., & Tainer, J. (2005). Structural Features of DNA Glycosylases and AP Endonucleases. In DNA Damage Recognition. https://doi.org/10.1201/9780849352683.pt3

Iyama, T., & Wilson, D. M., 3rd. (2013). DNA repair mechanisms in dividing and non-dividing cells. DNA Repair, 12(8), 620–636.

Iyer, R. R., Pluciennik, A., Burdett, V., & Modrich, P. L. (2006). DNA mismatch repair: functions and mechanisms. Chemical Reviews, 106(2), 302–323.

Jackson, S. P., & Bartek, J. (2009). The DNA-damage response in human biology and disease. Nature, 461(7267), 1071–1078.

Jacobs, A. L., & Schär, P. (2012). DNA glycosylases: in DNA repair and beyond. Chromosoma, 121(1), 1–20.

Jiang, P., & Mizushima, N. (2014). Autophagy and human diseases. In Cell Research (Vol. 24, Issue 1, pp. 69–79). https://doi.org/10.1038/cr.2013.161

Jiricny, J. (2006). MutLalpha: at the cutting edge of mismatch repair [Review of MutLalpha: at the cutting edge of mismatch repair]. Cell, 126(2), 239–241.

Joy, S., Thirunavukkarasu, L., Agrawal, P., Singh, A., Sagar, B. K. C., Manjithaya, R., & Surolia, N. (2018). Basal and starvation-induced autophagy mediates parasite survival during intraerythrocytic stages of Plasmodium falciparum. Cell Death Discovery, 4, 43.

Kamada, Y., Yoshino, K.-I., Kondo, C., Kawamata, T., Oshiro, N., Yonezawa, K., & Ohsumi, Y. (2010). Tor directly controls the Atg1 kinase complex to regulate autophagy. Molecular and Cellular Biology, 30(4), 1049–1058.

Kanaar, R., Wyman, C., & Rothstein, R. (2008). Quality control of DNA break metabolism: in the "end", it's a good thing. The EMBO Journal, 27(4), 581–588.

Karantza-Wadsworth, V., Patel, S., Kravchuk, O., Chen, G., Mathew, R., Jin, S., & White, E. (2007). Autophagy mitigates metabolic stress and genome damage in mammary tumorigenesis. Genes & Development, 21(13), 1621–1635.

Kastan, M. B., & Bartek, J. (2004). Cell-cycle checkpoints and cancer. Nature, 432(7015), 316–323.

Katoh, M., Nakajima, M., Yamazaki, H., & Yokoi, T. (2000). Pharmaceutical Research (Vol. 17, Issue 10, pp. 1189–1197). https://doi.org/10.1023/a:1007568811691

Katsuki, Y., & Takata, M. (2016). Defects in homologous recombination repair behind the human diseases: FA and HBOC. In Endocrine-Related Cancer (Vol. 23, Issue 10, pp. T19–T37). https://doi.org/10.1530/erc-16-0221

Kaur, J., & Debnath, J. (2015). Autophagy at the crossroads of catabolism and anabolism. In Nature Reviews Molecular Cell Biology (Vol. 16, Issue 8, pp. 461–472). https://doi.org/10.1038/nrm4024

Kaushik, S., & Cuervo, A. M. (2012). Chaperone-mediated autophagy: a unique way to enter the lysosome world. Trends in Cell Biology, 22(8), 407–417.

Kim, H. J., Lee, S., & Jung, J. U. (2010). When autophagy meets viruses: a double-edged sword with functions in defense and offense. Seminars in Immunopathology, 32(4), 323–341.

Kim, K.-H., Park, J.-H., Kim, E.-Y., Ko, J.-J., Park, K.-S., & Lee, K.-A. (2016). The role of Rad51 in safeguarding mitochondrial activity during the meiotic cell cycle in mammalian oocytes. Scientific Reports, 6, 34110.

Kinsella, T. J. (2009). Coordination of DNA mismatch repair and base excision repair processing of chemotherapy and radiation damage for targeting resistant cancers. Clinical Cancer Research: An Official Journal of the American Association for Cancer Research, 15(6), 1853–1859.

Kitagawa, R., Bakkenist, C. J., & McKinnon, P. J. (2004). Phosphorylation of SMC1 is a critical downstream event in the ATM–NBS1–BRCA1 pathway. Genes. http://genesdev.cshlp.org/content/18/12/1423.short

Kleine, H., & Lüscher, B. (2009). Learning How to Read ADP-Ribosylation. In Cell (Vol. 139, Issue 1, pp. 17–19). https://doi.org/10.1016/j.cell.2009.09.018

Ko, J.-C., Chen, J.-C., Wang, T.-J., Zheng, H.-Y., Chen, W.-C., Chang, P.-Y., & Lin, Y.-W. (2016). Astaxanthin down-regulates Rad51 expression via inactivation of AKT kinase to enhance mitomycin C-induced cytotoxicity in human non-small cell lung cancer cells. Biochemical Pharmacology, 105, 91–100.

Kocaturk, N. M., & Gozuacik, D. (2018). Crosstalk Between Mammalian Autophagy and the Ubiquitin-Proteasome System. Frontiers in Cell and Developmental Biology, 6, 128.

Korolchuk, V. I., Mansilla, A., Menzies, F. M., & Rubinsztein, D. C. (2009). Autophagy inhibition compromises degradation of ubiquitin-proteasome pathway substrates. Molecular Cell, 33(4), 517–527.

Kovtun, I. V., & McMurray, C. T. (2007). Crosstalk of DNA glycosylases with pathways other than base excision repair. DNA Repair, 6(4), 517–529.

Krokan, H. E., & Bjoras, M. (2013). Base Excision Repair. In Cold Spring Harbor Perspectives in Biology (Vol. 5, Issue 4, pp. a012583–a012583). https://doi.org/10.1101/cshperspect.a012583

Kunkel, T. A. (2009). Evolving Views of DNA Replication (In)Fidelity. In Cold Spring Harbor Symposia on Quantitative Biology (Vol. 74, Issue 0, pp. 91–101). https://doi.org/10.1101/sqb.2009.74.027

Kunkel, T. A., & Erie, D. A. (2005). DNA MISMATCH REPAIR. In Annual Review of Biochemistry (Vol. 74, Issue 1, pp. 681–710). https://doi.org/10.1146/annurev.biochem.74.082803.133243

Laddha, S. V., Ganesan, S., Chan, C. S., & White, E. (2014). Mutational landscape of the essential autophagy gene BECN1 in human cancers. Molecular Cancer Research: MCR, 12(4), 485–490.

Lang, T., Dalal, S., Chikova, A., DiMaio, D., & Sweasy, J. B. (2007). The E295K DNA polymerase beta gastric cancer-associated variant interferes with base excision repair and induces cellular transformation. Molecular and Cellular Biology, 27(15), 5587–5596.

Lee, W.-S., Sung, M.-S., Lee, E.-G., Yoo, H.-G., Cheon, Y.-H., Chae, H.-J., & Yoo, W.-H. (2015). A pathogenic role for ER stress-induced autophagy and ER chaperone

GRP78/BiP in T lymphocyte systemic lupus erythematosus. In Journal of Leukocyte Biology (Vol. 97, Issue 2, pp. 425–433). https://doi.org/10.1189/jlb.6a0214-097r

Lei, Y., Zhang, D., Yu, J., Dong, H., Zhang, J., & Yang, S. (2017). Targeting autophagy in cancer stem cells as an anticancer therapy. Cancer Letters, 393, 33–39.

Levine, B., & Kroemer, G. (2008). Autophagy in the pathogenesis of disease. Cell, 132(1), 27–42.

Lieber, M. R., Gu, J., Lu, H., Shimazaki, N., & Tsai, A. G. (2010). Nonhomologous DNA End Joining (NHEJ) and Chromosomal Translocations in Humans. In H.-P. Nasheuer (Ed.), Genome Stability and Human Diseases (pp. 279–296). Springer Netherlands.

Li, G.-M. (2008). Mechanisms and functions of DNA mismatch repair. Cell Research, 18(1), 85–98.

Li, G.-M. (2014). New insights and challenges in mismatch repair: Getting over the chromatin hurdle. In DNA Repair (Vol. 19, pp. 48–54). https://doi.org/10.1016/j.dnarep.2014.03.027

Li, H., Sekine, M., Tung, N., & Avraham, H. K. (2010). Wild-Type BRCA1, but not Mutated BRCA1, Regulates the Expression of the Nuclear Form of -Catenin. In Molecular Cancer Research (Vol. 8, Issue 3, pp. 407–420). https://doi.org/10.1158/1541-7786.mcr-09-0403

Li, M., Zhang, Q., Liu, L., Lu, W., Wei, H., Li, R. W., & Lu, S. (2013). Expression of the mismatch repair gene hMLH1 is enhanced in non-small cell lung cancer with EGFR mutations. PloS One, 8(10), e78500.

Lindahl, T. (1993). Instability and decay of the primary structure of DNA. Nature, 362(6422), 709–715.

Lindahl, T., & Barnes, D. E. (2000). Repair of endogenous DNA damage. Cold Spring Harbor Symposia on Quantitative Biology, 65, 127–133.

Lin, L.-T., Dawson, P. W. H., & Richardson, C. D. (2010). Viral interactions with macroautophagy: a double-edged sword. Virology, 402(1), 1–10.

Lin, M. G., & Hurley, J. H. (2016). Structure and function of the ULK1 complex in autophagy. In Current Opinion in Cell Biology (Vol. 39, pp. 61–68). https://doi.org/10.1016/j.ceb.2016.02.010

Lin, W., Yuan, N., Wang, Z., Cao, Y., Fang, Y., Li, X., Xu, F., Song, L., Wang, J., Zhang, H., Yan, L., Xu, L., Zhang, X., Zhang, S., & Wang, J. (2015). Autophagy confers DNA damage repair pathways to protect the hematopoietic system from nuclear radiation injury. In Scientific Reports (Vol. 5, Issue 1). https://doi.org/10.1038/srep12362

Lin, X., & Howell, S. B. (2006). DNA mismatch repair and p53 function are major determinants of the rate of development of cisplatin resistance. Molecular Cancer Therapeutics, 5(5), 1239–1247.

Lin, X., Kong, L.-N., Huang, C., Ma, T.-T., Meng, X.-M., He, Y., Wang, Q.-Q., & Li, J. (2015). Hesperetin derivative-7 inhibits PDGF-BB-induced hepatic stellate cell activation and proliferation by targeting Wnt/β-catenin pathway. International Immunopharmacology, 25(2), 311–320.

Lin, Y., Dion, V., & Wilson, J. H. (2006). Transcription and Triplet Repeat Instability. In Genetic Instabilities and Neurological Diseases (pp. 691–704). https://doi.org/10.1016/b978-012369462-1/50045-4

Li, S.-J., Sun, S.-J., Gao, J., & Sun, F.-B. (2016). Wogonin induces Beclin-1/PI3K and reactive oxygen species-mediated autophagy in human pancreatic cancer cells. In Oncology Letters (Vol. 12, Issue 6, pp. 5059–5067). https://doi.org/10.3892/ol.2016.5367

Liu, E. Y., Xu, N., O'Prey, J., Lao, L. Y., Joshi, S., Long, J. S., O'Prey, M., Croft, D. R., Beaumatin, F., Baudot, A. D., Mrschtik, M., Rosenfeldt, M., Zhang, Y., Gillespie, D. A., & Ryan, K. M. (2015). Loss of autophagy causes a synthetic lethal deficiency in DNA repair. In Proceedings of the National Academy of Sciences (Vol. 112, Issue 3, pp. 773–778). https://doi.org/10.1073/pnas.1409563112

Liu, P., & Demple, B. (2010). DNA repair in mammalian mitochondria: Much more than we thought? Environmental and Molecular Mutagenesis, 51(5), 417–426.

Li, X., & Heyer, W.-D. (2008). Homologous recombination in DNA repair and DNA damage tolerance. Cell Research, 18(1), 99–113.

Li, Z., Wen, J., Lin, Y., Wang, S., Xue, P., Zhang, Z., Zhou, Y., Wang, X., Sui, L., Bi, L.-J., & Zhang, X.-E. (2011). A Sir2-like protein participates in mycobacterial NHEJ. PloS One, 6(5), e20045.

Malivert, L., Ropars, V., Nunez, M., Drevet, P., Miron, S., Faure, G., Guerois, R., Mornon, J.-P., Revy, P., Charbonnier, J.-B., Callebaut, I., & de Villartay, J.-P. (2010). Delineation of the Xrcc4-interacting region in the globular head domain of cernunnos/XLF. The Journal of Biological Chemistry, 285(34), 26475–26483.

Mari, M., Griffith, J., Rieter, E., Krishnappa, L., Klionsky, D. J., & Reggiori, F. (2010). An Atg9-containing compartment that functions in the early steps of autophagosome

biogenesis. In Journal of Cell Biology (Vol. 190, Issue 6, pp. 1005–1022). https://doi.org/10.1083/jcb.200912089

Marini, F., Nardo, T., Giannattasio, M., Minuzzo, M., Stefanini, M., Plevani, P., & Muzi Falconi, M. (2006). DNA nucleotide excision repair-dependent signaling to checkpoint activation. Proceedings of the National Academy of Sciences of the United States of America, 103(46), 17325–17330.

Mari, P.-O., Florea, B. I., Persengiev, S. P., Verkaik, N. S., Brüggenwirth, H. T., Modesti, M., Giglia-Mari, G., Bezstarosti, K., Demmers, J. A. A., Luider, T. M., Houtsmuller, A. B., & van Gent, D. C. (2006). Dynamic assembly of end-joining complexes requires interaction between Ku70/80 and XRCC4. Proceedings of the National Academy of Sciences of the United States of America, 103(49), 18597–18602.

Maron, B. J. (2009). Clinical Outcome and Phenotypic Expression in LAMP2 Cardiomyopathy. In JAMA (Vol. 301, Issue 12, p. 1253). https://doi.org/10.1001/jama.2009.371

Marteijn, J. A., Lans, H., Vermeulen, W., & Hoeijmakers, J. H. J. (2014). Understanding nucleotide excision repair and its roles in cancer and ageing. Nature Reviews. Molecular Cell Biology, 15(7), 465–481.

Martin, S. A., Lord, C. J., & Ashworth, A. (2010). Therapeutic targeting of the DNA mismatch repair pathway. Clinical Cancer Research: An Official Journal of the American Association for Cancer Research, 16(21), 5107–5113.

Martin, S. A., McCabe, N., Mullarkey, M., Cummins, R., Burgess, D. J., Nakabeppu, Y., Oka, S., Kay, E., Lord, C. J., & Ashworth, A. (2010). DNA polymerases as potential

therapeutic targets for cancers deficient in the DNA mismatch repair proteins MSH2 or MLH1. Cancer Cell, 17(3), 235–248.

Marti, T. M., Hefner, E., Feeney, L., Natale, V., & Cleaver, J. E. (2006). H2AX phosphorylation within the G1 phase after UV irradiation depends on nucleotide excision repair and not DNA double-strand breaks. Proceedings of the National Academy of Sciences of the United States of America, 103(26), 9891–9896.

Maskey, D., Yousefi, S., Schmid, I., Zlobec, I., Perren, A., Friis, R., & Simon, H.-U. (2013). ATG5 is induced by DNA-damaging agents and promotes mitotic catastrophe independent of autophagy. Nature Communications, 4, 2130.

Masutani, C., Sugasawa, K., Yanagisawa, J., Sonoyama, T., Ui, M., Enomoto, T., Takio, K., Tanaka, K., van der Spek, P. J., & Bootsma, D. (1994). Purification and cloning of a nucleotide excision repair complex involving the xeroderma pigmentosum group C protein and a human homologue of yeast RAD23. The EMBO Journal, 13(8), 1831–1843.

Matsuoka, S., Ballif, B. A., Smogorzewska, A., McDonald, E. R., 3rd, Hurov, K. E., Luo, J., Bakalarski, C. E., Zhao, Z., Solimini, N., Lerenthal, Y., Shiloh, Y., Gygi, S. P., & Elledge, S. J. (2007). ATM and ATR substrate analysis reveals extensive protein networks responsive to DNA damage. Science, 316(5828), 1160–1166.

Ma, Y., & Lieber, M. R. (2002). Binding of inositol hexakisphosphate (IP6) to Ku but not to DNA-PKcs. The Journal of Biological Chemistry, 277(13), 10756–10759.

Meek, K., Dang, V., & Lees-Miller, S. P. (2008). DNA-PK: the means to justify the ends? Advances in Immunology, 99, 33–58.

Menck, C. F., & Munford, V. (2014). DNA repair diseases: What do they tell us about cancer and aging? Genetics and Molecular Biology, 37(1 Suppl), 220–233.

Mercer, T. J., Gubas, A., & Tooze, S. A. (2018). A molecular perspective of mammalian autophagosome biogenesis. In Journal of Biological Chemistry (Vol. 293, Issue 15, pp. 5386–5395). https://doi.org/10.1074/jbc.r117.810366

Mihaylova, V. T., Bindra, R. S., Yuan, J., Campisi, D., Narayanan, L., Jensen, R., Giordano, F., Johnson, R. S., Rockwell, S., & Glazer, P. M. (2003). Decreased expression of the DNA mismatch repair gene Mlh1 under hypoxic stress in mammalian cells. Molecular and Cellular Biology, 23(9), 3265–3273.

Mimitou, E. P., & Symington, L. S. (2010). Ku prevents Exo1 and Sgs1-dependent resection of DNA ends in the absence of a functional MRX complex or Sae2. The EMBO Journal, 29(19), 3358–3369.

Misteli, T., & Soutoglou, E. (2009). The emerging role of nuclear architecture in DNA repair and genome maintenance. Nature Reviews. Molecular Cell Biology, 10(4), 243–254.

Mizushima, N. (2007). Autophagy: process and function. In Genes & Development (Vol. 21, Issue 22, pp. 2861–2873). https://doi.org/10.1101/gad.1599207

Mizushima, N., & Komatsu, M. (2011). Autophagy: Renovation of Cells and Tissues. In Cell (Vol. 147, Issue 4, pp. 728–741). https://doi.org/10.1016/j.cell.2011.10.026

Mizushima, N., Levine, B., Cuervo, A. M., & Klionsky, D. J. (2008). Autophagy fights disease through cellular self-digestion. Nature, 451(7182), 1069–1075.

Mocquet, V., Lainé, J. P., Riedl, T., Yajin, Z., Lee, M. Y., & Egly, J. M. (2008). Sequential recruitment of the repair factors during NER: the role of XPG in initiating the resynthesis step. In The EMBO Journal (Vol. 27, Issue 1, pp. 155–167). https://doi.org/10.1038/sj.emboj.7601948

Møllersen, L., Rowe, A. D., Illuzzi, J. L., Hildrestrand, G. A., Gerhold, K. J., Tveterås, L., Bjølgerud, A., Wilson, D. M., 3rd, Bjørås, M., & Klungland, A. (2012). Neil1 is a genetic modifier of somatic and germline CAG trinucleotide repeat instability in R6/1 mice. Human Molecular Genetics, 21(22), 4939–4947.

Mo, N., Lu, Y.-K., Xie, W.-M., Liu, Y., Zhou, W.-X., Wang, H.-X., Nong, L. I., Jia, Y.-X., Tan, A.-H., Chen, Y., Li, S.-S., & Luo, B.-H. (2014). Inhibition of autophagy enhances the radiosensitivity of nasopharyngeal carcinoma by reducing Rad51 expression. In Oncology Reports (Vol. 32, Issue 5, pp. 1905–1912). https://doi.org/10.3892/or.2014.3427

Moser, J., Kool, H., Giakzidis, I., Caldecott, K., Mullenders, L. H. F., & Fousteri, M. I. (2007). Sealing of chromosomal DNA nicks during nucleotide excision repair requires XRCC1 and DNA ligase III alpha in a cell-cycle-specific manner. Molecular Cell, 27(2), 311–323.

Murphy, D. L., Donigan, K. A., Jaeger, J., & Sweasy, J. B. (2012). The E288K colon tumor variant of DNA polymerase β is a sequence specific mutator. Biochemistry, 51(26), 5269–5275.

Nakamura, H., Tanimoto, K., Hiyama, K., Yunokawa, M., Kawamoto, T., Kato, Y., Yoshiga, K., Poellinger, L., Hiyama, E., & Nishiyama, M. (2008). Human mismatch

repair gene, MLH1, is transcriptionally repressed by the hypoxia-inducible transcription factors, DEC1 and DEC2. Oncogene, 27(30), 4200–4209.

Nimonkar, A. V., Genschel, J., & Kinoshita, E. (2011). BLM–DNA2–RPA–MRN and EXO1–BLM–RPA–MRN constitute two DNA end resection machineries for human DNA break repair. Genes. http://genesdev.cshlp.org/content/25/4/350.short

Nishi, R., Okuda, Y., Watanabe, E., Mori, T., Iwai, S., Masutani, C., Sugasawa, K., & Hanaoka, F. (2005). Centrin 2 Stimulates Nucleotide Excision Repair by Interacting with Xeroderma Pigmentosum Group C Protein. In Molecular and Cellular Biology (Vol. 25, Issue 13, pp. 5664–5674). https://doi.org/10.1128/mcb.25.13.5664-5674.2005

Odell, I. D., Wallace, S. S., & Pederson, D. S. (2013). Rules of engagement for base excision repair in chromatin. Journal of Cellular Physiology, 228(2), 258–266.

Orenstein, S. J., & Cuervo, A. M. (2010). Chaperone-mediated autophagy: Molecular mechanisms and physiological relevance. In Seminars in Cell & Developmental Biology (Vol. 21, Issue 7, pp. 719–726). https://doi.org/10.1016/j.semcdb.2010.02.005

Pang, D., Vidic, B., Rodgers, J., Berman, B. L., & Dritschilo, A. (1997). Atomic force microscope imaging of DNA and DNA repair proteins:Applications in radiobiological research. In Radiation Oncology Investigations (Vol. 5, Issue 4, pp. 163–169). https://doi.org/10.1002/(sici)1520-6823(1997)5:4<163::aid-roi1>3.0.co;2-w

Panier, S., & Boulton, S. J. (2014). Double-strand break repair: 53BP1 comes into focus. Nature Reviews. Molecular Cell Biology, 15(1), 7–18.

Pankiv, S., Lamark, T., Bruun, J.-A., Øvervatn, A., Bjørkøy, G., & Johansen, T. (2010). Nucleocytoplasmic shuttling of p62/SQSTM1 and its role in recruitment of nuclear

polyubiquitinated proteins to promyelocytic leukemia bodies. The Journal of Biological Chemistry, 285(8), 5941–5953.

Park, C., Suh, Y., & Cuervo, A. M. (2015). Regulated degradation of Chk1 by chaperone-mediated autophagy in response to DNA damage. Nature Communications, 6, 6823.

Park, J. M., Tougeron, D., Huang, S., Okamoto, K., & Sinicrope, F. A. (2014). Beclin 1 and UVRAG confer protection from radiation-induced DNA damage and maintain centrosome stability in colorectal cancer cells. PloS One, 9(6), e100819.

Parzych, K. R., & Klionsky, D. J. (2014). An overview of autophagy: morphology, mechanism, and regulation. Antioxidants & Redox Signaling, 20(3), 460–473.

Pyo, J.-O., Jang, M.-H., Kwon, Y.-K., Lee, H.-J., Jun, J.-I., Woo, H.-N., Cho, D.-H., Choi, B., Lee, H., Kim, J.-H., Mizushima, N., Oshumi, Y., & Jung, Y.-K. (2005). Essential roles of Atg5 and FADD in autophagic cell death: dissection of autophagic cell death into vacuole formation and cell death. The Journal of Biological Chemistry, 280(21), 20722–20729.

Paulsen, R. D., Soni, D. V., Wollman, R., Hahn, A. T., Yee, M.-C., Guan, A., Hesley, J. A., Miller, S. C., Cromwell, E. F., Solow-Cordero, D. E., Meyer, T., & Cimprich, K. A. (2009). A genome-wide siRNA screen reveals diverse cellular processes and pathways that mediate genome stability. Molecular Cell, 35(2), 228–239.

Peltomaki, P. (2001). Deficient DNA mismatch repair: a common etiologic factor for colon cancer. In Human Molecular Genetics (Vol. 10, Issue 7, pp. 735–740). https://doi.org/10.1093/hmg/10.7.735

Perry, J. J. P., Yannone, S. M., Holden, L. G., Hitomi, C., Asaithamby, A., Han, S., Cooper, P. K., Chen, D. J., & Tainer, J. A. (2006). WRN exonuclease structure and molecular

mechanism imply an editing role in DNA end processing. Nature Structural & Molecular Biology, 13(5), 414–422.

Pfeiffer, P., Goedecke, W., & Obe, G. (2000). Mechanisms of DNA double-strand break repair and their potential to induce chromosomal aberrations. Mutagenesis, 15(4), 289–302.

Pollard, J., & Curtin, N. (2018). Targeting the DNA Damage Response for Anti-Cancer Therapy. Springer.

Ramadan, K., Shevelev, I., & Hübscher, U. (2004). The DNA-polymerase-X family: controllers of DNA quality? Nature Reviews. Molecular Cell Biology, 5(12), 1038–1043.

Ray, P. D., & Fry, R. C. (2015). Chapter 2 - The Cell: The Fundamental Unit in Systems Biology. In R. C. Fry (Ed.), Systems Biology in Toxicology and Environmental Health (pp. 11–42). Academic Press.

Rello-Varona, S., Lissa, D., Shen, S., Niso-Santano, M., Senovilla, L., Mariño, G., Vitale, I., Jemaá, M., Harper, F., Pierron, G., Castedo, M., & Kroemer, G. (2012). Autophagic removal of micronuclei. Cell Cycle , 11(1), 170–176.

Reynolds, P., Cooper, S., Lomax, M., & O'Neill, P. (2015). Disruption of PARP1 function inhibits base excision repair of a sub-set of DNA lesions. Nucleic Acids Research, 43(8), 4028–4038.

Riley, T., Sontag, E., Chen, P., & Levine, A. (2008). Transcriptional control of human p53-regulated genes. Nature Reviews. Molecular Cell Biology, 9(5), 402–412.

Robertson, A. B., Klungland, A., Rognes, T., & Leiros, I. (2009). DNA repair in mammalian cells: Base excision repair: the long and short of it. Cellular and Molecular Life Sciences: CMLS, 66(6), 981–993.

Roberts, S. A., Strande, N., Burkhalter, M. D., Strom, C., Havener, J. M., Hasty, P., & Ramsden, D. A. (2010). Ku is a 5'-dRP/AP lyase that excises nucleotide damage near broken ends. Nature, 464(7292), 1214–1217.

Robert, T., Vanoli, F., Chiolo, I., Shubassi, G., Bernstein, K. A., Rothstein, R., Botrugno, O. A., Parazzoli, D., Oldani, A., Minucci, S., & Foiani, M. (2011). HDACs link the DNA damage response, processing of double-strand breaks and autophagy. In Nature (Vol. 471, Issue 7336, pp. 74–79). https://doi.org/10.1038/nature09803

Rogakou, E. P., Pilch, D. R., Orr, A. H., Ivanova, V. S., & Bonner, W. M. (1998). DNA double-stranded breaks induce histone H2AX phosphorylation on serine 139. The Journal of Biological Chemistry, 273(10), 5858–5868.

Rothkamm, K., Krüger, I., Thompson, L. H., & Löbrich, M. (2003). Pathways of DNA double-strand break repair during the mammalian cell cycle. Molecular and Cellular Biology, 23(16), 5706–5715.

Rowe, B. P., & Glazer, P. M. (2010). Emergence of rationally designed therapeutic strategies for breast cancer targeting DNA repair mechanisms. In Breast Cancer Research (Vol. 12, Issue 2). https://doi.org/10.1186/bcr2566

Rytelewski, M., Tong, J. G., Buensuceso, A., Leong, H. S., Vareki, S. M., Figueredo, R., Di Cresce, C., Wu, S. Y., Herbrich, S. M., Baggerly, K. A., Romanow, L., Shepherd, T., Deroo, B. J., Sood, A. K., Chambers, A. F., Vincent, M., Ferguson, P. J., & Koropatnick, J. (2014). BRCA2 inhibition enhances cisplatin-mediated alterations in

tumor cell proliferation, metabolism, and metastasis. In Molecular Oncology (Vol. 8, Issue 8, pp. 1429–1440). https://doi.org/10.1016/j.molonc.2014.05.017

Sachadyn, P. (2010). Conservation and diversity of MutS proteins. In Mutation Research/Fundamental and Molecular Mechanisms of Mutagenesis (Vol. 694, Issues 1-2, pp. 20–30). https://doi.org/10.1016/j.mrfmmm.2010.08.009

Sagona, A. P., Nezis, I. P., & Stenmark, H. (2014). Association of CHMP4B and autophagy with micronuclei: implications for cataract formation. BioMed Research International, 2014, 974393.

Sakai, W., Swisher, E. M., Karlan, B. Y., Agarwal, M. K., Higgins, J., Friedman, C., Villegas, E., Jacquemont, C., Farrugia, D. J., Couch, F. J., Urban, N., & Taniguchi, T. (2008). Secondary mutations as a mechanism of cisplatin resistance in BRCA2-mutated cancers. In Nature (Vol. 451, Issue 7182, pp. 1116–1120). https://doi.org/10.1038/nature06633

Sattler, T., & Mayer, A. (2000). Cell-free reconstitution of microautophagic vacuole invagination and vesicle formation. The Journal of Cell Biology, 151(3), 529–538.

Scharer, O. D. (2013). Nucleotide Excision Repair in Eukaryotes. In Cold Spring Harbor Perspectives in Biology (Vol. 5, Issue 10, pp. a012609–a012609). https://doi.org/10.1101/cshperspect.a012609

Schatz, D. G., & Swanson, P. C. (2011). V(D)J Recombination: Mechanisms of Initiation. In Annual Review of Genetics (Vol. 45, Issue 1, pp. 167–202). https://doi.org/10.1146/annurev-genet-110410-132552

Schipler, A., & Iliakis, G. (2013). DNA double-strand-break complexity levels and their possible contributions to the probability for error-prone processing and repair pathway

choice. In Nucleic Acids Research (Vol. 41, Issue 16, pp. 7589–7605). https://doi.org/10.1093/nar/gkt556

Schreiber, V., Dantzer, F., Ame, J.-C., & de Murcia, G. (2006). Poly(ADP-ribose): novel functions for an old molecule. Nature Reviews. Molecular Cell Biology, 7(7), 517–528.

Schwertman, P., Lagarou, A., Dekkers, D. H. W., Raams, A., van der Hoek, A. C., Laffeber, C., Hoeijmakers, J. H. J., Demmers, J. A. A., Fousteri, M., Vermeulen, W., & Marteijn, J. A. (2012). UV-sensitive syndrome protein UVSSA recruits USP7 to regulate transcription-coupled repair. In Nature Genetics (Vol. 44, Issue 5, pp. 598–602). https://doi.org/10.1038/ng.2230

Scrima, A., Konícková, R., Czyzewski, B. K., Kawasaki, Y., Jeffrey, P. D., Groisman, R., Nakatani, Y., Iwai, S., Pavletich, N. P., & Thomä, N. H. (2008). Structural basis of UV DNA-damage recognition by the DDB1-DDB2 complex. Cell, 135(7), 1213–1223.

Shah, S. Z. A., Zhao, D., Hussain, T., Sabir, N., Mangi, M. H., & Yang, L. (2018). p62-Keap1-NRF2-ARE Pathway: A Contentious Player for Selective Targeting of Autophagy, Oxidative Stress and Mitochondrial Dysfunction in Prion Diseases. Frontiers in Molecular Neuroscience, 11, 310.

Shakeri, A., Cicero, A. F. G., Panahi, Y., Mohajeri, M., & Sahebkar, A. (2019). Curcumin: A naturally occurring autophagy modulator. Journal of Cellular Physiology, 234(5), 5643–5654.

Sharma, A., Alswillah, T., Kapoor, I., Debjani, P., Willard, B., Summers, M. K., Gong, Z., & Almasan, A. (2020). USP14 is a deubiquitinase for Ku70 and critical determinant of non-homologous end joining repair in autophagy and PTEN-deficient cells. Nucleic Acids Research, 48(2), 736–747.

Sharma, V., Verma, S., Seranova, E., Sarkar, S., & Kumar, D. (2018). Selective Autophagy and Xenophagy in Infection and Disease. In Frontiers in Cell and Developmental Biology (Vol. 6). https://doi.org/10.3389/fcell.2018.00147

Sorokina, I. V., Denisenko, T. V., Imreh, G., Tyurin-Kuzmin, P. A., Kaminskyy, V. O., Gogvadze, V., & Zhivotovsky, B. (2017). Involvement of autophagy in the outcome of mitotic catastrophe. Scientific Reports, 7(1), 14571.

Soutoglou, E., Dorn, J. F., Sengupta, K., Jasin, M., Nussenzweig, A., Ried, T., Danuser, G., & Misteli, T. (2007). Positional stability of single double-strand breaks in mammalian cells. Nature Cell Biology, 9(6), 675–682.

Soutoglou, E., & Misteli, T. (2008). Activation of the Cellular DNA Damage Response in the Absence of DNA Lesions. In Science (Vol. 320, Issue 5882, pp. 1507–1510). https://doi.org/10.1126/science.1159051

Starcevic, D., Dalal, S., & Sweasy, J. B. (2004). Is There a Link Between DNA Polymerase Beta and Cancer? Cell Cycle , 3(8), 996–999.

Stavnezer, J. (2008). Faculty Opinions recommendation of Ubiquitylated PCNA plays a role in somatic hypermutation and class-switch recombination and is required for meiotic progression. In Faculty Opinions – Post-Publication Peer Review of the Biomedical Literature. https://doi.org/10.3410/f.1124350.581517

Stracker, T. H., & Petrini, J. H. J. (2011). The MRE11 complex: starting from the ends. Nature Reviews. Molecular Cell Biology, 12(2), 90–103.

Sun, S.-Y., Hu, X.-T., Yu, X.-F., Zhang, Y.-Y., Liu, X.-H., Liu, Y.-H., Wu, S.-H., Li, Y.-Y., Cui, S.-X., & Qu, X.-J. (2021). Nuclear translocation of ATG5 induces DNA mismatch

repair deficiency (MMR-D)/microsatellite instability (MSI) via interacting with Mis18α in colorectal cancer. British Journal of Pharmacology, 178(11), 2351–2369.

Sun, Y., Jiang, X., Chen, S., Fernandes, N., & Price, B. D. (2005). A role for the Tip60 histone acetyltransferase in the acetylation and activation of ATM. Proceedings of the National Academy of Sciences of the United States of America, 102(37), 13182–13187.

Su, Z., Wang, T., Zhu, H., Zhang, P., Han, R., Liu, Y., Ni, P., Shen, H., Xu, W., & Xu, H. (2015). HMGB1 modulates Lewis cell autophagy and promotes cell survival via RAGE-HMGB1-Erk1/2 positive feedback during nutrient depletion. Immunobiology, 220(5), 539–544.

Svilar, D., Goellner, E. M., Almeida, K. H., & Sobol, R. W. (2011). Base excision repair and lesion-dependent subpathways for repair of oxidative DNA damage. Antioxidants & Redox Signaling, 14(12), 2491–2507.

Takata, M., Sasaki, M. S., Sonoda, E., Morrison, C., Hashimoto, M., Utsumi, H., Yamaguchi-Iwai, Y., Shinohara, A., & Takeda, S. (1998). Homologous recombination and non-homologous end-joining pathways of DNA double-strand break repair have overlapping roles in the maintenance of chromosomal integrity in vertebrate cells. The EMBO Journal, 17(18), 5497–5508.

Tang, Y., Jacobi, A., Vater, C., Zou, L., Zou, X., & Stiehler, M. (2015). Icariin Promotes Angiogenic Differentiation and Prevents Oxidative Stress-Induced Autophagy in Endothelial Progenitor Cells. In STEM CELLS (Vol. 33, Issue 6, pp. 1863–1877). https://doi.org/10.1002/stem.2005

Tham, K.-C., Kanaar, R., & Lebbink, J. H. G. (2016). Mismatch repair and homeologous recombination. DNA Repair, 38, 75–83.

Tubbs, A., & Nussenzweig, A. (2017). Endogenous DNA Damage as a Source of Genomic Instability in Cancer. Cell, 168(4), 644–656.

Van Houten, B., Santa-Gonzalez, G. A., & Camargo, M. (2018). DNA repair after oxidative stress: current challenges. Current Opinion in Toxicology, 7, 9–16.

Vitale, I., Galluzzi, L., Castedo, M., & Kroemer, G. (2011). Mitotic catastrophe: a mechanism for avoiding genomic instability. Nature Reviews. Molecular Cell Biology, 12(6), 385–392.

Volker, M., Moné, M. J., Karmakar, P., van Hoffen, A., Schul, W., Vermeulen, W., Hoeijmakers, J. H., van Driel, R., van Zeeland, A. A., & Mullenders, L. H. (2001). Sequential assembly of the nucleotide excision repair factors in vivo. Molecular Cell, 8(1), 213–224.

Wakasugi, M., Kawashima, A., Morioka, H., Linn, S., Sancar, A., Mori, T., Nikaido, O., & Matsunaga, T. (2002). DDB Accumulates at DNA Damage Sites Immediately after UV Irradiation and Directly Stimulates Nucleotide Excision Repair. In Journal of Biological Chemistry (Vol. 277, Issue 3, pp. 1637–1640). https://doi.org/10.1074/jbc.c100610200

Wang, L., Patel, U., Ghosh, L., & Banerjee, S. (1992). DNA polymerase beta mutations in human colorectal cancer. Cancer Research, 52(17), 4824–4827.

Wang, Y., Zhang, N., Zhang, L., Li, R., Fu, W., Ma, K., Li, X., Wang, L., Wang, J., Zhang, H., Gu, W., Zhu, W.-G., & Zhao, Y. (2016). Autophagy Regulates Chromatin Ubiquitination in DNA Damage Response through Elimination of SQSTM1/p62. Molecular Cell, 63(1), 34–48.

Wang, Z., Lin, H., Hua, F., & Hu, Z.-W. (2013). Repairing DNA damage by XRCC6/KU70 reverses TLR4-deficiency-worsened HCC development via restoring senescence and autophagic flux. Autophagy, 9(6), 925–927.

Wan, K., Wang, Y. A., Kaper, M., Fritzemeier, M., & Babbar, N. (2018). The prevalence of PIK3CA mutations in HR /HER2– metastatic breast cancer (BELLE2, BELLE3 and BOLERO2 clinical trials). In Annals of Oncology (Vol. 29, p. viii95). https://doi.org/10.1093/annonc/mdy272.289

Weterings, E., & Chen, D. J. (2008). The endless tale of non-homologous end-joining. Cell Research, 18(1), 114–124.

Wirawan, E., Vanden Berghe, T., Lippens, S., Agostinis, P., & Vandenabeele, P. (2012). Autophagy: for better or for worse. Cell Research, 22(1), 43–61.

Yaneva, M., Kowalewski, T., & Lieber, M. R. (1997). Interaction of DNA-dependent protein kinase with DNA and with Ku: biochemical and atomic-force microscopy studies. The EMBO Journal, 16(16), 5098–5112.

Yang, Z., Goronzy, J. J., & Weyand, C. M. (2015). Autophagy in autoimmune disease. In Journal of Molecular Medicine (Vol. 93, Issue 7, pp. 707–717). https://doi.org/10.1007/s00109-015-1297-8

Yang, Z., & Klionsky, D. J. (2010). Mammalian autophagy: core molecular machinery and signaling regulation. Current Opinion in Cell Biology, 22(2), 124–131.

Yang, Z., Zhong, L., Zhong, S., Xian, R., & Yuan, B. (2015). Hypoxia induces microglia autophagy and neural inflammation injury in focal cerebral ischemia model. Experimental and Molecular Pathology, 98(2), 219–224.

Yan, S., Liu, L., Ren, F., Gao, Q., Xu, S., Hou, B., Wang, Y., Jiang, X., & Che, Y. (2017). Sunitinib induces genomic instability of renal carcinoma cells through affecting the interaction of LC3-II and PARP-1. Cell Death & Disease, 8(8), e2988.

Yoo, S., Kimzey, A., & Dynan, W. S. (1999). Photocross-linking of an Oriented DNA Repair Complex. In Journal of Biological Chemistry (Vol. 274, Issue 28, pp. 20034–20039). https://doi.org/10.1074/jbc.274.28.20034

Yorimitsu, T., & Klionsky, D. J. (2005). Autophagy: molecular machinery for self-eating. Cell Death and Differentiation, 12 Suppl 2, 1542–1552.

Yousefi, S., Perozzo, R., Schmid, I., Ziemiecki, A., Schaffner, T., Scapozza, L., Brunner, T., & Simon, H.-U. (2006). Calpain-mediated cleavage of Atg5 switches autophagy to apoptosis. Nature Cell Biology, 8(10), 1124–1132.

Yu, L., McPhee, C. K., Zheng, L., Mardones, G. A., Rong, Y., Peng, J., Mi, N., Zhao, Y., Liu, Z., Wan, F., Hailey, D. W., Oorschot, V., Klumperman, J., Baehrecke, E. H., & Lenardo, M. J. (2010). Termination of autophagy and reformation of lysosomes regulated by mTOR. In Nature (Vol. 465, Issue 7300, pp. 942–946). https://doi.org/10.1038/nature09076

Yun, C. W., & Lee, S. H. (2018). The Roles of Autophagy in Cancer. International Journal of Molecular Sciences, 19(11). https://doi.org/10.3390/ijms19113466

Zhao, Z., Oh, S., Li, D., Ni, D., Pirooz, S. D., Lee, J.-H., Yang, S., Lee, J.-Y., Ghozalli, I., Costanzo, V., Stark, J. M., & Liang, C. (2012). A dual role for UVRAG in maintaining chromosomal stability independent of autophagy. Developmental Cell, 22(5), 1001–1016.

Zhou, B. B., & Elledge, S. J. (2000). The DNA damage response: putting checkpoints in perspective. Nature, 408(6811), 433–439.

Zhu, H., Tannous, P., Johnstone, J. L., Kong, Y., Shelton, J. M., Richardson, J. A., Le, V., Levine, B., Rothermel, B. A., & Hill, J. A. (2007). Cardiac autophagy is a maladaptive response to hemodynamic stress. The Journal of Clinical Investigation, 117(7), 1782–1793.

Ziv, Y., Bielopolski, D., Galanty, Y., Lukas, C., Taya, Y., Schultz, D. C., Lukas, J., Bekker-Jensen, S., Bartek, J., & Shiloh, Y. (2006). Chromatin relaxation in response to DNA double-strand breaks is modulated by a novel ATM-and KAP-1 dependent pathway. Nature Cell Biology, 8(8), 870–876.

APPENDIX A

MATERIAL LIST

Name of Material/ Equipment Company Catalog Number	Company	Catalog Number
Acrylamide/Bis-Acrylamide Solution	Sigma	A3574
Alexa fluor 546 phalloidin	Molecular Probes	A22283
Anti mouse IgG, HRP conjugated	Jackson Immuno.	115035003
Anti-Mouse IgG Alexa Fluor 488	Invitrogen	A11001
Anti-rabbit IgG HRP conjugated	Jackson Immuno.	1110305144
Anti-Rabbit IgG Alexa Fluor 568	Invitrogen	A11011
ATG5 Antibody	Sigma	A0856
Bradford Solution	Sigma	6916
Bromophenol blue	Applichem	A3640.0005
BSA	Sigma	A4503
CCCP	Sigma	C2759
Coumeric Acid	Sigma	C9008
Coverslides	Jena Bioscience	CSL-103
DMEM (high glucose) PAN Biotech	PAN Biotech	P04-03500
DMSO	Sigma	VWRSAD2650
EBSS	Biological Industries	BI02-010-1A
Fetal bovine serum (FBS)	Biowest	S1810-500
Flag Antibody	Sigma	F3165
Flag M2 Beads Sigma	Sigma	A2220
Glutaraldehyde	Sigma	G5882
Glycerol	Applichem	A4453
Hemocytometer	Sigma	Z359629-1EA
Hydrogen Peroxide	Merck	K35522500604
L-glutamine	Biological Industries	BI03-020-1B
Luminol	Fluka	9253
MG132	Enzo Life Sciences	BML-PI102-0005
MOPS	Sigma	M1254
Nitocellulose membrane	GE Healthcare	A10083108
Non-Fat milk	Applichem	A0830
Non-targeting SiRNA	Dharmacon	D-0011210-02-20
NP-40	Applichem	A16694.0250

P62 Antibody	Abnova	H00008878-M01
Paraformaldehyde (PFA)	Sigma	15812-7
PBS	PAN Biotech	P04-36500
Penicillin/streptomycin solution 03-031-1B	Biological Industries	03-031-1B
Phenol red	Sigma	114537-5G
PhosphoSer65-Ub Antibody	Millipore	ABS1513
Poly-L-Lysine	Sigma	P8920
Protease inhibitor	Sigma	P8340
Protein A-Agarose Beads	Santa Cruz Biotechnology	Sc-2001
Protein G-Agarose Beads	Santa Cruz Biotechnology	Sc-2002
Rapamycin	Sigma	R0395
Saponin	Sigma	84510
Slides	Isolab	I.075.02.005
Sodium Azide	Riedel de Haen	13412
Sodium Chloride	Applichem	A9242.5000
Sodium deoxycholate	Sigma	30970
Sodium dodecyl sulphate (SDS)	Biochemika	A2572
Sodium orthovanadate	Sigma	450243
Staurosporine	Sigma	S5921
Sucrose Sigma	Sigma	S0389
Torin	Tocris	4247
Triton-X	Applichem	4975
Trizma Base	Sigma	T1503
Trypan Blue	Sigma	A4503
Trypsin EDTA Solution A	Biological Industries	BI03-050-1A
Tween 20	Sigma	P5927
X-ray Films	Fujifilm	47410 19289
â-Actin Antibody	Sigma	A5441
â-Mercaptoethanol	Applichem	A1108.0250

PUBLICATIONS

S. Sarikaya., H. Çakır., D. Gözüaçık., Y. Akkoç., ‘‘Crosstalk between autophagy and DNA repair systems.’’ Available online: 09.06.2021. DOI: 10.3906/biy-2103-51 in press.

S. Sarikaya. et al., A novel ATG5 interaction with Ku70 potentiates DNA repair upon genotoxic stress. submitted

Poster Presentations:

Sinem Demirbağ-Sarıkaya, Jörn Dengjel and Devrim Gozuacik, Investigation of links and crosstalk between autophagy and DNA damage responses. The AIM Center's 2020 International eSymposium, 25th November 2020.